To the Graduate Council:

We are submitting herewith a thesis written by **Zorawar Singh Kooner** entitled **"Surface Complexation Modeling of Metal Adsorption onto Goethite in Aqueous Systems."** We have examined the final copy of this thesis for form and content and recommend that it be accepted in partial fulfillment of the requirements for the degree of Master of Science with a major in Environmental Engineering.

Dr. C. D. Cox, Major Professor

Dr. J. L. Smoot, Major Professor

We have read this thesis
and recommend its acceptance:

Accepted for the Council:

Associate Vice Chancellor
and Dean of The Graduate School

STATEMENT OF PERMISSION TO USE

In presenting this thesis in partial fulfillment of the requirements for a Master's degree at the university of Tennessee, Knoxville, I agree that the library shall make it available to borrowers under rules of the Library. Brief quotations from this thesis are allowable without special permission, provided that accurate acknowledgement of the source is made.

Permission for extensive quotation from or reproduction of this thesis may be granted by my major professors, or in their absence, by the Head of Interlibrary Services when, in the opinion of either, the proposed use of the material is for scholarly purposes. Any copying or use of the material in this thesis for financial gain shall not be allowed without my written permission.

Signature ZS Koonce

Date Apr 5, 1994

Surface Complexation Modeling of Metal Adsorption onto Goethite in Aqueous Systems

A Thesis

Presented for the

Master of Science

Degree

The University of Tennessee, Knoxville

Zorawar Singh Kooner

May 1994

Dedicated

to

Reshma and Preetma

for the time we lost

during my work on this thesis

ACKNOWLEDGEMENTS

I would like to express my sincere thanks to Dr C. C. Cox and Dr. J. L. Smoot, my coadvisors for their constant help, encouragement and guidance throughout the course of this study.

My thanks are also due to Dr. M. M. Ghosh, my committee member, for his help and critique of the manuscripts. The assistance of Mr. F. M. Hoffman in computer modeling is gratefully acknowledged.

I want to take this opportunity to express my indebtedness to my best friend and wife, Nasib Kaur Kooner for many sacrifices she had to make so that I could complete this study.

ABSTRACT

The triple layer surface complexation model has been used to model the adsorption behavior of copper(II), lead(II), and zinc(II) onto goethite as function of pH, total dissolved metal concentration, the surface area of goethite, and ionic strength. A single reaction involving adsorption of Me^{2+} onto negative surface site ($SOH + Me^{2+} = SOMe^{+} + H^{+}$) as an inner-sphere complex proved successful in describing adsorption of copper, lead, and zinc under the experimental conditions. The estimated values of the weighted average equilibrium constant of above the reactions are $10^{1.95}$, $10^{1.19}$, and $10^{0.34}$ for copper, lead, and zinc, respectively. The adsorption equilibrium constants were related to the first hydrolysis constant by a linear free-energy relationship.

TABLE OF CONTENTS

Chapter		Page
1.	INTRODUCTION	1
	1.A Introduction	1
	1.B Objectives	3
2.	LITERATURE REVIEW	4
	2.A Introduction	4
	2.B Triple Layer Model	5
	2.C Previous Work	11
3.	MATERIALS AND METHODS	19
	3.A Introduction	19
	3.B Materials	19
	3.C Experimental Methods	20
4.	RESULTS AND DISCUSSION	30
	4.A Introduction	30
	4.B Hydrolysis of Metals in Aqueous System	30
	4.C Adsorption Modeling	34
5.	CONCLUSIONS	52
	5.A Summary	52
	5.B Recommendations for future research	53
LIST OF REFERENCES		56
APPENDICES		64
	APPENDIX A. Data for chapter 3	65
	APPENDIX B. Data for chapter 4	71
	APPENDIX C. Figures for chapter 4	94
VITA		115

LIST OF TABLES

Table		Page
2.1.	Comparison of the properties of metals	15
3.1.	Range of experimental variables	29
4.1.	Equilibrium constants for hydrolysis reactions	35
4.2.	Parameters for modeling	37
4.3.	Equilibrium constants for reaction 4.1	43
5.1	EPA Primary Drinking Water Standards	54

LIST OF FIGURES

Figure **Page**

2.1. A Schematic representation of potential and charge distribution in the electrical double layer.....6

2.2. Adsorption of metals onto goethite: Comparison of the adsorption edges; ΣMe = 5 ppm; Surface area = 30 m^2/l; I = 0.1 M $NaNO_3$.....13

2.3. Adsorption of metals onto goethite: Comparison of distribution coefficients, ΣMe = 5 ppm; Surface area = 30 m^2/l; I = 0.1 M $NaNO_3$.....17

3.1. Adsorption (kinetics) experiments at pH 5.8: (corrected for pH and the mass of goethite); ΣCu = 5.0 ppm (7.87 x 10^{-5} M); Surface area = 30 m^2/l; I = 0.1 M $NaNO_3$.....24

3.2. Reversibility of copper adsorption onto goethite; ΣCu = 5.0 ppm; (7.87 x 10^{-5} M); Surface area = 30 m^2/l; I = 0.1 M $NaNO_3$.....25

3.3.. Reproducibility of copper adsorption onto goethite; ΣCu = 0.5 ppm; (7.87 x 10^{-6} M); Surface area = 30 m^2/l; I = 0.1 M $NaNO_3$.....27

3.4. Reproducibility of lead adsorption onto goethite; Surface area = 30 m^2/l; I = 0.1 M $NaNO_3$.....28

LIST OF FIGURES (Cont.)

Figure **Page**

4.1. Species distribution of copper in an aqueous Cu(II) solution; ΣCu = 5.0 ppm (7.87×10^{-5} M); I = 0.1 M $NaNO_3$ 31

4.2. Species distribution of lead in an aqueous Pb(II) solution; ΣPb = 5.0 ppm (2.41×10^{-5} M); I = 0.1 M $NaNO_3$ 32

4.3. Species distribution of zinc in an aqueous Zn(II) solution; ΣZn = 5.0 ppm (7.65×10^{-5} M); I = 0.1 M $NaNO_3$ 33

4.4. Modeling the adsorption of copper onto goethite; ΣCu = 5 ppm (7.87×10^{-5} M); Surface area = 30 m^2/l; I = 0.1 M $NaNO_3$; $SOH + Cu^{2+} = SOCu^{+} + H^{+}$ 39

4.5. Modeling the adsorption of copper onto goethite; ΣCu = 5 ppm (7.87×10^{-5} M); Surface area = 30 m^2/l; I = 0.1 M $NaNO_3$; $SOH + CuOH^{+} = SOCuOH + H^{+}$ 40

4.6. Modeling the adsorption of copper onto goethite; ΣCu = 5 ppm (7.87×10^{-5} M); Surface area = 30 m^2/l; I = 0.1 M $NaNO_3$; $SOH + CuOH^{+} = SO^{-}\text{-}CuOH^{+} + H^{+}$ 42

LIST OF FIGURES (Cont.)

Figure **Page**

4.7. Modeling the adsorption of lead onto goethite; Effect of surface area; ΣPb = 5.0 ppm (2.41×10^{-5} M); I = 0.1 M $NaNO_3$ 46

4.8. Modeling the adsorption of lead onto goethite; Effect of lead concentration; Surface area = 30 m^2/l I = 0.1 M $NaNO_3$ 47

4.9. Modeling the adsorption of lead onto goethite; Effect of ionic strength; ΣPb = 5.0 ppm (2.41×10^{-5} M); Surface area = 30 m^2/l 48

4.10. Correlation of log $K^{int}_{Me^{2+}}$ with first hydrolysis constants for divalent metals 51

C.1. Modeling the adsorption of copper onto goethite; ΣCu = 0.5 ppm (7.87×10^{-6} M); Surface area = 30 m^2/l; I = 0.1 M $NaNO_3$ 95

C.2. Modeling the adsorption of copper onto goethite; ΣCu = 1.0 ppm (1.57×10^{-5} M); Surface area = 280 m^2/l; I = 0.1 M $NaNO_3$ 96

C.3. Modeling the adsorption of copper onto goethite; ΣCu = 5.0 ppm (7.87×10^{-5} M); Surface area = 30 m^2/l; I = 0.1 M $NaNO_3$ 97

LIST OF FIGURES (Cont.)

Figure **Page**

C.4. Modeling the adsorption of copper onto goethite;
ΣCu = 5.0 ppm (7.87×10^{-5} M);
Surface area = 60 m^2/l; I = 0.1 M $NaNO_3$.....98

C.5. Modeling the adsorption of copper onto goethite;
ΣCu = 5.0 ppm (7.87×10^{-5} M);
Surface area = 145 m^2/l; I = 0.1 M $NaNO_3$.....99

C.6. Modeling the adsorption of copper onto goethite;
ΣCu = 5.0 ppm (7.87×10^{-5} M);
Surface area = 280 m^2/l; I = 0.1 M $NaNO_3$.....100

C.7. Modeling the adsorption of copper onto goethite;
ΣCu = 5.0 ppm (7.87×10^{-5} M);
Surface area = 30 m^2/l; I = 0.01 M $NaNO_3$.....101

C.8. Modeling the adsorption of copper onto goethite;
ΣCu = 10.0 ppm (1.57×10^{-4} M);
Surface area = 30 m^2/l; I = 0.1 M $NaNO_3$.....102

C.9. Modeling the adsorption of copper onto goethite;
ΣCu = 10.0 ppm (1.57×10^{-4} M);
Surface area = 280 m^2/l; I = 0.1 M $NaNO_3$.....103

C.10. Modeling the adsorption of lead onto goethite;
ΣPb = 2.0 ppm (9.65×10^{-6} M);
Surface area = 12 m^2/l; I = 0.1 M $NaNO_3$.....104

LIST OF FIGURES (Cont.)

Figure **Page**

C.11. Modeling the adsorption of lead onto goethite;
ΣPb = 2.0 ppm (9.65×10^{-6} M);
Surface area = 30 m^2/l; I = 0.1 M $NaNO_3$.....105

C.12. Modeling the adsorption of lead onto goethite;
ΣPb = 5.0 ppm (2.41×10^{-5} M);
Surface area = 30 m^2/l; I = 0.1 M $NaNO_3$.....106

C.13. Modeling the adsorption of lead onto goethite;
ΣPb = 5.0 ppm (2.41×10^{-5} M);
Surface area = 60 m^2/l; I = 0.1 M $NaNO_3$.....107

C.14. Modeling the adsorption of lead onto goethite;
ΣPb = 5.0 ppm (2.41×10^{-5} M);
Surface area = 120 m^2/l; I = 0.1 M $NaNO_3$.....108

C.15. Modeling the adsorption of lead onto goethite;
ΣPb = 5.0 ppm (2.41×10^{-5} M);
Surface area = 30 m^2/l; I = 0.01 M $NaNO_3$.....109

C.16. Modeling the adsorption of lead onto goethite;
ΣPb = 5.0 ppm (2.41×10^{-5} M);
Surface area = 30 m^2/l; I = 0.5 M $NaNO_3$.....110

C.17. Modeling the adsorption of lead onto goethite;
ΣPb = 10.0 ppm (4.83×10^{-5} M);
Surface area = 30 m^2/l; I = 0.1 M $NaNO_3$.....111

LIST OF FIGURES (Cont.)

Figure **Page**

C.18. Modeling the adsorption of lead onto goethite;
ΣPb = 15.0 ppm (7.24×10^{-5} M);
Surface area = 30 m^2/l; I = 0.1 M $NaNO_3$.....112

C.19. Modeling the adsorption of zinc onto goethite;
ΣZn = 5.0 ppm (7.65×10^{-5} M);
Surface area = 30 m^2/l; I = 0.1 M $NaNO_3$.....113

4.20. Modeling the adsorption of zinc onto goethite;
ΣZn = 5.0 ppm (7.65×10^{-5} M);
Surface area = 30 m^2/l; I = 0.01 M $NaNO_3$.....114

CHAPTER 1
INTRODUCTION

1.A INTRODUCTION

The fate of hazardous wastes, including metals, in groundwater is becoming an increasingly important issue in the United States and other countries. Metals are known to migrate much further from a buried disposal site than expected (Means et al. 1978). Aqueous transport is the main process by which buried waste can migrate from its site. The natural environment contains a wide variety of mineral surfaces that, through interactions at the mineral/solute interface, are capable of removing metals from aqueous solutions in a variety of systems, including seawater, streams, soils, and groundwater. Such interactions can be classified as adsorption, ion exchange, precipitation and coprecipitation. The adsorption of metals by solid surfaces is an important mechanism that controls trace metal concentration in aqueous systems (Hem 1972, 1976; and Schindler 1967) and is widely recognized as the most important phenomenon in retarding metal migration in aqueous systems (Dudley et al. 1988; Fuller and Davis 1987; James and Leckie 1974; McCarthy and Zachara 1989; Parks 1975; and Zachara et al. 1989). An understanding of the adsorption process forms the basis for burial site selection, design of landfills and remedial action at certain waste facilities.

Iron oxides, common constituents of soils, sediments, and aquifers, have high surface areas and are capable of adsorbing a significant quantity of metals. They are dominant adsorbents in the environment because they are finely dispersed and tend to coat other particles. Thus, they are believed to play a role in controlling the transport of metals in aqueous systems. Goethite (α-FeOOH),

was selected for this study because it can be reproducibly synthesized in the laboratory within a short time. Further, the surface-chemical characteristics of goethite sample that was synthesized by a nearly identical procedure are available in the literature (Hayes 1987).

The mobility of metals in the aqueous phase can be characterized by a distribution coefficient (K_d), defined as the ratio of the amount of metal adsorbed onto the solid phase to the amount of metal in the aqueous phase at equilibrium. Distribution coefficients act as an indicator of the tendency of the metal to be mobile in the aqueous medium. A high distribution coefficient indicates that most of the metal is retained by the adsorbent by sorption processes. Distribution coefficients were used in previous studies (Kooner 1992, 1993) to describe the adsorption of copper, lead, and zinc at the goethite/water interface.

Although empirical approaches, like K_d, have been successful in describing adsorption data, they do not give any insight into the mechanism of adsorption, and cannot be used to predict the metal behavior outside the experimental conditions under which the data were taken. Metals in aqueous systems generally exist in the form of several aquometal species whose concentrations depend upon ionic strength, pH, temperature and the total amount of the metal. Distribution coefficients, K_d, are calculated based on the total metal concentration instead of the concentration of free metal ion and adsorbing metal complex, if any.

Adsorption behavior of a free metal ion might differ from its various metal complexes. Any one of these species might be able to take part in surface adsorption. It is equally possible that more than one species might take part in the adsorption reaction. The K_d approach does not account for the chemical processes which are responsible for the partitioning of the metal between the solid and

liquid phase, nor does it take into consideration possible changes in the oxidation state of metals during (e.g. cobalt) adsorption (Murray and Dillard 1979). A more rational approach may facilitate prediction of adsorption behavior under various conditions and provide a useful tool for scientists and engineers involved in fate and transport, risk assessment, and site remediation techniques.

1.B OBJECTIVES

Surface complexation models (SCM) based on electrical double layer (EDL) theory describe adsorption in terms of the chemical and physical interactions between ions and the surface. They may be preferable to the K_d approach in that data representing a wider range of experimental conditions can be represented using a single set of parameters and a more fundamental understanding of the phenomena is possible.

The purpose of this study is to model the previously collected data (Kooner 1992, 1993) using a surface complexation model with the following objectives:

- to investigate whether the data could be described by a SCM
- to determine the equilibrium constants for metal adsorption
- to determine the metal species which control solution-surface partitioning

CHAPTER 2
LITERATURE REVIEW

2.A INTRODUCTION

A model is a simplified representation of a system that considers only the characteristics of the system important to the problem. If a model describes data without any theoretical background, it is referred to as an ***empirical model***. If the model describes data consistent with the chemical properties of the system based on theoretical considerations, it is called a ***chemical model***. Use of distribution coefficients, K_d, to explain adsorption phenomenon is a typical example of an empirical model. Unfortunately, it has a limited range of applicability because it is a parameter which is conditional upon the chemical conditions under which it has been measured.

Unlike empirical models, surface complexation models are chemical models that are based on general molecular description of adsorption phenomenon using a equilibrium approach and are based on thermodynamic properties of the system and may be used under different conditions. These models are based on the well known electrical double layer (EDL) theory proposed by Gouy (1910) and Chapman (1913) later extended by Stern (1924) and Grahame (1947).

Several models have been developed based on EDL theories but they differ from each other because of slightly different assumptions made in the development of each model. As a result, the fitted parameters of one model cannot be compared with those of another, but the ability of the models to fit the data can be compared. The major difference between the models lies in the description of the

EDL. Though the surface complexation models of the EDL may vary from one another, they all share a common fundamental framework, as follows:

- oxides have specific site at which the sorption takes place
- mass law equations can be used to quantitatively describe the sorption onto the oxide
- sorption reactions at the surface result in surface charge
- EDL theory can be used to account for the effect of surface charge

The model selected for the present work, the triple layer model (TLM), was originally developed by Davis and coworkers (Davis et al. 1978; and Davis and Leckie 1978b, 1980) and is an extension of site the binding-model developed by Yates et al. (1974). Later, the model was modified by Hayes and Leckie (1987) to better represent the effects of ionic strength on adsorption.

2. B TRIPLE LAYER MODEL

A simplified diagram of the original triple layer model, along with associated charge and potential is shown in Figure 2.1. It is assumed that all ions except H^+, when adsorbed, remain at a distance β from the surface, whereas H^+ can approach the surface to almost zero distance. This concept was modified by Hayes and Leckie (1987) in that metal ions were assumed to be able to form either inner-sphere or outer-sphere complexes, depending on the affinity of the metal for the surface. Metals that form inner-sphere complexes are assigned to the surface plane, while metals that form outer-sphere complexes are assigned to the β plane. This modification was invoked to explain the effect of ionic strength on metal adsorption. The modified version of TLM is successful in explaining the ionic strength effect on both weakly and strongly

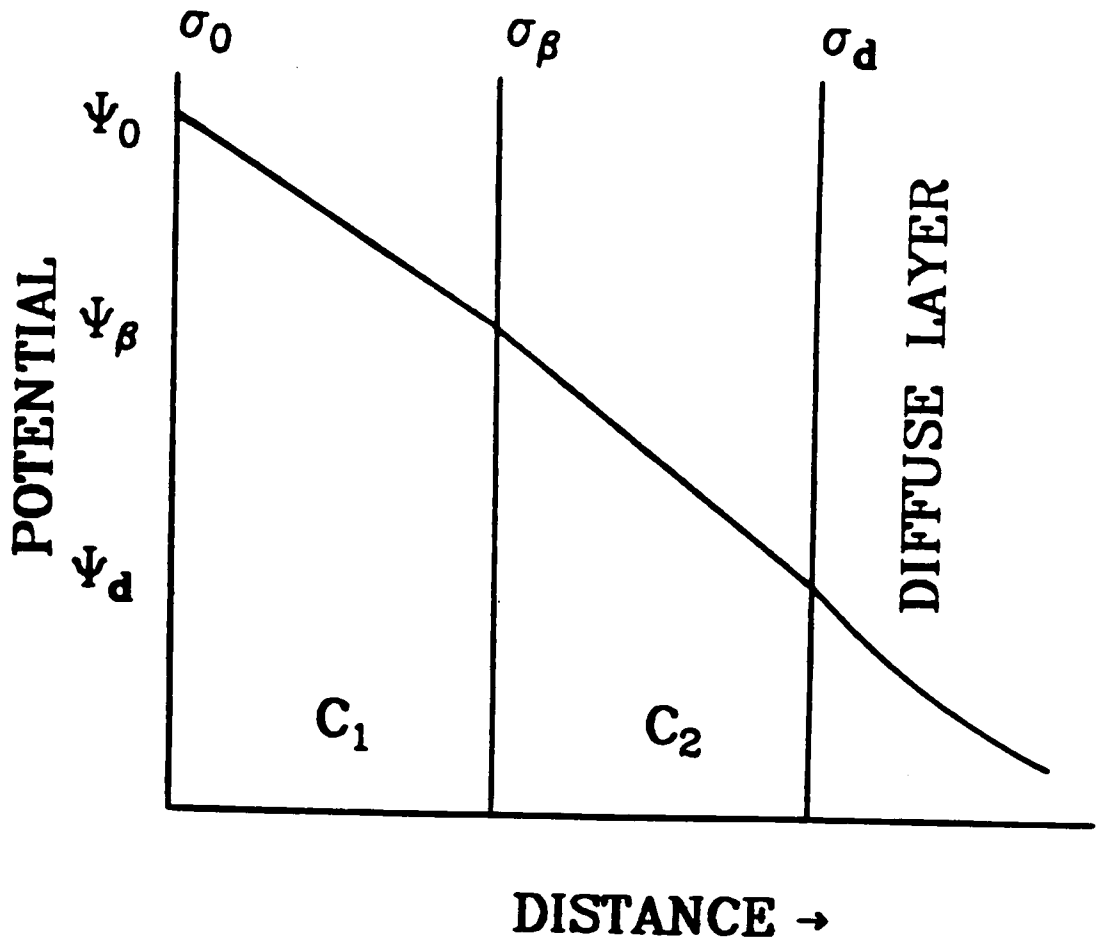


Figure 2.1 A schematic representation of potential and charge distribution in the electrical double layer. ψ stands for potential, and σ stands for charge. C_1 and C_2 represent capacitance in inner and outer layers respectively. The subscript 0, β, and d refer to the 0-plane, β-plane and the diffuse layer respectively.

bonding surface complexes (Hayes and Leckie, 1987; and Hayes et al. 1988). Other SCMs treat only either inner-sphere complex (Stumm et al. 1970, 1976) or outer sphere complexes (Davis and Leckie 1978) but not both.

Oxide surface in aqueous solution are assumed to have acidic, basic, and neutral sites depending upon the pH of the solution. At values of pH less than point of zero charge (PZC), the surface acquires a positive (acidic) charge, where as at pH values higher than PZC, the surface acquires a negative (basic) charge. PZC is defined as the pH at which the surface does not have any net charge. These positive or negative surfaces are created by the adsorption or desorption of protons at the neutral surface. These reactions can be represented as follows:

$$SOH_2^+ = SOH + H^+ \quad (2.1)$$

$$SOH = SO^- + H^+ \quad (2.2)$$

Where SOH_2^+, SOH, and SO^- represents the positively charged, neutral and negatively charged oxide surface sites. Apparent equilibrium constant for the above reaction may be written as follows:

$$K_{a1} = (SOH)[H^+]/(SOH_2^+) \quad (2.3)$$

$$K_{a2} = (SO^-)[H^+]/(SOH) \quad (2.4)$$

where ( ) represent molar concentrations, and [ ] represent activities. K_{a1} and K_{a2} are called apparent equilibrium constants because term $[H^+]$ used in above equations refers to the bulk solution and not the adsorption surface, the site of the reaction. The work required to transport an ion from the bulk solution across a potential gradient to the surface, causes a change in the activity of the ion. Assuming H_s^+ is the activity of the hydrogen ion at the

surface, the intrinsic equilibrium constants of reaction 2.1 and 2.2 can be represented as follows:

$$K^{int}_{a1} = (SOH)[H_s^+]/(SOH_2^+) \quad (2.5)$$

$$K^{int}_{a2} = (SO^-)[H_s^+]/(SOH) \quad (2.6)$$

where K^{int}_{a1} and K^{int}_{a2} are independent of surface charge and ionic strength and H_s^+ is related to the bulk hydrogen activity as follows:

$$[H_s^+] = [H^+]\exp(-F\Psi_0/RT) \quad (2.7)$$

where Ψ_0 represents the surface potential at the surface (zero) plane (Fig. 2.1) compared to the reference potential in the bulk solution, and F, R, and T are Faraday constant, gas constant and absolute temperature, respectively. Taking into account the above electrostatic interactions, the intrinsic equilibrium constants for reaction 2.1 and 2.2 can be rewritten as follows:

$$K^{int}_{a1} = (SOH)[H^+]\exp(-F\Psi_0/RT)/(SOH^{2+}) \quad (2.8)$$

$$K^{int}_{a2} = (SO^-)[H^+]\exp(-F\Psi_0/RT)/(SOH) \quad (2.9)$$

A similar scheme can be used to represent reactions for the adsorption of metals onto the oxide. One of the reactions which might take place during adsorption is as follows:

$$SOH + Me^{2+} = SOMe^+ + H^+ \quad (2.10)$$

where Me^{2+} represents a divalent metal ion and $SOMe^+$ represents an inner-sphere complex of the metal with the surface. Some other possible reaction combinations will be discussed in Chapter 4. The intrinsic equilibrium constant of reactions 2.10 is given by the following equation:

$$K^{int}_{Me^{2+}} = (SOMe^{+})[H^{+}]\exp(-F\Psi_0/RT)/(SOH)[Me^{2+}] \quad (2.11)$$

Another important surface reaction is the interaction of the background electrolyte (e. g. $NaNO_3$ in this study) with the surface, which can be represented by the following reactions:

$$SOH + Na^{+} = SO^{-}\text{-}Na^{+} + H^{+} \quad (2.12)$$

$$SOH + NO_3^{-} + H^{+} = SOH_2^{+}\text{-}NO_3^{-} \quad (2.13)$$

where SO^{-}-Na^{+} and SOH_2^{+}-NO_3^{-} represent outer-sphere complexes and the corresponding equilibrium constants for reactions 2.12 and 2.13 may be written as follows:

$$K^{int}_{Na^{+}} = (SO^{-}\text{-}Na^{+})[H^{+}]\exp(-F\Psi_0/RT)/(SOH)[Na^{+}]\exp(-F\Psi_\beta/RT) \quad (2.14)$$

$$K^{int}_{NO_3^{-}} = (SOH^{+}_2\text{-}NO_3^{-})/(SOH)[H^{+}][NO_3^{-}]\exp(-F\Psi_0/RT)\exp(+F\Psi_\beta/RT) \quad (2.15)$$

where Ψ_β represents the surface potential at the β plane (Fig. 2.1) compared to the reference potential in the bulk solution.

Assuming Na^{+}, NO_3^{-}, and Me^{2+} are the only adsorbing ions, it is now possible to an write equation for surface charge at the surface (zero) plane (σ_0), beta plane (σ_β), and at the diffuse layer (σ_d) as follows:

$$\sigma_0 = B([SOH^{+}_2] + [SOH^{+}_2\text{-}NO_3^{-}] + [SOMe^{+}] - [SO^{-}] - [SO^{-}\text{-}Na^{+}]) \quad (2.16)$$

$$\sigma_\beta = B([SO^{-}\text{-}Na^{+}] - [SOH^{+}_2\text{-}NO_3^{-}]) \quad (2.17)$$

where B is a conversion factor calculated as $10^6F/A$ with A as the surface area available per liter of solution. Further, the solution must be electrically neutral:

$$\sigma_0 + \sigma_\beta + \sigma_d = 0 \quad (2.18)$$

C_1 and C_2 are inner and outer capacitance (Fig. 2.1) and are assumed to be constant between the layers and relate the EDL potentials and charges to one another as follows:

$$\psi_0 - \psi_\beta = \sigma_0/C_1 \quad (2.19)$$

$$\psi_\beta - \psi_d = \sigma_d/C_2 \quad (2.20)$$

$$\sigma_d = -(8c\varepsilon RT)^{1/2}\sinh(ZF\psi_d/ZRT) \quad (2.21)$$

where c is the electrolyte concentration and ε is the permitivity of water.

The surface species are distributed among the total number of sites (N) described by the following equation:

$$N = B([SOH^+_2] + [SOH] + [SO^-] + [SO^-Na^+] + [SOH^+_2\text{-}NO_3^-] + [SOMe^+]) \quad (2.22)$$

The parameters of TLM are obtained by fitting the model to experimental data. For example, N, K^{int}_{a1}, K^{int}_{a1}, K^{int}_{Na}, $K^{int}_{NO_3^-}$, C_1 and C_2 are obtained by fitting surface titration data at various electrolyte concentrations. Parameters to describe metal sorption are defined in a similar manner. FITEQL (Westall, 1982), a nonlinear least-square optimization program based on the Newton-Raphson method is designed to extract estimates of chemical equilibrium model parameters from experimental data.

The TLM implemented by Davis et al. (1978) has been used to successfully model the adsorption behavior of metal ions, ligands and metal-ligand complexes at oxide/aqueous interface (Davis et al. 1978; and Davis and Leckie 1978a, 1978b, 1979, 1980). Balistrieri and Murray (1979, 1981, 1982a, 1982b) have found that the TLM is adequate in modeling adsorption of ions onto oxides suspended in seawater. James et al. (1978) have been successful in

modeling the conductometric and potentiometric titration data of ionizable latices with the TLM.

The triple layer model has also been used for modeling adsorption of ions onto other types of soil constituents. A two-site version of the TLM was used by James and Parks (1982) to model the clay ion-exchange data of Marshall and coworkers (Marshall and Bergman 1942; Marshall and Krinbill 1942). Kleijn (1981) has developed a two-site SCM for clay and oxide minerals based on TLM and the addition of isomorphic substitution charge.

Charlet (1986) has modeled the adsorption of major cations onto an oxisol using the modified version of the TLM of Hayes and Leckie (1987). The modified version of the TLM was used by Hayes and Leckie (1987) for the adsorption of lead and cadmium onto goethite to explain the effect of ionic strength and by Hayes et al. (1988) for the adsorption of selenite and selenate onto goethite. Cox and Ghosh (1994) used a two-site version of the TLM to model the adsorption behavior of methylated arsenates onto hydrous oxide as inner-sphere complexes. Ghosh et al. (1994) used the TLM to model selenium adsorption; inner- and outer-sphere complexes were proposed for selenite and selenate, respectively.

2.C PREVIOUS WORK

This section summarizes work previously reported in the literature (Kooner 1992, 1993) and is included here for the convenience of the reader. The adsorption behavior of copper, lead, and zinc (Kooner 1992, 1993) was found to be similar to that of other hydrolyzable metal ions as reported by Anderson and Christensen (1988); Balistrieri and Murray (1982a); Benjamin and Leckie (1981); Davis and Leckie (1978a); Forbes et al. (1976), and Padmanabham (1983).

Adsorption isotherms

Adsorption edges of all three metals onto goethite (surface area = 30 m^2/l) at various metal concentrations were dependent on initial metal concentration. With an increase in the concentration of metal, the adsorption edge moved to a higher pH (i.e. at constant surface area of goethite, a higher pH is required to achieve the same fractional adsorption as that observed at lower metal concentrations). At high goethite concentration (280 m^2/l) the adsorption edge was independent of initial copper concentration. At low surface area, the number of binding sites per copper ion decreases with the increase in the copper concentration, and copper ion has to compete with other copper ions for the available binding sites. As a result, the percentage of copper adsorbed decreases. However, as the copper concentration is increased at high surface area, the number of binding sites per copper ion decreases, but the total number of binding sites is sufficiently large that copper ions do not have to compete for available sites. The adsorption edge moved to a lower pH with an increase in the goethite surface area at constant metal concentration. At constant pH with an increase in surface area, more goethite is present in the suspension to remove metal. As a result, the percentage of metal adsorbed increases, which results in the shift of adsorption edge to a lower pH. A decrease in ionic strength did not have any significant effect on the adsorption of copper, lead, and zinc. This is not unusual, considering that nitrate does not significantly complex with any of these metals and sodium and nitrate do not strongly interact with the goethite surface. Hayes and Leckie (1987) reported similar results in a study in which the concentration of lead was almost 100 times higher than that reported here.

The adsorption edges of the three metals—lead, copper, and zinc—are compared in Figure 2.2. The adsorption edges of copper and lead are similar, and adsorption increases sharply from pH 4 to 7.

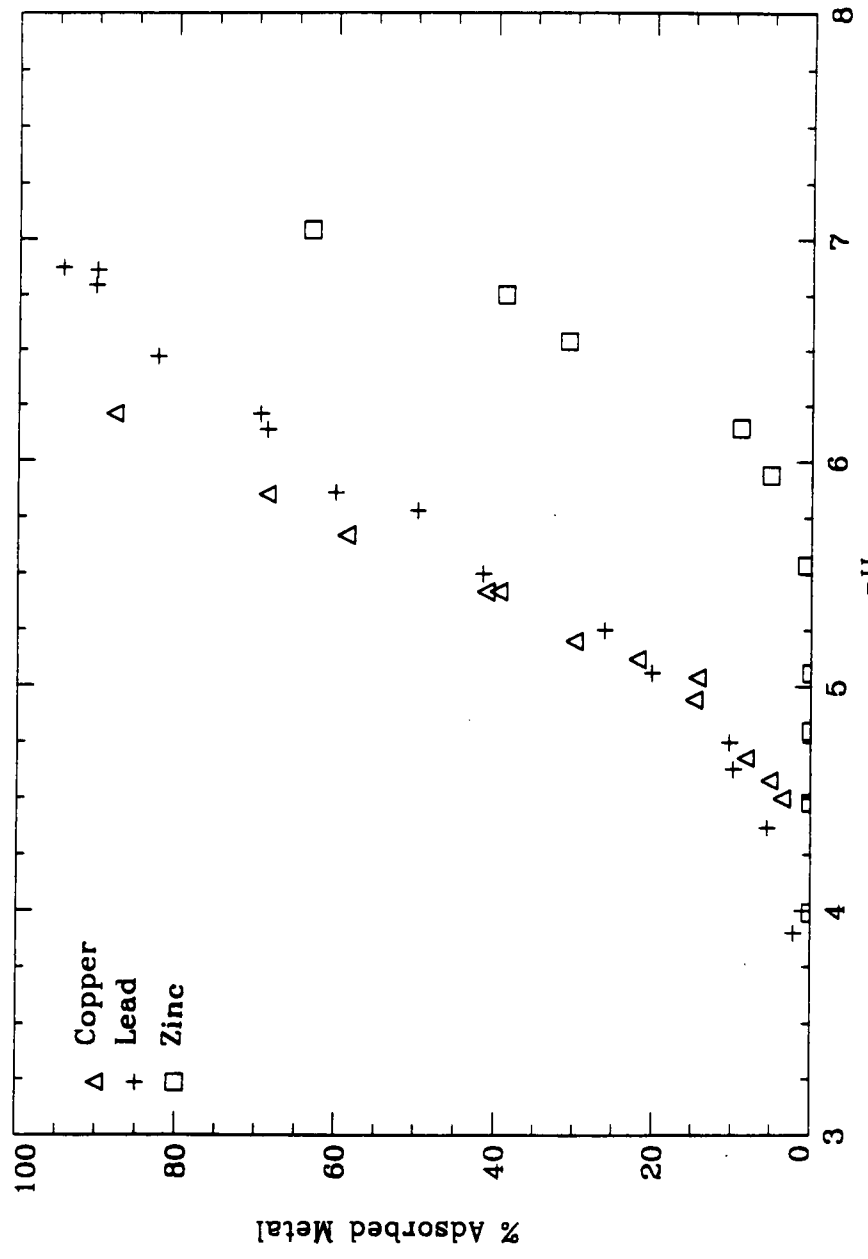


Figure 2.2 Adsorption of metals onto goethite: Comparison of the adsorption edges; ΣMe = 5 ppm; Surface area = 30 m^2/l; I = 0.1 M $NaNO_3$

However, zinc shows a different adsorption edge shifted by almost one and half pH units toward higher pH. The copper and lead adsorption curves reach almost 100%, whereas zinc barely reaches 60% adsorption by neutral pH. As a result, 40% of the zinc will remain available for transport in an aqueous environment around neutral pH, whereas copper and lead will be completely bound to goethite. Although copper is not adsorbed below pH 4, lead shows slight adsorption under these conditions. The relative position of the adsorption curves for these three metals is related to the ability of the metals to hydrolyze in aqueous solution. Fifty percent adsorption of copper, lead, and zinc (Figure 2.2) occurs at pH 5.5, 5.7, and 7.0, respectively, which shows the same trend as the first hydrolysis constant (pK_1) of these metals (Table 2.1).

Distribution coefficients

The distribution coefficient K_d for an aqueous system may be defined by the following equation:

$$K_d\,(ml/g) = [SO\text{-}Me]/[Me^{2+}] \quad (2.23)$$

where SO-Me is moles of metal adsorbed per gram of goethite, and Me^{2+} is equilibrium metal concentration in moles per milliliter and can be calculated as follow:

$$[SO\text{-}Me] = \%Me_{ad}Me_T/100[S] \quad (2.24)$$

$$[Me^{2+}] = 1000(100\text{-}\%Me_{ad})Me_T/100 \quad (2.25)$$

where $\%Me_{ad}$ is percentage of metal adsorbed by goethite, Me_T is the total metal added to the suspension, and S is goethite concentration in suspension in grams per liter. Substituting equations 2.24 and 2.25 in equation 2.23 will result in the following equation:

Table 2.1

Comparison of the properties of metals

Metal	$pK_1 (I = 0)$	pH_{50}
Copper[1]	7.7 to 8.0	5.5
Lead[2]	7.7	5.7
Zinc[3]	9.0	7.0

pK_1 = first hydrolysis constant.
pH_{50} = pH at which 50% of the metal is adsorbed.

[1]Allison (1991), Lindsay (1979), Stumm and Morgan (1981)
[2]Lindsay (1979)
[3]Lindsay (1979)

$$K_d\ (ml/g) = 1000\%Me_{ad}/[(100 - \%Me_{ad})S] \quad (2.26)$$

Equation 2.26 was used to calculate the distribution coefficients of several sets of data of copper, lead, and zinc.

Distribution coefficients became larger with higher pH depending on the pH, goethite surface area, and metal concentration but were independent of a tenfold decrease in the ionic strength of the medium. Lower K_d means little metal is bound to the goethite, which leaves most of the metal in the solution where it is available for geochemical reactions and may also be transported with aqueous solution. As a result, metal will be more mobile at low rather than neutral pH values.

Although an increase in surface area has a significant effect on the adsorption edge, it does not affect the magnitude of distribution coefficients. K_d by definition (equation 2.23), is the ratio of metal concentration in the solid phase to that in the solution at equilibrium. At constant pH and constant metal concentration, as the amount of goethite increases, metal distribution in solid and solution phase is adjusted so that the $[\%Me_{ad}/S]$ term in equation 2.26 remains constant. It follows that with an increase in goethite concentration at constant metal concentration, the total amount of metal adsorbed per gram of goethite decreases. The calculated amount of metal adsorbed per gram of goethite showed a systematic decrease with the increase in goethite surface area. As long as the total amount of goethite in the suspension remains in excess, the magnitude of distribution coefficient should not be affected by the decrease in goethite concentration. In this study a tenfold decrease in the amount of goethite did not effect the magnitude of K_d.

The distribution coefficients of the three metals—lead, copper, and zinc—are compared in Figure 2.3. The three data sets form straight

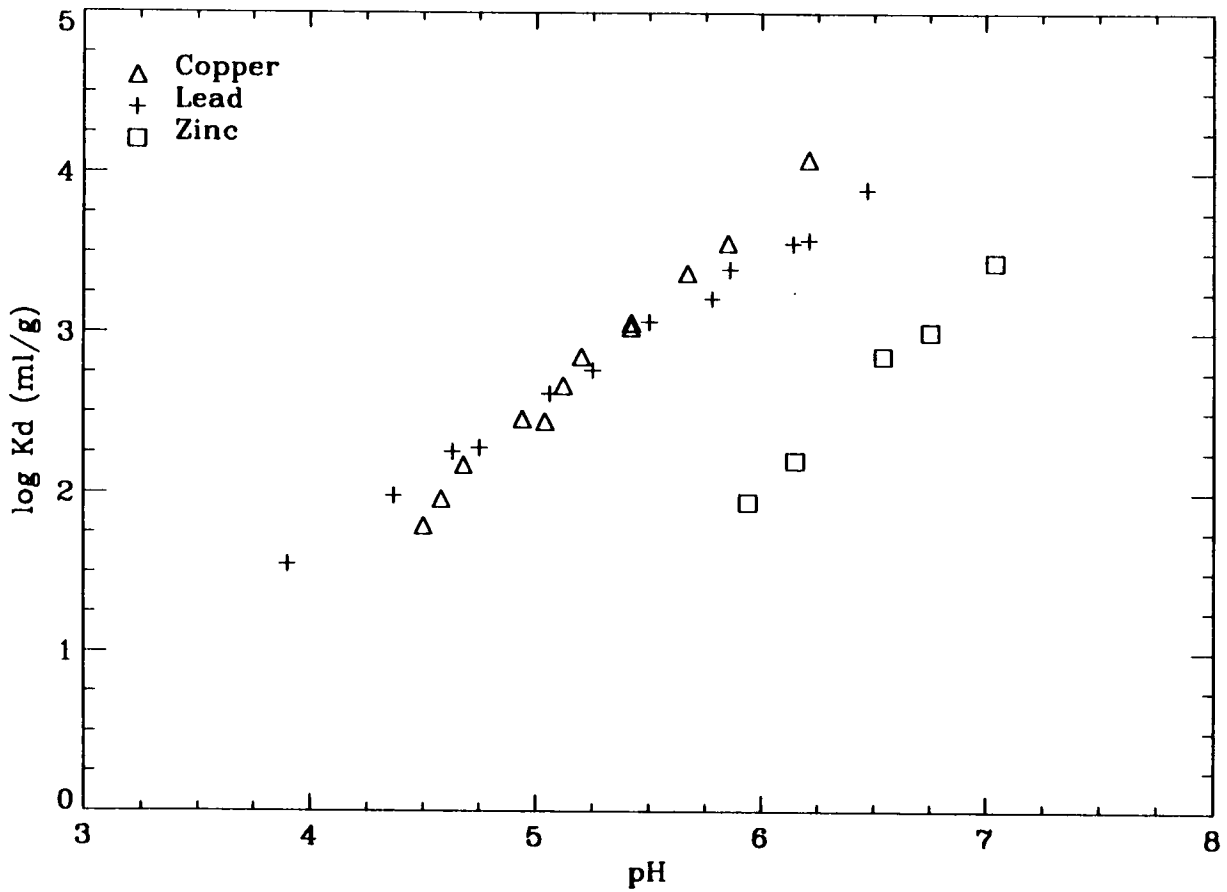


Figure 2.3 Adsorption of metals onto goethite: Comparison of the distribution coefficients; ΣMe = 5 ppm; Surface area = 30 m^2/l; I = 0.1 M $NaNO_3$

lines, with lines for lead and copper superimposed and the linear data set of zinc displaced to higher pH values. At pH 6, the distribution coefficients of copper and lead are 60 and 40 times larger than zinc, respectively. Comparing the value of K_d for the three metals (between pH 4 to 7) and their relative magnitude as a function of pH, it was concluded that under similar conditions, more zinc is available in solution than lead or copper. In comparison with copper or lead, a higher pH is required to remove the same percentage of zinc from the solution via adsorption onto goethite surface.

CHAPTER 3
MATERIALS AND METHODS

3.A INTRODUCTION

The purpose of this thesis is to reinterpret the data collected in an earlier study (Kooner 1992, 1993) for the adsorption of copper, lead, and zinc on goethite in terms of surface complexation modeling. The analytical methods, experimental techniques, materials used and experimental work performed are presented here as an aid to the reader in understanding how the data was collected.

3.B MATERIALS

Reagents

Ferric nitrate, GR crystal (> 98 percent), and cupric oxide, GR reagent (> 99 percent), were supplied by EM Science. Sodium nitrate, as crystal (99.6 percent), was supplied by J. T. Baker Inc. A 10 N certified sodium hydroxide solution and a 0.1 N certified nitric acid solution, supplied by Fisher Scientific, were used. Copper, lead, and zinc reference solution (certified 1000 ppm; suitable for atomic absorption spectroscopy) were also supplied by Fisher Scientific. Deionized water, prepared by a Milli-Q system, was used for all of the experiments. Aqueous solution of copper, lead and zinc were prepared by diluting the 1000 ppm reference solution.

Synthesis of Goethite

Goethite (α-FeOOH) was prepared by hydrolysis and aging of a ferric nitrate solution according to the method described by Atkinson et al. (1967) and later used by other researchers (Balistrieri and Murray 1982a; Hayes and et al. 1987; and Tripathi 1983). The method consists of the following steps:

- 50.53 g of ferric nitrate was dissolved in 225 ml of deionized water in polypropylene container.
- 2.5 M NaOH solution was added rapidly while stirring to bring the final pH between 11.8 and 12.0.
- The suspension was aged at 63^0 C in a water bath for four to five days.
- The precipitate was washed with deionized water by repeated centrifugation and decantation until the pH of the suspension was between 7.5 and 8.0 (close to the point of zero charge of goethite).

Following this procedure, goethite was stored as a suspension (not dried) in a polypropylene container. X-ray diffraction analysis of the synthesized goethite (as paste) showed evidence of the presence of goethite and no other iron oxide. Goethite used for experiments was always less than two weeks old.

3.C EXPERIMENTAL METHODS

Metal analysis

Metal concentrations in the solutions were analyzed by a Perkin Elmer Atomic Absorption Spectrophotometer (model 560). The spectrophotometer was calibrated by standard solutions for each

run. The error on the adsorption measurement for samples was estimated to be within ± 2 percent .

pH measurement

The pH of the suspension was measured with an Orion Research pH meter (EA 950) using a Fisher glass electrode. VWR Scientific buffers (pH 4, 7, and 10) were used for calibration.

Determination of Surface Area in Suspensions of Goethite

Aqueous goethite suspensions of known volumes were dried in an oven at 80^0 C for 4 h to evaporate moisture. The weight of the dry goethite was plotted against the volume of the aqueous goethite suspension to obtain a volume vs weight calibration curve. A calibration curve was obtained for each batch of goethite. Balistrieri and Murray (1982a), Hayes et al. (1987), and Tripathi (1983) found the specific surface area of goethite synthesized in the same way to be 51.8, 52, and 50.0 m^2/g, respectively. Based on their work, a specific surface area of 50 m^2/g was used for further calculations. The surface area of goethite in the adsorption experiment was calculated from the volume vs weight calibration curve and the specific surface area of 50 m^2/g.

Adsorption procedure

A known amount of goethite suspension was added to a polypropylene bottle (125 ml). The ionic strength was adjusted to the desired value by adding a known amount of 0.25 M $NaNO_3$. The required amount of 100 ppm metal solution was added to adjust the copper concentration in the bottle to the desired level. The total volume of the suspension was made to 100 ml by adding deionized water. The pH was adjusted by the addition of 0.1 M NaOH or 0.1 M HNO_3. The amount of sodium hydroxide or nitric acid used did not

significantly change the ionic strength of the suspension. The suspension was shaken in a water bath at 25.0° C for a predetermined length of time. The final pH of the suspension was measured, after which the suspension was centrifuged and decanted and the supernatant transferred to another bottle. The pH of the supernatant was immediately adjusted to approximately 3 by adding nitric acid to prevent loss of copper to the container wall. A standard solution (pH ~ 3) containing no goethite was prepared in the same way. The total volume of the standard solution was also adjusted to 100 ml. This solution was used to calibrate the atomic absorption spectrophotometer. A new standard solution was prepared for each series of measurements.

Adsorption of Metal on Container Walls

Metal adsorption on container walls (polypropylene) was investigated for aqueous solutions at the ionic strength of 0.1 M $NaNO_3$. The suspensions were prepared as described earlier, except that no goethite was added; the only adsorbent was the container surface. No metal loss from adsorption on container walls was detected within analytical precision.

Calculation of Percent Metal(II) Adsorbed onto Goethite

Total metal (Me_{tl}) present in the experimental system is distributed, within experimental error, in three reservoirs: metal in solution (Me_{aq}), metal adsorbed on goethite (Me_{ad}), and metal lost as a result of adsorption on container walls (Me_{cn}). Because loss of metal on the container walls (me_{cn}) was found to be negligible, metal adsorbed onto goethite can be calculated as

$$Me_{ad} = Me_{tl} - Me_{aq}$$
$$\%\, Me_{ad} = 100 Me_{ad}/Me_{tl}$$

Establishing the Time Required for Equilibration

To determine the time required to attain equilibrium, a large number (~30) of adsorption experiments were conducted at reaction times ranging from 30 min to 30 h, with [Cu] = 5.0 ppm (7.87×10^{-5} M) and goethite surface area = 30 m^2/l. The results are given in Appendix A.1 and are plotted in Figure 3.1. The adsorption process was fast, and equilibrium was established within 1 h. There are several reports in the literature (Balistrieri and Murray 1982a; Forbes et al. 1976; and Hayes and Leckie 1987) that show that the equilibrium time for adsorption reaction is a few hours. An equilibration time of 16 to 20 h was used for all subsequent experiments to ensure equilibrium and for operational convenience.

Reversibility

The following experiments were designed to study the reversibility of the adsorption reaction at a 5.0 ppm (7.87×10^{-5} M) copper concentration. The results of two duplicate sets of experiments are shown in Appendix A.2 and are plotted in Figure 3.2. Points in set A represent overnight adsorption equilibrium results for a 5.0 ppm (7.87×10^{-5} M) copper concentration within a pH range of 4-6. The suspensions in the set B (pH range of 4-6), prepared along with set A, were kept for overnight shaking but, unlike set A, were not removed and analyzed for copper adsorption. Instead, the pH of suspensions of set B were readjusted by adding 0.1 M NaOH or 0.1 M HNO_3. Suspensions with a pH of 4-5 were readjusted to a pH of 5-6, and suspensions with a pH of 5-6 were readjusted to a pH of 4-5. Set B was kept for shaking for another 24 h and was analyzed for copper adsorption. The results of both sets of experiments, shown in Figure 3.2, confirms that the adsorption of copper onto goethite is reversible. Based on the copper results, the adsorption of lead and zinc onto goethite was also assumed to be reversible.

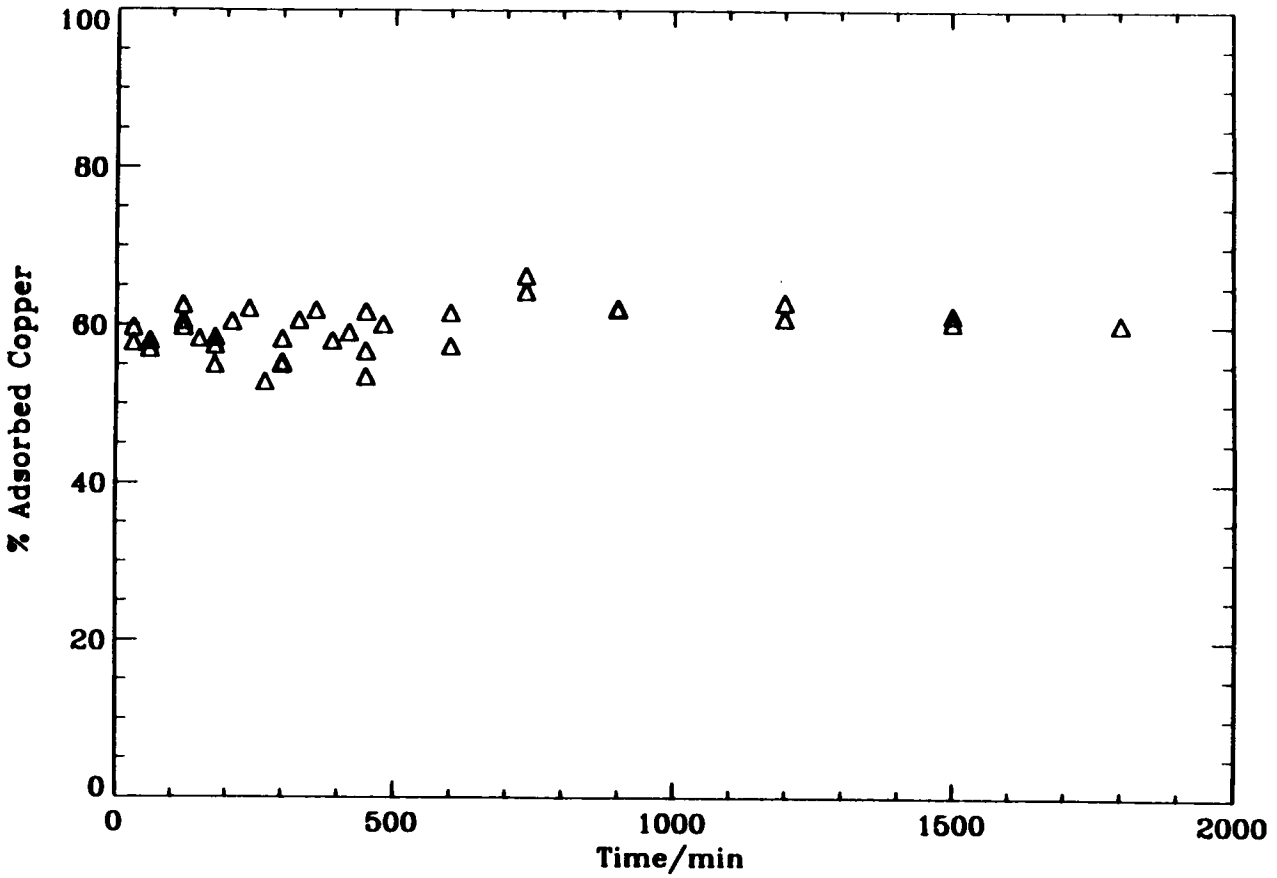


Figure 3.1 Adsorption (Kinetics) Experiments at pH 5.8 (corrected for pH and the mass of goethite)
ΣCu = 5.0 ppm (7.87×10^{-5} M); Surface area = 30 m^2/l; I = 0.1 M $NaNO_3$

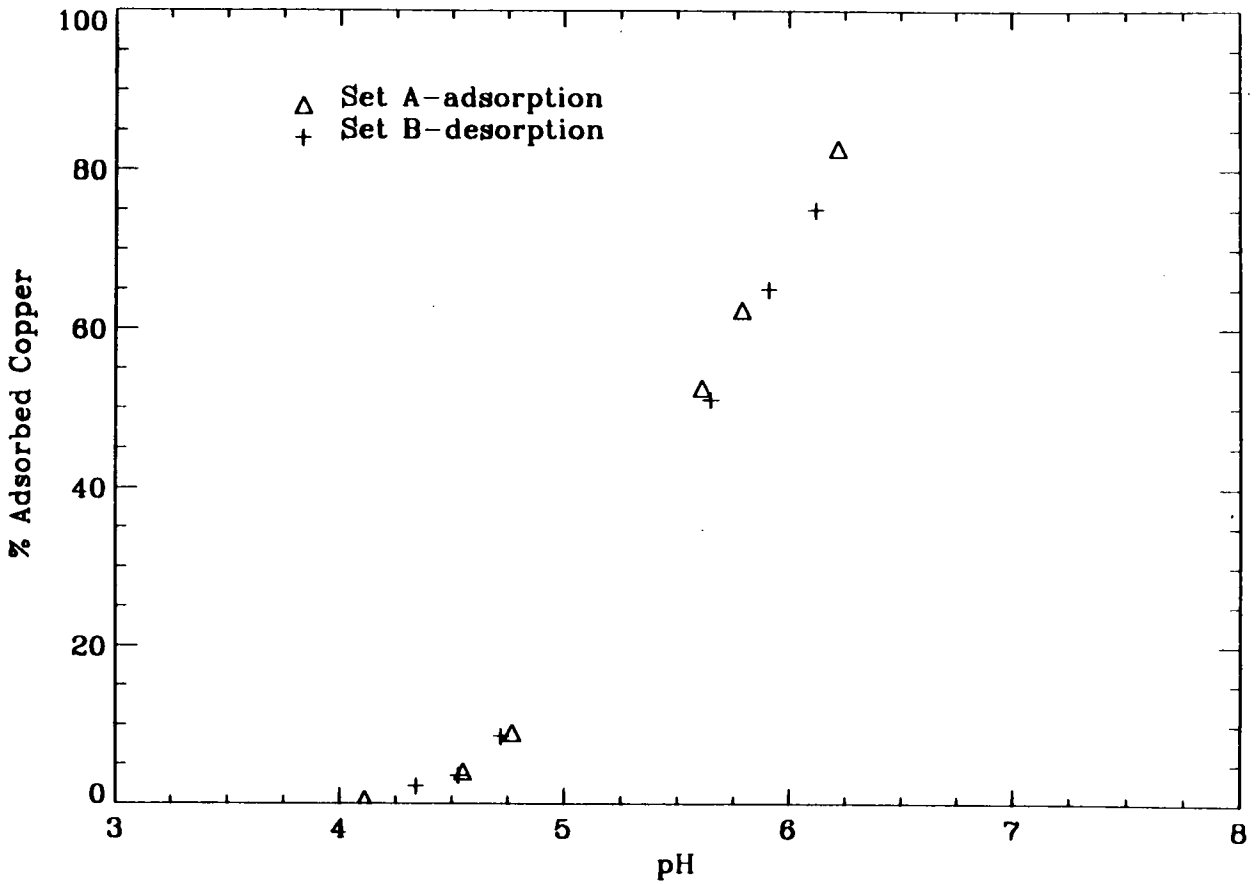


Figure 3.2. Reversibility of copper adsorption onto goethite ΣCu = 5.0 ppm (7.87 x 10^{-5} M); surface area = 30 m^2/l; I = 0.1 M $NaNO_3$

Reproducibility

Figure 3.3 presents (data is shown in Appendix A.2) three replicate sets of adsorption experiments at [Cu] = 0.5 ppm (7.87 X 10^{-6} M) and surface area = 30 m^2/l to demonstrate the consistency of the experimental procedure. Two sets of experiments utilized identical batches of reagents and goethite but were obtained on different days, whereas the third set utilized a different batch of goethite. The proximity of the three data sets indicates excellent reproducibility. Duplicate adsorption experiments for lead were also performed at two concentrations and a goethite surface area of 30 m^2/L. The experimental results given in Appendix A.3 are presented in Figure 3.4. The total lead concentration in Batch A and Batch B was 2.0 ppm (9.64 x 10^{-6} M), whereas Batch C and Batch D had 15.0 ppm (7.26 x 10^{-5} M) of lead. A different batch of goethite was used in each experiment. Here again like copper, the proximity between the two sets indicates excellent reproducibility. The adsorption results at 5.0 ppm of lead were also in excellent agreement with that of Balistrieri and Murray (1982a), and Forbes et al. (1976) whose experimental conditions were similar. The range of experimental variables for the adsorption isotherms is shown in Table 3.1

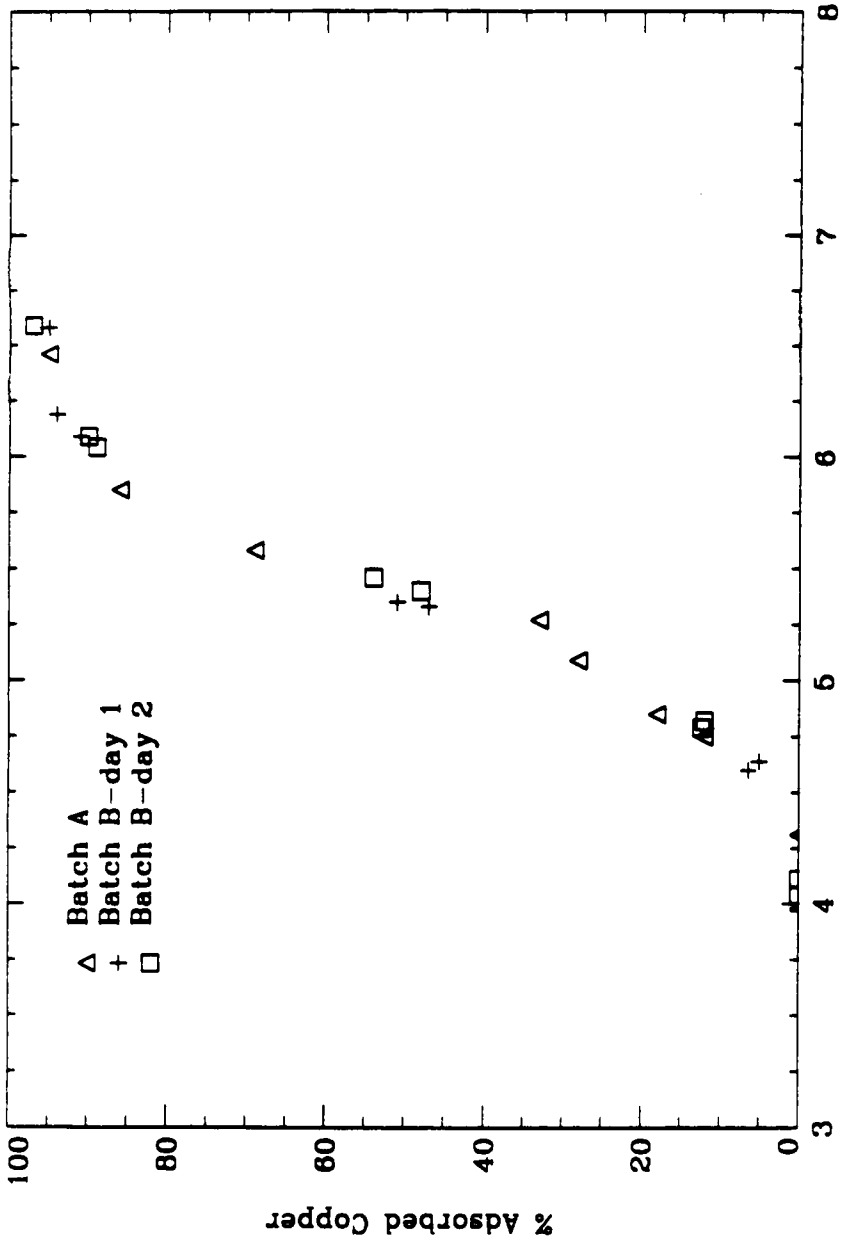


Figure 3.3. Reproducibility of copper adsorption onto goethite
ΣCu = 0.5 ppm (7.87×10^{-6} M); surface area = 30 m^2/l; I = 0.1 M $NaNO_3$

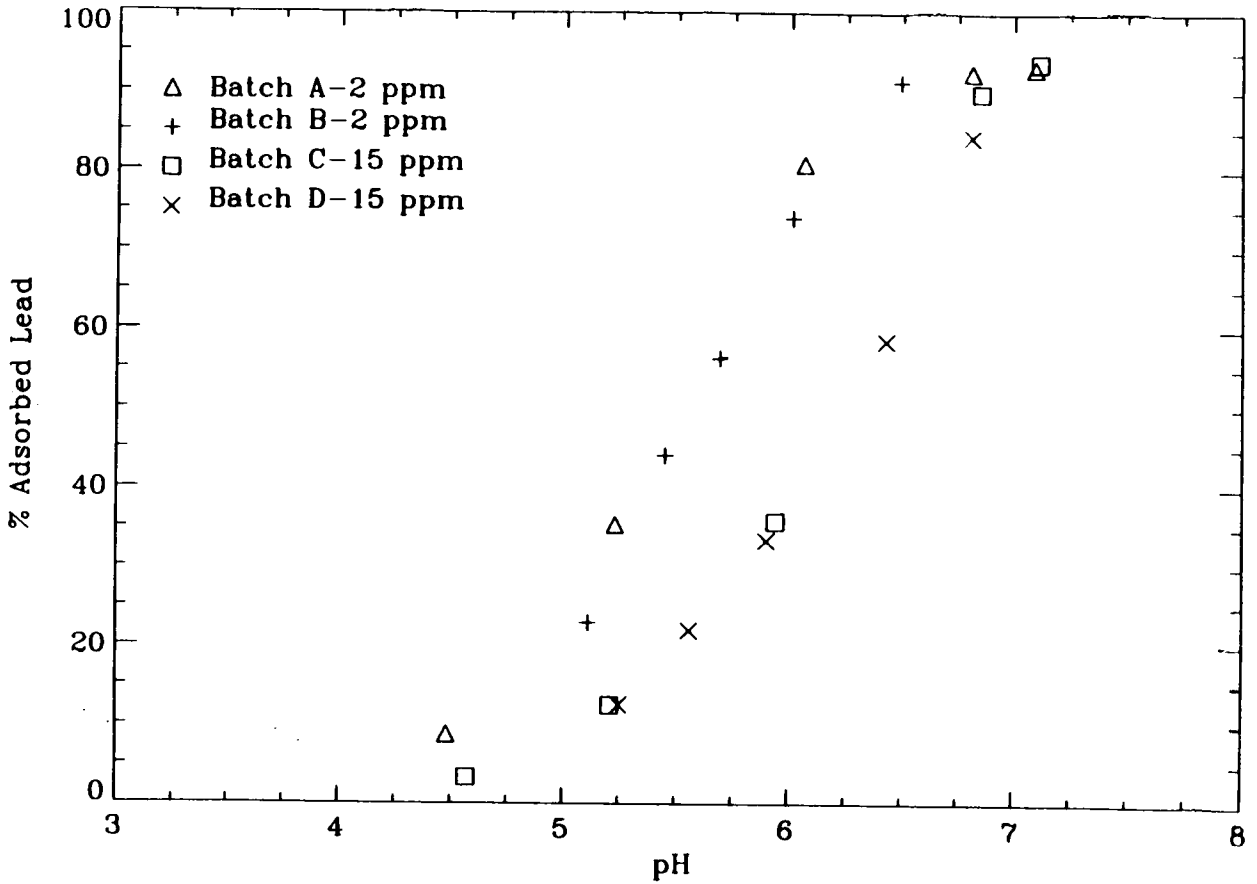


Figure 3.4. Reproducibility of lead adsorption onto goethite
Surface area = 30 m^2/l; I = 0.1 M $NaNO_3$

Table 3.1

Range of experimental variables

Metal	Variable	Range
Copper	Temperature	25° C
	pH	4 - 7
	Initial concentration	0.5 -10.0 ppm
	Ionic Strength	0.01 - 0.10 M $NaNO_3$
	Surface Area	11.4 - 280 m^2/l
Lead	Temperature	25° C
	pH	4 - 7
	Initial concentration	2.0 -15.0 ppm
	Ionic Strength	0.01 - 0.50 M $NaNO_3$
	Surface Area	12 - 120 m^2/l
Zinc	Temperature	25° C
	pH	4 - 7
	Initial concentration	5.0 ppm
	Ionic Strength	0.10 M $NaNO_3$
	Surface Area	30 m^2/l

CHAPTER 4
RESULTS AND DISCUSSION

4.A INTRODUCTION

Experimental data is modeled for various reasons by different investigators. Models can be used to test a hypothesis, replicate some experimental observations or predict the behavior of a system. Using a model to test a hypothesis might help in understanding the working of the system. In this case a surface complexation model is used to test whether the experimental adsorption results can be used to predict a surface reaction(s) and to estimate the equilibrium constant(s) of the reaction(s). The adsorption data used for modeling has been reported in Appendix B (kooner 1992, 1993).

4.B HYDROLYSIS OF METALS IN AQUEOUS SYSTEM

In aqueous solution, free metal ions are complexed with water giving rise to several hydroxometal complexes or species. The concentration of these complexes are strongly dependent on pH of the system and the concentration of the free metal. For modeling purposes it is important to know which aqueous species of any metal are present in the system so that some of the species (which are not present at certain pH and free metal concentration) can be eliminated from consideration. The purpose of this is to identify only those species which might be taking part in the surface reaction(s). Speciation of copper, lead, and zinc, as calculated from the thermodynamic data using MINEQL (Westall et al. 1976) between pH range 4 to 7 at total metal concentrations of 5 ppm in 0.1 M $NaNO_3$ are shown in Figures 4.1 - 4.3. The concentration of

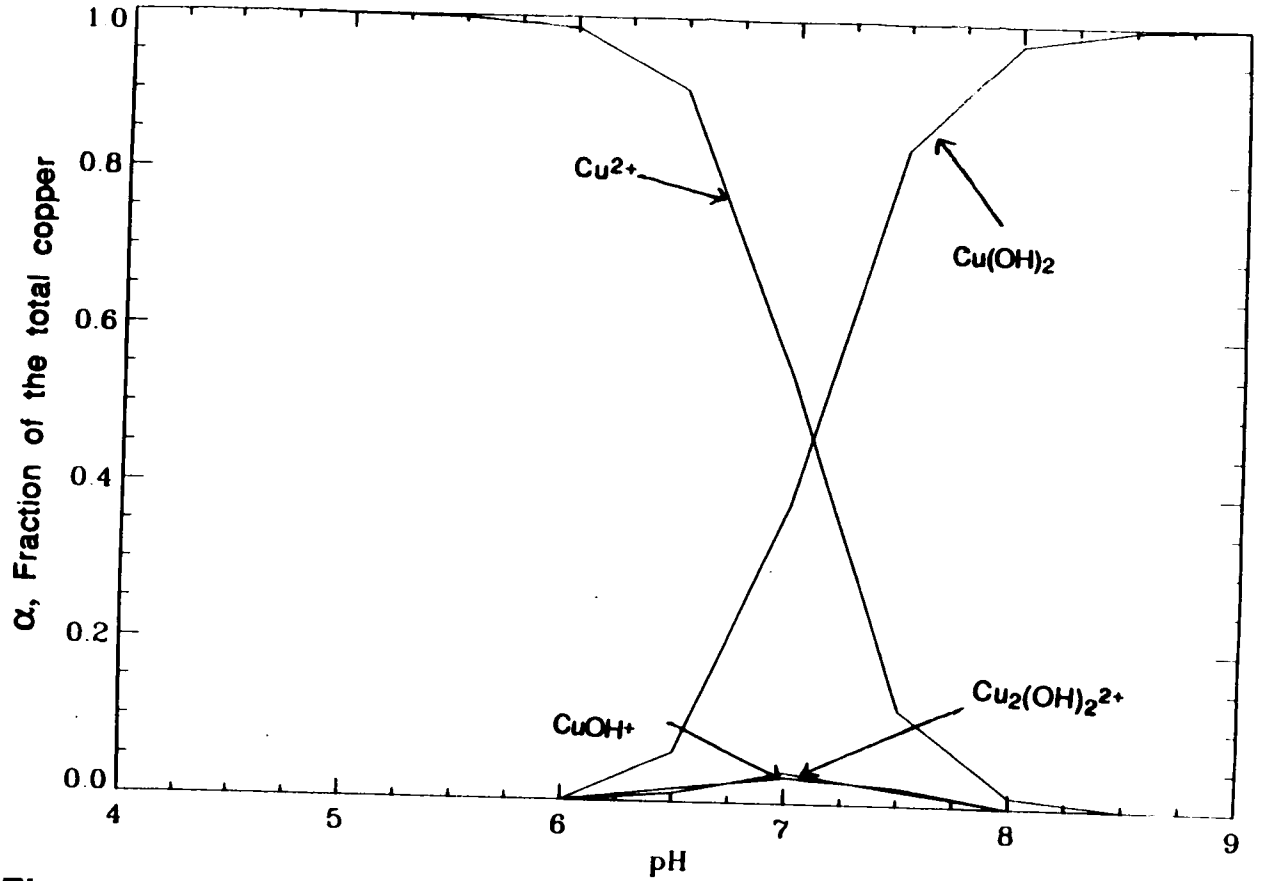


Figure 4.1 Species distribution of copper in an aqueous Cu(II) solution ΣCu = 5.0 ppm (7.87×10^{-5}M); I = 0.1 M $NaNO_3$

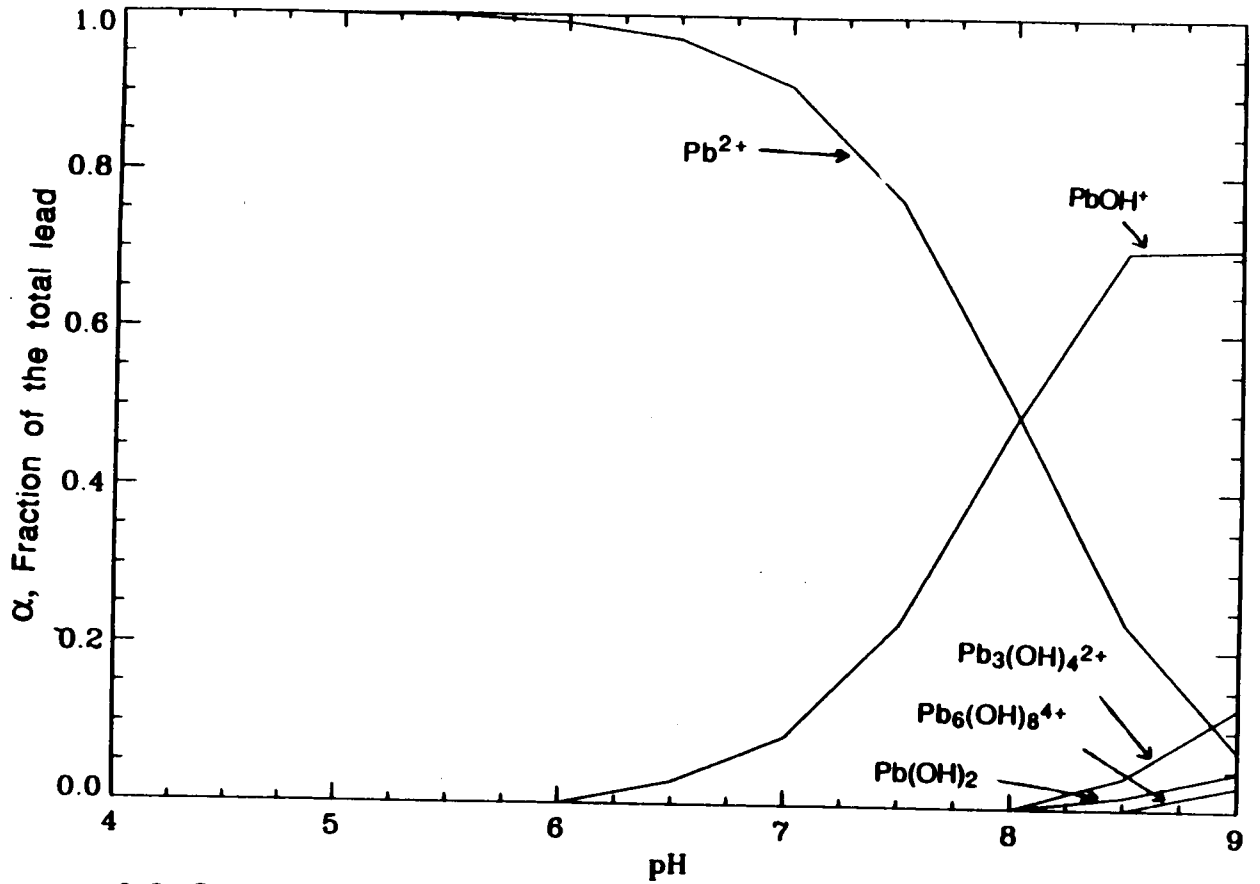


Figure 4.2 Species distribution of lead in an aqueous Pb(II) solution ΣPb = 5.0 ppm (2.41×10^{-5}M); I = 0.1 M $NaNO_3$

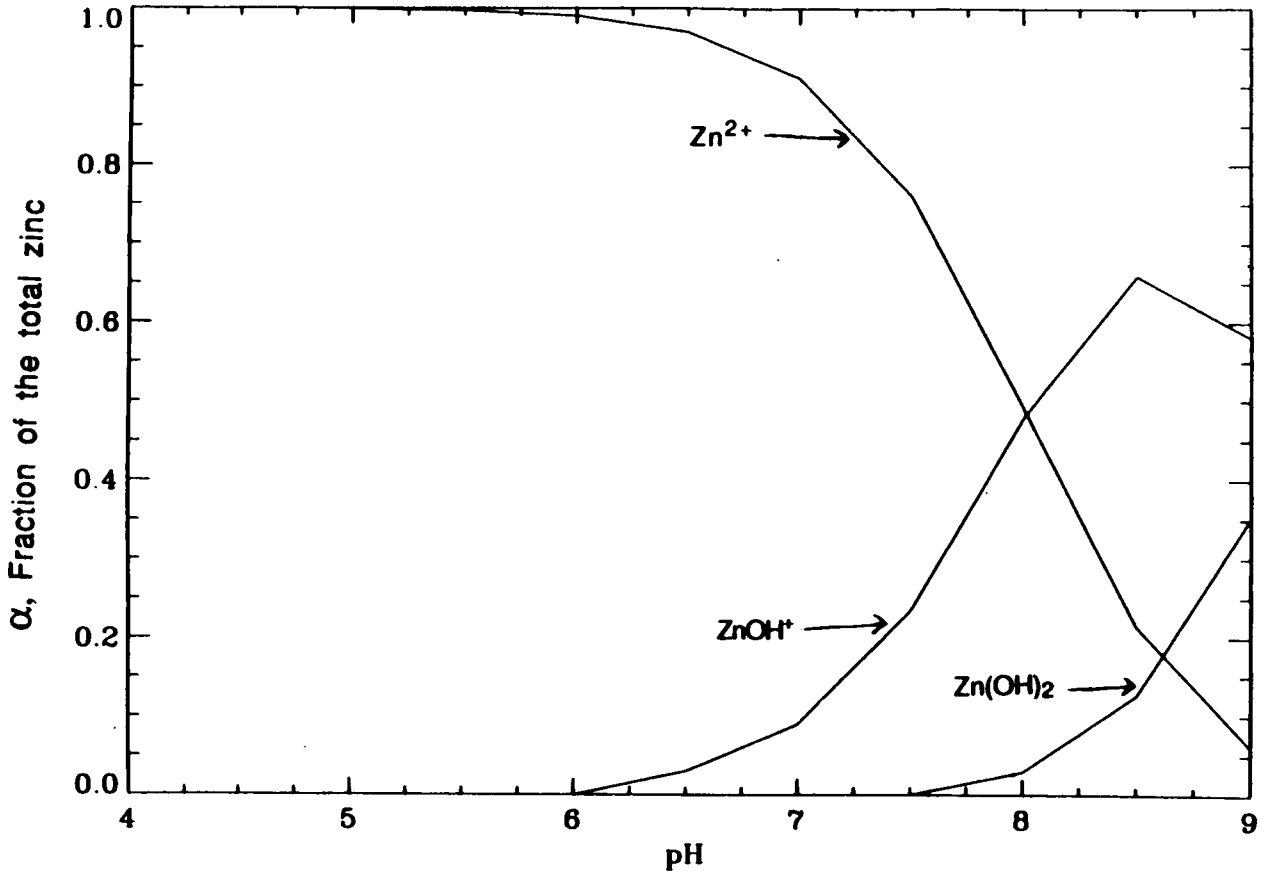


Figure 4.3 Species distribution of zinc in an aqueous Zn(II) solution ΣZn = 5.0 ppm (7.65×10^{-5}M); I = 0.1 M $NaNO_3$

these species is based on the thermodynamic equilibrium constants of the various hydrolysis reactions given in Table 4.1. It is evident from Figures 4.1-4.3 that in addition to Me^{2+} the other major species which might be able to take part in the surface reaction between pH 4 to 7 is $MeOH^{+}$. For modeling purposes these were the only two species which were considered for surface reactions.

4.C ADSORPTION MODELING

Modeling parameters

Goethite surface has been studied by many investigators and as a result all the parameters required for modeling purposes are well documented in the literature. Table 4.2 shows all the parameters used for the model.

Strategy for modeling

The goals in attempting to model the metal adsorption were threefold:

- to investigate whether the data could be described by electrical double layer theory
- to determine the equilibrium constants for metal adsorption if there is reasonable success in data modeling
- to determine the metal species which take part in the surface reaction.

Since only positively charged metal species were present in the solution in the pH range of interest (i.e. Me^{2+} and $MeOH^{+}$), only a negative surface was tried. The following three reactions were considered:

Table 4.1

Equilibrium constants for hydrolysis reactions

Reaction	log $K^{int}_{Me^{2+}}$	Reference	Ave. log $K^{int}_{Me^{2+}}$
$Cu^{2+} + H_2O = CuOH^+ + H^+$	-8.00	Allison (1991)	-7.90
	-7.70	Lindsay (1979)	
	-8	Stumm and Morgan (1981)	
$Cu^{2+} + 2H_2O = Cu(OH)_2 + 2H^+$	-13.68	Allison (1991)	-13.73
	-13.78	Lindsay(1979)	
$Cu^{2+} + 3H_2O = Cu(OH)_3^- + 3H^+$	-26.90	Allison (1991)	-26.65
	-26.75	Lindsay (1979)	
	-26.30	Stumm and Morgan (1981)	
$Cu^{2+} + 4H_2O = Cu(OH)_4^{2-} + 4H^+$	-39.60	Allison (1991)	-39.52
	-39.56	Lindsay (1979)	
	-39.40	Stumm and Morgan (1981)	
$2Cu^{2+} + 2H_2O = Cu_2(OH)_2^{2+} + 2H^+$	-10.36	Allison (1991)	-10.66
	-10.68	Lindsay(1979)	
	-10.95	Stumm and Morgan (1981)	

Table 4.1 (cont.)

Reaction	log $K^{int}_{Me^{2+}}$	Reference
$Pb^{2+} + H_2O = PbOH^+ + H^+$	-7.70	Lindsay (1979)
$Pb^{2+} + 2H_2O = Pb(OH)_2 + 2H^+$	-17.75	Lindsay (1979)
$Pb^{2+} + 3H_2O = Pb(OH)_3^- + 3H^+$	-28.09	Lindsay (1979)
$Pb^{2+} + 4H_2O = Pb(OH)_4^{2-} + 4H^+$	-39.49	Lindsay (1979)
$2Pb^{2+} + H_2O = Pb_2OH^{3+} + H^+$	-6.40	Lindsay (1979)
$3Pb^{2+} + 4H_2O = Pb_3(OH)_4^{2+} + 4H^+$	-23.89	Lindsay (1979)
$4Pb^{2+} + 4H_2O = Pb_4(OH)_4^{4+} + 4H^+$	-20.89	Lindsay (1979)
$6Pb^{2+} + 8H_2O = Pb_6(OH)_8^{4+} + 8H^+$	-43.58	Lindsay (1979)
$Zn^{2+} + H_2O = ZnOH^+ + H^+$	-9.00	Lindsay (1979)
$Zn^{2+} + 2H_2O = Zn(OH)_2 + 2H^+$	-16.80	Lindsay (1979)
$Zn^{2+} + 3H_2O = Zn(OH)_3^- + 3H^+$	-27.68	Lindsay (1979)
$Zn^{2+} + 4H_2O = Zn(OH)_4^{2-} + 4H^+$	-38.29	Lindsay (1979)

Table 4.2

Parameters for modeling*

Parameter	Value
Inner Helmholtz capacitance, C_1	1.1 F m^{-2}
Outer Helmholtz capacitance, C_2	0.2 F m^{-2}
Number of sites, N	7 sites/nm^2
Specific surface area, S	50 m^2 g^{-1}
Equilibrium constant, K^{int}_{a1}	5.80
Equilibrium constant, K^{int}_{a2}	.11.10
Equilibrium constant, $K^{int}_{Na^+}$	-8.8
Equilibrium constant, $K^{int}_{NO_3^-}$	7.7

* Hayes (1987)

$$SOH + Me^{2+} = SOMe^{+} + H^{+} \quad (4.1)$$

$$SOH + MeOH^{+} = SOMeOH + H^{+} \quad (4.2)$$

$$SOH + MeOH^{+} = SO^{-}\text{-}MeOH^{+} + H^{+} \quad (4.3)$$

Reactions 4.1 and 4.2 are inner-sphere complexes and 4.3 is an outer-sphere complex. For an inner-sphere complex, the metal is assigned to the 0 plane, making a stronger bond as compared to outer-sphere complex where metal is assigned to the β plane.

Modeling

The adsorption edge for copper at a concentration of 5 ppm and goethite surface area of 30 m^2/l was used for initial model calibration. Both reactions 4.1 and 4.2 were able to fit the adsorption data, but the fit for reaction 4.1 was almost 8 times better than the fit for reaction 4.2 as quantified by the overall variance. The overall variance is defined as the ratio of the sum of squares of the residuals divided by the degrees of freedom. Comparison of the model calculations with experimental data for both reactions are shown in Figures 4.4 - 4.5. Reaction 4.1 was able to fit the data for most of the pH range except in the lower range (pH 4-4.5), whereas, modeling using reaction 4.2 either underestimated or overestimated the data. As evident from Figure 4.1, most of the copper metal is presented as Cu^{2+} in the aqueous system. Therefore, it is not surprising that reaction using Cu^{2+} instead $CuOH^{+}$ was better suited to fit the data. The discrepancy between the model fit and the data in the lower pH range (4-4.5) of Figure 4.4 may be due to the fact that either a different reaction or a combination of reaction 4.1 with another reaction is taking place in this region. Some of the parameters used in modeling (e.g number of sites, and surface area) are best estimates and are assumed to be constant over the whole pH range. There is no study which confirms that surface area and number of sites on the adsorbing surface are independent of pH. Surface area is generally

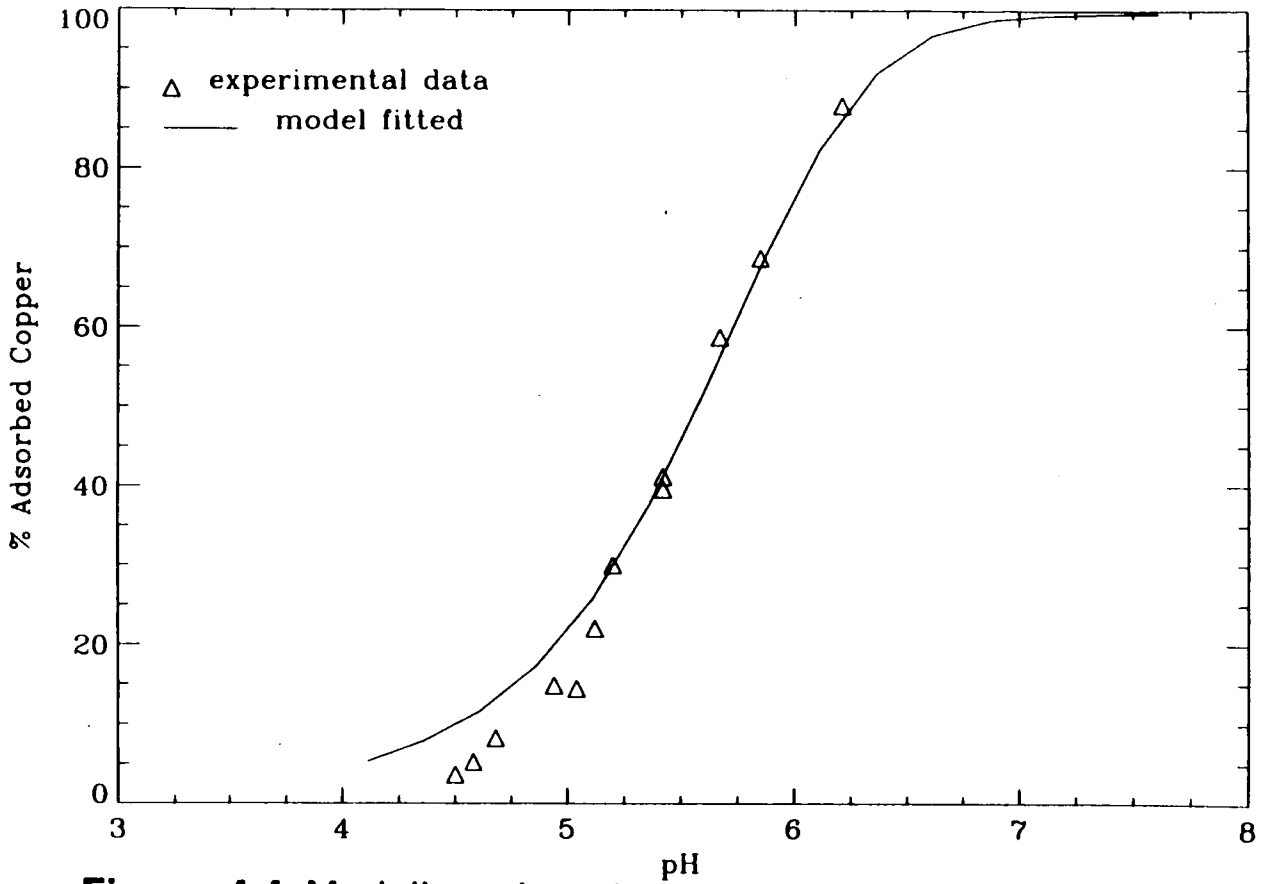


Figure 4.4 Modeling the adsorption of copper onto goethite
ΣCu = 5 ppm (7.87×10^{-5} M); Surface area = 30 m^2/l; I = 0.1 M $NaNO_3$

$$SOH + Cu^{2+} = SOCu^{+} + H^{+}$$

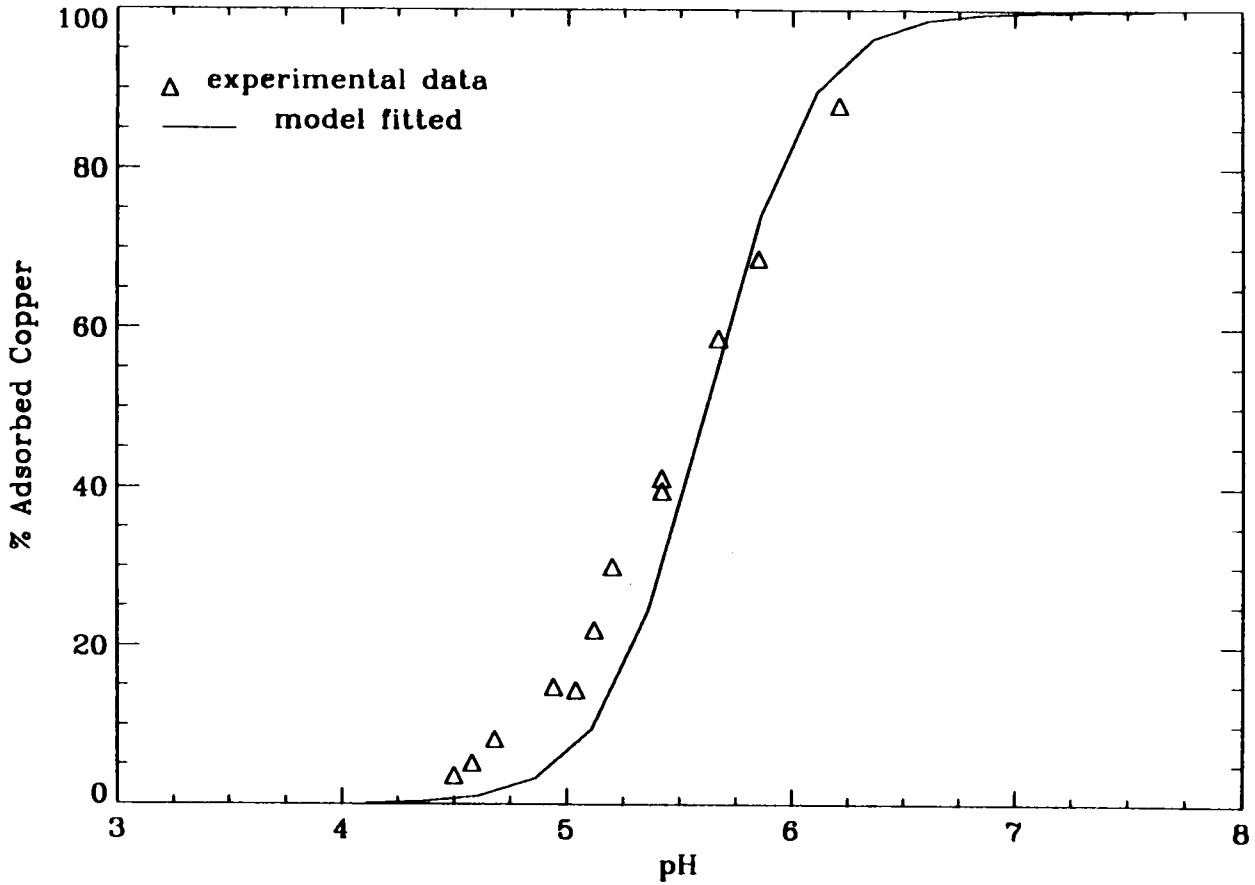


Figure 4.5 Modeling the adsorption of copper onto goethite
ΣCu = 5 ppm (7.87×10^{-5} M); Surface area = 30 m^2/l; I = 0.1 M $NaNO_3$

$$SOH + CuOH^+ = SOCuOH + H^+$$

measured around neutral pH and not in the lower pH range. It is possible that both or one of these parameters are pH dependent which might results in the discrepancy between the experimental and modeled results. EDL theory is really a surface complex activity coefficient theory, and short comings in the theory may result in deviations in the model. Reactions 4.3, depicting outer-sphere complex was also tried which resulted in a very poor fits (Fig. 4.6) showing that outer-sphere reaction is not suitable for this model. Therefore, reaction 4.1 was selected because it gave the best fit. Combination of either reaction 4.2 or 4.3 with reaction 4.1 did not improve the fit. Similar results were obtained for the adsorption data of lead and zinc with metal concentration of 5 ppm and goethite surface area of 30 m^2/l. Based on the above observations, only reaction 4.1 was considered for modeling all the remaining adsorption data. The results indicate that adsorption of all three metals are best modeled as an inner-sphere complex with goethite. Similar results have already been reported by Leckie and coworkers (Hayes and Leckie, 1987; and Hayes et al., 1988). The intrinsic equilibrium constants (i.e. $K^{int}_{Cu^{2+}}$, $K^{int}_{Pb^{2+}}$, and $K^{int}_{Zn^{2+}}$) for all three metal was found to be independent of ionic strength which is a further indication of relatively strong bonding affinities of copper, lead, and zinc, hence inner-sphere complex formation. If the metals were making a outer-sphere complex, then $K^{int}_{Me^{2+}}$ should have been ionic strength dependent (Hayes and Leckie 1987) and reaction 4.3 would be expected to fit the data better.

Each data set was modeled independently using reaction 4.1 and a intrinsic equilibrium constant was determined for each set. The intrinsic equilibrium constants determined by this method along with the standard deviation in the equilibrium constants are shown in Table 4.3. It is desirable to have a single value of the intrinsic equilibrium constant for each metal even at the cost of some additional errors in the equilibrium constant.

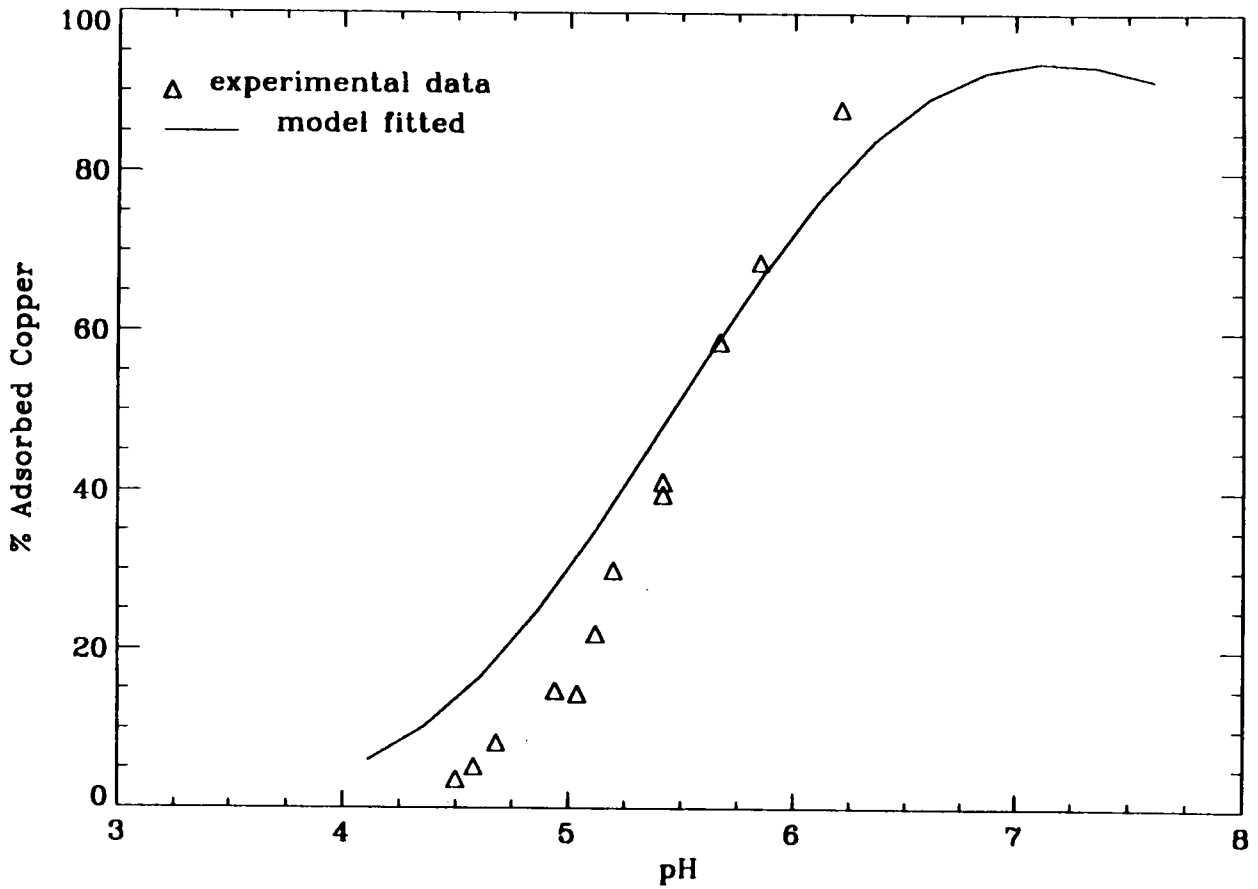


Figure 4.6 Modeling the adsorption of copper onto goethite
ΣCu = 5 ppm (7.87×10^{-5} M); Surface area = 30 m^2/l; I = 0.1 M $NaNO_3$

$$SOH + CuOH^+ = SO^-\text{-}CuOH^+ + H^+$$

Table 4.3

Equilibriun constants for reaction 4.1[a]

S. No.	[Metal](ppm)	[Goethite](m^2/l)	log $K^{int}_{Me^{2+}}$	$\sigma^{b}_{\log K^{int}_{Me^{2+}}}$
Copper				
1	0.5	30	1.598	0.00796
2	1	280	0.922	0.00879
3	5	30	2.876	0.01491
4	5	60	2.479	0.01273
5	5	145	2.059	0.01087
6	5	280	1.574	0.00898
7	5	30	2.289[c]	0.01579
8	10	30	2.563	0.02980
9	10	280	2.366	0.00932
Lead				
10	2	12	1.201	0.01516
11	2	30	0.922	0.01038

Table 4.3 (cont.)

S. No.	[Metal](ppm)	[Goethite](m^2/l)	log $K^{int}_{Me^{2+}}$	$\sigma^{b}_{\log K^{int}_{Me^{2+}}}$
12	5	30	1.215	0.00990
13	5	60	1.203	0.01417
14	5	120	1.217	0.01203
15	5	30	1.241[c]	0.01140
16	5	30	1.043[d]	0.02238
17	10	30	1.155	0.01256
18	15	30	1.515	0.01265
Zinc				
19	5	30	0.193	0.02576
20	5	30	0.491[c]	0.02713

[a] all the data is at 0.1 M $NaNO_3$ unless specified otherwise

[b] standard deviation on log K

[c] data at 0.01 M $NaNO_3$

[d] data at 0.50 M $NaNO_3$

Following Dzombak and Morel (1990), the best estimate of intrinsic equilibrium constant was determined by a weighted average of optimum log $K^{int}_{Me^{2+}}$ values. The weighing factor used is

$$W_i = (1/\sigma_{\log K^{int}_{Me^{2+}}})_i / \Sigma(1/\sigma_{\log K^{int}_{Me^{2+}}})_i \qquad (4.4)$$

where $\sigma_{\log K^{int}_{Me^{2+}}}$ is the estimated standard deviation calculated by the FITEQL for the ith data set. The best estimate for log $K^{int}_{Me^{2+}}$ is given by

$$\log K^{int}_{Me^{2+}} = \Sigma(W_i(\log K^{int}_{Me^{2+}})_i) \qquad (4.5)$$

The values of weighted-average log $K^{int}_{Me^{2+}}$ calculated by this method are 1.95, 1.19, and 0.34 for adsorption of copper, lead, and zinc respectively. Experimental data is compared with the model output using the individual log $K^{int}_{Me^{2+}}$ (Table 4.3) for that data set and the weighted-average log $K^{int}_{Me^{2+}}$ for each metal in Figures C.1-C.20 (appendix C). The solid line in each graph represents the model output using the optimum log $K^{int}_{Me^{2+}}$ for that data set, whereas the broken line represents the model output using the weighted-average log $K^{int}_{Me^{2+}}$. This enables easy evaluation of the quality of optimum fits and the general validity of the best estimate log $K^{int}_{Me^{2+}}$ values. As can be seen from the graphs, the model gave a reasonable fit to the experimental data except in some cases where model output is not as good (Figs. C.2, C.3, C.12, and C.13). The possible reason for this discrepancy may be the fact that a different reaction or a combination of some reactions are taking place and are not accounted for in the model used.

The sensitivity of the model to a change in one of the experimental conditions is illustrated in figures 4.7-4.9. In each case the model output shows a similar trend as demonstrated by the experimental

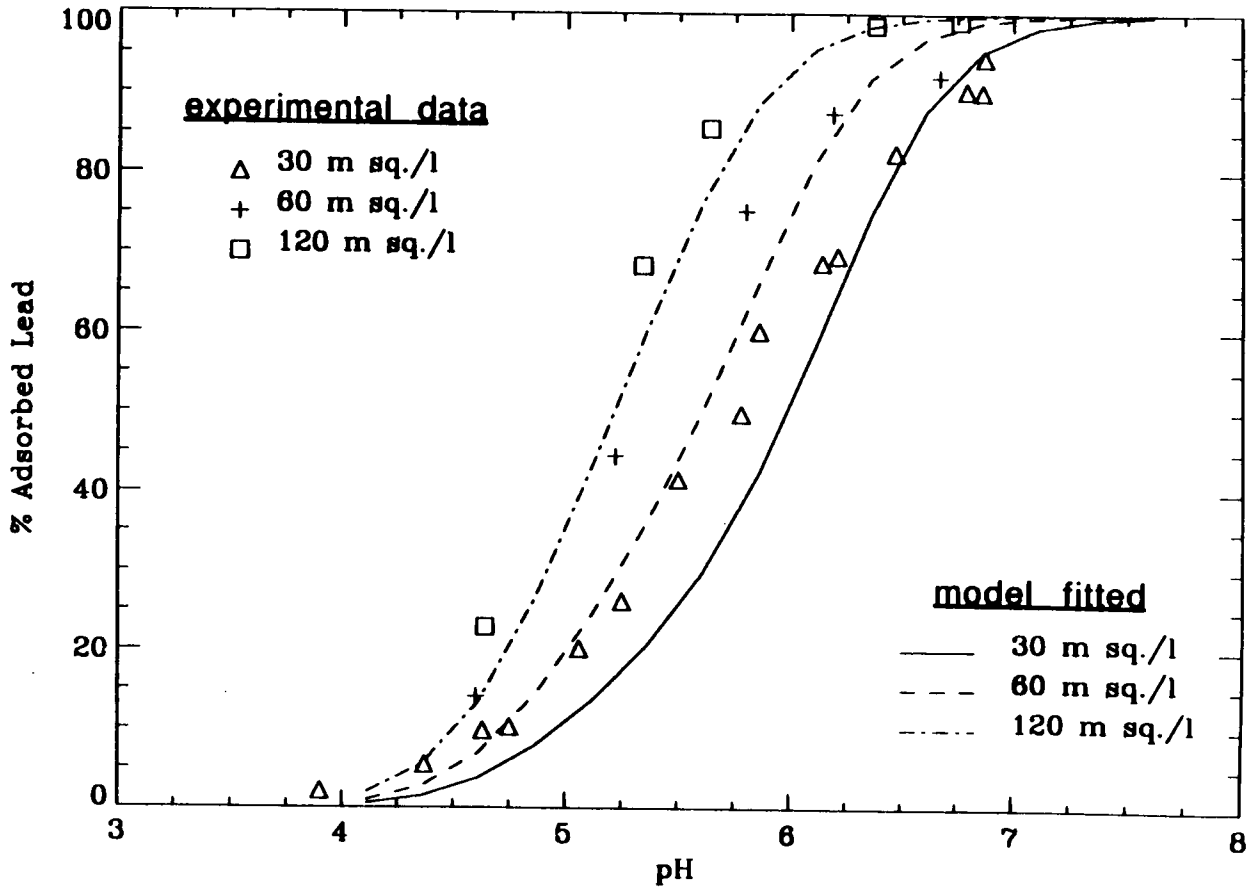


Figure 4.7 Modeling the adsorption of lead onto goethite: Effect of surface area; ΣPb = 5.0 ppm (2.41×10^{-5} M); I = 0.1 M $NaNO_3$

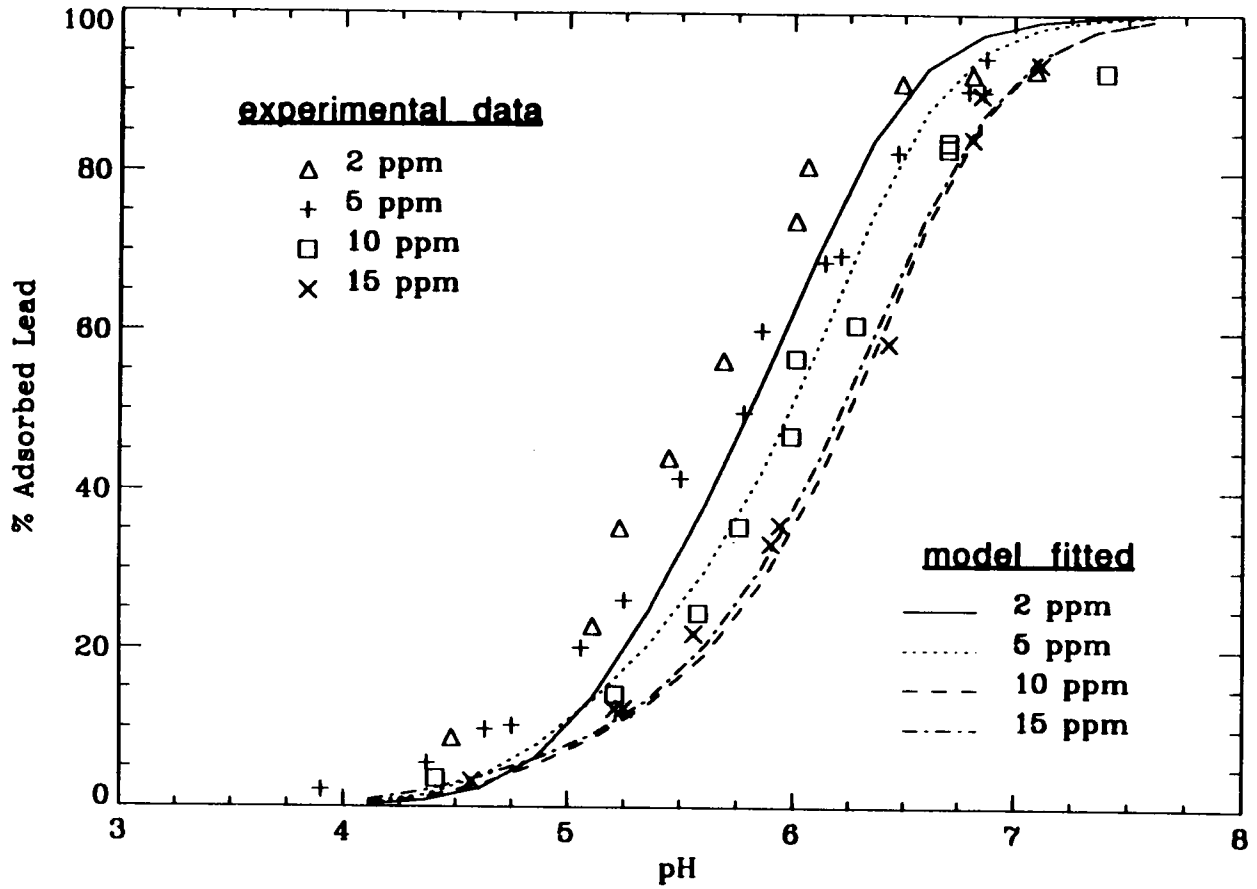


Figure 4.8 Modeling the adsorption of lead onto goethite: Effect of lead concentration; Surface area = 30 m^2/l; I = 0.1 M $NaNO_3$

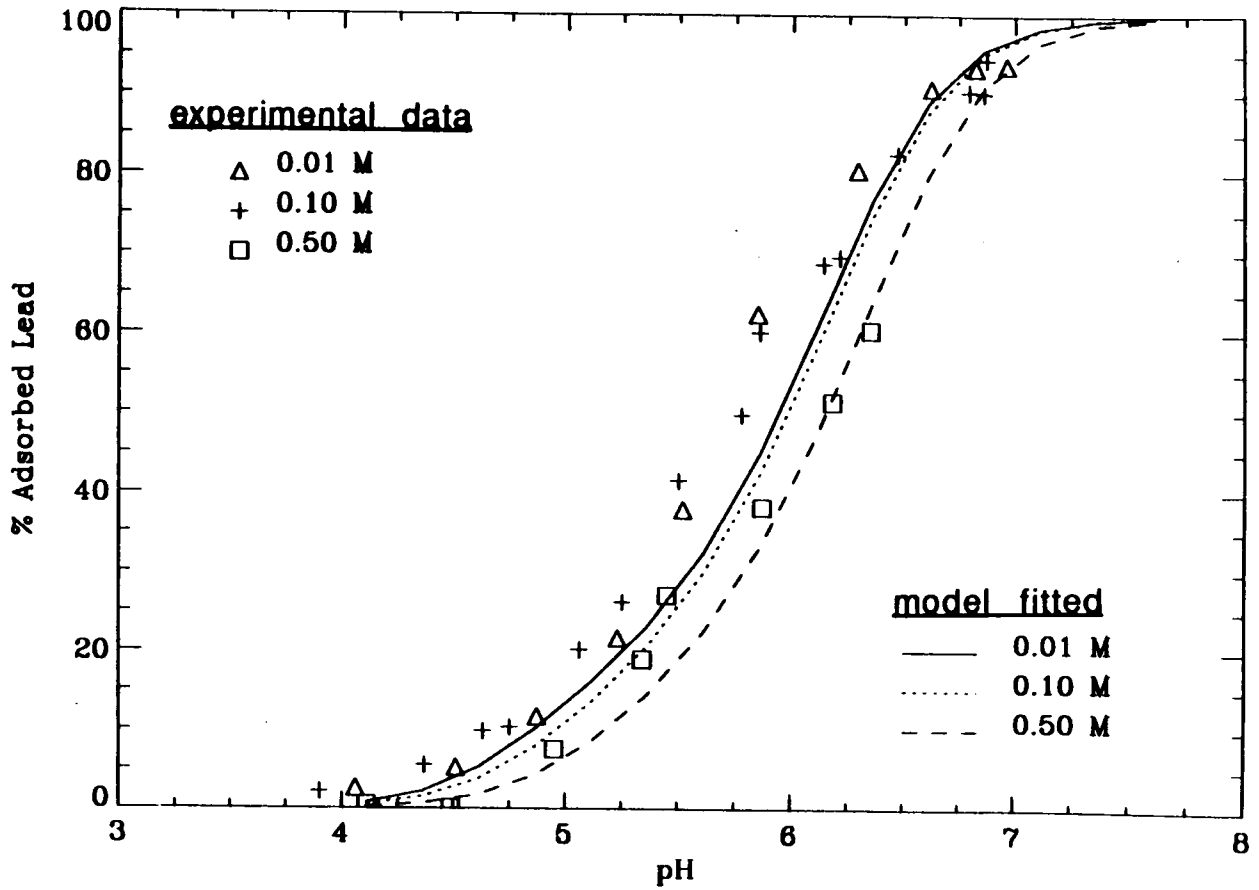


Figure 4.9 Modeling the adsorption of lead onto goethite: Effect of ionic strength; ΣPb = 5.0 ppm (2.41×10^{-5} M); Surface area = 30 m^2/l

data. Figure 4.7 shows the effect of an increase in goethite surface area on lead adsorption. The experimental data show that the adsorption edge has moved to lower pH with the increase in surface area. The change in the adsorption edge is almost 1 pH unit with a surface area increase from 30 m^2/l to 120 m^2/l. The model was able to predict the change in the adsorption edge to lower pH as well as the magnitude of the change (i.e. 1 pH unit).

The effect of lead concentration on the adsorption edge is shown in Figure 4.8. As the concentration of lead is increased from 2 ppm to 15 ppm, the adsorption edge has moved toward higher pH. The model was able to show a similar trend except for 15 ppm lead concentration where model output does not show any change in the adsorption edge from that at 10 ppm lead.

As discussed earlier, intrinsic equilibrium constant of the inner-sphere complexes should be independent of ionic strength. This is shown in Figure 4.9 where ionic strength is changed from 0.01 M to 0.5 M and there is virtually no change in the model output for 0.01 M and 0.1 M data but the data for 0.5 M show slight dependence on the ionic strength. The activity of the hydrogen is estimated using Davies equation which is true only at low concentration and may not hold at 0.5 M $NaNO_3$. Therefore, the model output at 0.5 M concentration may show greater deviations from observed results when compared to the model output at lower concentrations.

As pointed out in Chapter 1, it is important to be able to make predictions based on the experimental data and extrapolate the results to different experimental conditions. One of the tools which provides a quantitative basis for comparing related classes of reactions is the linear free-energy relationships (LFERs) where log $K^{int}_{Me^{2+}}$ of metal adsorption is plotted against the log of the first hydrolysis constant of the metal. The results of this study

are presented in Figure 4.10 along with some literature values. The plot shows a positive correlation between the hydrolysis constant of the metal and equilibrium constant of the adsorption reaction except in the case of lead adsorption which deviates from the relationship. A similar relationship has been observed by Dzombak and Morel (1990) for the adsorption of several metals onto hydrous ferric oxide. This relationship can be used to obtain a first estimate of the equilibrium constant of metal adsorption based on its hydrolysis constant if no adsorption data is available.

Assuming the model is correct, it can be concluded from the modeling results that only Me^{2+} and not any other species is taking part in the adsorption reaction. However, it should be cautioned that other SCMs may lead to different conclusions in that regard. The K_d approach cannot be used to make such predictions because it is not dependent upon the species taking part in the adsorption reaction. Moreover, unlike K_d, the intrinsic equilibrium constant is independent of ionic strength and pH, and can be used to make predictions outside the experimental conditions for which the data are taken. By using the LFER plot, the first hydrolysis constant for a selected metal can be used to obtain an estimate of log $K^{int}_{Me^{2+}}$ without obtaining any adsorption isotherms.

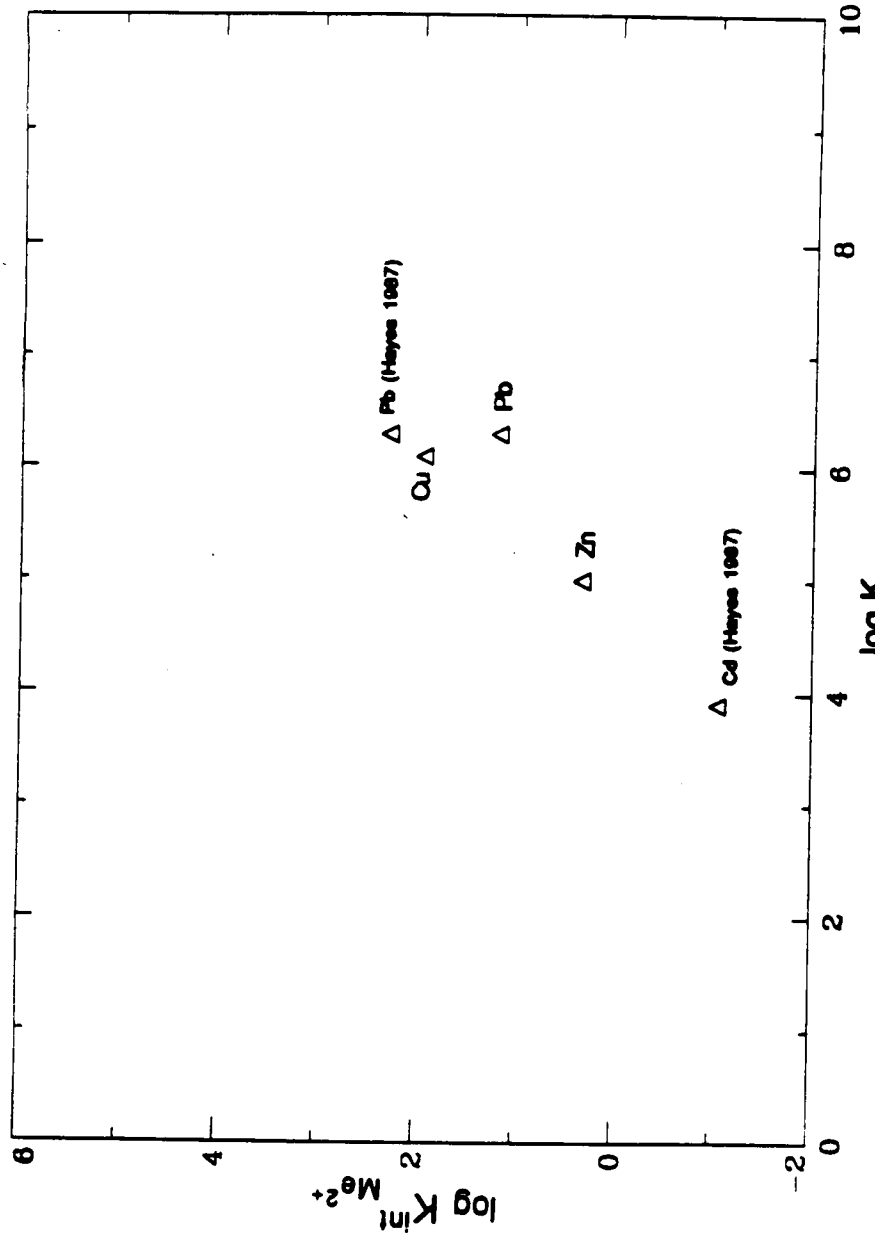


Figure 4.10 Correlation of log $K^{int}_{Me^{2+}}$ with first hydrolysis constants for divalent metals

CHAPTER 5
CONCLUSIONS

5.A SUMMARY

Transport of metals in aqueous solutions is an important aspect of many geological and environmental processes. Transport of metals is facilitated by a decrease in aqueous pH and by the adsorption of metals onto suspended matter. In contrast, an increase in pH and/or adsorption of metals onto surface of fixed materials such as rock, soil, and sediments, retards the transport of metals. Adsorption of metals by solid surfaces is an important phenomenon in retarding metal migration in the subsurface.

Empirical models based on distribution coefficients (K_d) although simple to use, do not account for ongoing chemical processes responsible for partitioning of metals between solid and solution phases. In contrast to the K_d approach, chemical models based on the chemical and physical interactions between metal and the adsorbent can be used to estimate the intrinsic equilibrium constant for adsorption reactions and to identify the metal species taking part in the reaction.

In this research, adsorption of divalent metals (copper, lead, and zinc) onto synthetic goethite has been studied at room temperature as a function of pH, total dissolved metal, ionic strength, and adsorbate/adsorbent ratio. A surface complexation model based on electrical double layer theory was successful in describing the adsorption behavior under various laboratory conditions. The intrinsic equilibrium constant for the adsorption of metals onto goethite were estimated under different experimental conditions. The results have been used to obtain a weighted-average intrinsic

equilibrium constant for each metal. The weighted-average constants were shown to be related to the first hydrolysis constant of the metal, and as a result, the hydrolysis constant for other metals can be helpful in predicting their behavior without obtaining experimental adsorption data.

5.B RECOMMENDATIONS FOR FUTURE RESEARCH

Several areas for further research have been identified and are discussed in this section:

The present research should be extended to include other metals especially those which are harmful to human health and are found in potable water sources.

It is also recommended that metal adsorption be studied at very low (< 1 ppm) total metal concentration to see if the reaction used in this study can be used to describe adsorption under such conditions. EPA Primary Drinking Water Standards (Table 5.1) limits the presence of several metals in drinking water to only a few ppb. Therefore, it is important to get more information about these metals under low concentration conditions.

Co-contaminant associations of inorganic and organic waste can significantly alter the adsorption and transport of metals relative to the independent, singular adsorption processes of each metal. Because many waters will have mixtures of inorganic and organic contaminants, studies which investigate the kinetics and thermodynamic controls on the release and transport of co-contaminants are needed. The effect of systematic increases in concentration of important contaminants (e.g. EDTA) on the adsorption processes of metals is an important area which has not been explored, and deserves attention.

Table 5.1

EPA Primary Drinking Water Standards

Metal	Limit (ppm)
Arsenic	0.05
Barium	1.0
Cadmium	0.005
Copper	1.3
Chromium	0.1
Lead	0.015
Mercury	0.002
Selenium	0.05
Silver	0.05

Despite the recognition that adsorbents in natural systems are complex mixtures of a variety of minerals and organic materials, nearly all experimental studies to date have focused on pure single-mineral adsorbents due to the ease with which such systems can be characterized, monitored, and interpreted. Knowledge of single-mineral systems, however, do not completely resolve and quantify the complex adsorption processes and interactions occuring in multimineralic soils and rocks. Many pressing technical issues, such as hazardous and nuclear waste management and the impact of acidic precipitation on watersheds, stand to benefit from an improved understanding of adsorption of metals on naturally occuring materials.

Mixtures of minerals provide one of the best analogs of soils and rocks that can be carefully characterized and controlled during laboratory studies of adsorption. A quantitative understanding of adsorption of metals in mixtures could provide significant insight into the adsorption processes on rocks and soils. An important question in studying adsorption in adsorbent mixtures is whether the adsorption behavior of mixtures can be modeled as sum of the adsorption behavior of its components, and whether the behavior of the mixture can be predicted from knowledge of the behavior of constituent components.

LIST OF REFERENCES

LIST OF REFERENCES

Allison, J. D., D. S. brown, and K. J. Novo-Gradac, MINTEQA2/ PRODEFA2, a geochemical assessment model for environmental systems: Environmental Research Laboratory, U. S. Environmental Protection Agency, Athens, GA

Anderson, P. R., and T. H. Christensen, 1988, Distribution coefficients of Cd, Co, Ni, and Zn in soils: J. Soil Sci., **39**,15-22.

Atkinson, R. J., A. M. Posner, and J. P. Quirk, 1967, Adsorption of potential-determining ions at the ferric oxide-aqueous electrolyte interface: J. Phys. Chem., **71** (3), 550-558.

Balistrieri, L. S., and J. W. Murray, 1981, The surface chemistry of goethite (αFeOOH) in major ion seawater: Amer. J. Sci., **281**, 788-806.

Balistrieri, L. S., and J. W. Murray, 1982a, The adsorption of Cu, Pb, Zn, and Cd on goethite from major ion seawater: Geochim. Cosmochim. Acta, **46**, 1253-1265.

Balistrieri, L. S., and J. W. Murray, 1982b, The surface chemistry of δMnO_2 in major sea water: Geochim. Cosmochim. Acta, **46**, 1042-1051.

Balistrieri, L. S., and J. W. Murray, 1983, Metal-solid interactions in the marine environment: estimating apparent equilibrium binding constants: Geochim. Cosmochim. Acta, **47**, 1091-1098.

Benjamin, M. M., and J. O. Leckie, 1981, Multiple-site adsorption of Cd, Cu, Zn and Pb on amorphous iron oxyhydroxide: J Colloid Interface Sci., **79** (1), 209-221.

Chapman, D. L., 1913, A contribution to the theory of electrocapillarity: Philos. Mag., **6**, 475-481.

Charlet, L, 1986, Adsorption of some micronutrient ions on an oxisol: An application of the triple layer model: Ph. D. thesis, University of California at Riverside, Riverside, CA.

Cox, C. D. and M. M. Ghosh, 1994, Surface complexation of methylated arsenates by hydrous oxides: Water Research, in press.

Davis, J. A., R. O. James, and J. O. Leckie, 1978, Surface ionization and complexation at the oxide/water interface. I: Computation of electrical double layer properties in simple electrolyte: J. Colloid Interface Sci., **63** (1), 480-499.

Davis, J. A., and J. O. Leckie, 1978a, Surface ionization and complexation at the oxide/water interface. II: Surface properties of amorphous iron oxyhydroxide and adsorption of metal ions: J. Colloid Interface Sci., **67** (1), 90-107.

Davis, J. A., and J. O. Leckie, 1978b, Surface ionization and complexation at the oxide/water interface. III: Surface properties of amorphous iron oxyhydroxide and adsorption of anions: J. Colloid Interface Sci., **74** (1), 32-43.

Davis, J. A., and J. O. Leckie, 1978c, Effect of adsorbed complexing ligands on trace metal uptake by hydrous oxides: Environ. Sci. Technol., **12**, 1309-1315.

Davis, J. A., and J. O. Leckie, 1979, Speciation of adsorbed ions at the oxide/aqueous interface *in* E. A. Jenne, Ed., Chemical Modeling in Aqueous Systems, ACS symposium series no. 93, American chemical Society, Washington, D.C. p. 299-317.

Dudley, L. M., J. E. Mclean, R. C. Sims, and J. J. Jurinak, 1988, Sorption of copper and cadmium from the water soluble fraction of an acid mine waste by two calcareous soils: Soil Sci., **145**, 207-214.

Dzombak, D. A., and Morel, F. M. M., 1989, Surface Complexation Modeling: Hydrous Ferric Oxide: New York, NY, Wiley-Interscience Publication, p. 1-393.

Forbes, E. A., A. M. Posner, and J. P. Quirk, 1976, The specific adsorption of divalent Cd, Co, Cu, Pb, and Zn on goethite: J. Soil Sci., **27**, 154-166.

Fuller, C. C., and J. A. Davis, 1987, Processes and kinetics of Cd^{2+} sorption by a calcareous aquifer sand: Geochim. Cosmochim. Acta, **59**, 1491-1502.

Ghosh, M. M., C. D. Cox, and J. R. Yuan-Pan, 1994, Adsorption of selenium on hydrous oxides: Environmental Progress, in press.

Grahame, D. C., 1947, The electrical double layer and the theory of electrocapillarity: Chem. Rev. **41**, 441-501.

Gouy, G., 1910, Sur la constitution de la charge electrique a la surface d'um electrolyte: J. Phys., **9**, 457-468.

Hayes, K., 1987, Equilibrium, spectroscopic, and kinetics studies of ion adsorption at the oxide/aqueous interface: Ph. D. thesis, Department of Civil Engineering, Stanford University, CA.

Hayes, K. F., and J. O. Leckie, 1987, Modeling ionic strength effects on cation adsorption at hydrous oxide/solution interfaces: J. Colloid Interface Sci., **115**, 564-572.

Hayes, K. F., P. Charalambos, and J. O. Leckie, 1988, Modeling ionic strength effects on anion adsorption at hydrous oxide/solution interfaces: J. Colloid Interface Sci., **125** (2), 717-726.

Hayes, K. F., A. L. Roe, G. E. Brown, Jr., K. O. Hodgson, J. O. Leckie, and G. A. Parks,1987, In situ x-ray absorption study of surface complexes: Selenium oxyanions on α–FeO.OH: Science, **238**, 783-786.

Hem, J. D., 1972, Chemistry and occurrence of cadmium and zinc in surface water and groundwater: Water Resour. Res., **8**, 661-679.

Hem, J. D. , 1976, Geochemical controls on lead concentrations in stream water and sediments: Geochim. Cosmochim. Acta, **40**, 599-609.

Hohl, H., and W. Stumm, 1976, Interaction of Pb^{2+} with hydrous g-Al_2O_3: J. Colloid Interface Sci., **55** (2), 281-288.

James, R. O., and J. O. Leckie, 1974, Control mechanisms for trace metals in natural waters; *in* E. Rubin, ed., Aqueous-Environmental Chemistry of Metals: Ann Arbor, MI., Ann Arbor Science, p. 1-77.

James, R. O. and G. A. Parks, 1982, Characterization of aqueous colloids by their electrical double layer and intrinsic surface chemical properties: Surface and Colloid Science, **12**, 119-216.

Kleijn, W. B., 1981, The physical chemistry of clays and oxides: Ph. D. thesis, University of California at Riverside, Riverside, CA.

Kooner, Z. S., 1992, Adsorption of copper onto goethite in aqueous systems: Environ. Geol. Water Sci., **20** (3), 205-212.

Kooner, Z. S., 1993, Comparative study of the adsorption behavior of copper, lead, and zinc onto goethite in aqueous systems: Environ. Geol., **21** (4), 242-250.

Lindsey, W. L., 1979, Chemical Equilibrium in Soils; New York: John Wiley & Sons.

Loganathan, P., and R. G. Burau, 1973, Sorption of heavy metal ions by a hydrous manganese oxide: Geochim. Cosmochim. Acta, **37**, 1277-1293.

Marshall, C. E., and W. E. Bergan, 1942, The electrochemical properties of mineral membranes. II. Measurement of potassium-ion activities in colloidal clays: J. Phys. chem., **46**, 52-61.

Marshall, C. E., and C. A. Krinbill, 1942. The clays as colloidal electrolytes: J. Phys. Chem., **46**, 1077-1090.

McCarthy, J. F., and J. M. Zachara, 1989, Subsurface transport of contaminant: Environ. Sci. Technol., **23** (5), 496-502.

Means J. L., D. A. Crerar, and J. O. Duguid, 1978, Migration of radioactive waste: Radionuclide mobilization by complexing agents: Science, **200**, 1477-1481.

Murray, J. W. , and Dillard, J. G., 1979, The oxidation of cobalt(II) adsorbed on manganese dioxide: Geochim. Cosmochim. Acta, **43**, 781-787.

Padmanabham, M, 1983, Adsorption-desorption behaviour of copper(II) at the goethite-solution interface: Aust. J. Soil Res., **21**, 309-320.

Parks, G. A., 1975, Adsorption in marine environment; *in* J. P. Riley and G. Skirrow, eds., Chemical Oceanography, v. 1: New York: Academic Press, p. 241-308.

Schindler, P. W., 1967, Heterogeneous equilibria involving oxides, hydroxides, carbonates, and hydroxide carbonates; *in* W. Stumm, ed., Equilibrium Concepts in Natural Water Systems, Advances in Chemistry Series 67: Washington, D. C., American Chemical Society, 196-221.

Schindler, P. W., B. Furst, R. Dick, and P. U. Wolf, 1976, Ligand properties of surface silanol groups: Surface complex formation with Fe^{3+}, Cu^{2+}, cd^{2+}, and Pb^{2+}: J. Colloid Interface. Sci., **55** (2), 469-475.

Stern, O., 1924, Zur theorie der elektischen doppelschicht: Z. Elektrochem., **30**, 508-516.

Stumm, W., H. Hohl, and F. Dalang, 1976, Interaction of metal ions with hydrous oxide surfaces: Croatica Chem. Acta, **48**, 491-504.

Stumm, W., C. P. Huang, and S. R. Jenkins, 1970, Specific chemical interaction affecting the stability of dispersed systems: Croatica Chem. Acta, **42**, 223-245.

Stumm, W., and J. J. Morgan, 1981, Aquatic Chemistry, 2nd ed.: John Wiley & Sons, New York.

Tripathi, V. S., 1983, Uranium(VI) transport modeling: Geochemical data and submodel: Ph D. thesis, Department of Applied Earth Sciences, Stanford University, CA.

Westall, J. C.,1982, FITEQL: A program for the determination of chemical equilibrium constants from experimental data, Technical Report: Chemistry department, Oregon State University, Corvallis, OR.

Westall, J. C., J. L. Zachara, and M. M. M Francois, 1976, A computer program for the calculation of chemical equilibrium composition of aqueous system: Technical Note No. 18: Massachusetts Institute of Technology, Cambridge, MA.

Yates, D. E., S. Levine, T. W. Healy, 1974, Site-binding model of the electrical double layer at the oxide/water interface: J. Chem. Soc. Faraday Trans., **70** (3), 1807-1818.

Zachara, J. M., J. A. Kittrick, and J. B. Harsh, 1989, Solubility and surface spectroscopy of zinc precipitates on calcite: Geochim. Cosmochim. Acta, **53**, 9-19.

APPENDICES

APPENDIX A

A.1

Adsorption of copper onto goethite as a function of time at 25.0 C

[Cu]	=	5.0 ppm
Goethite	=	0.6 g/l
Ionic strength	=	0.1 M $NaNO_3$

Time/min	% Adsorption
30	57.8
30	59.7
60	58.0
60	57.0
120	62.6
120	60.6
120	59.8
150	58.4
180	55.0
180	57.5
180	58.5
210	60.5
240	62.2
270	52.9
300	55.1
300	55.0
300	58.3
330	60.7
360	61.9
390	58.1

A.1 (cont.)

Time/min	% Adsorption
420	59.1
450	61.8
450	56.7
450	53.5
480	60.1
600	57.4
600	61.6
735	66.4
735	64.4
900	62.1
900	62.3
1200	63.0
1200	61.0
1500	61.4
1500	60.5
1800	60.3

A.2

Adsorption of copper onto goethite as a function of pH at 25.0 C

[Cu]	=	5.0 ppm
Goethite	=	0.6 g/l
Ionic strength	=	0.1 M $NaNO_3$

Set A-adsorption		Set B-desorption	
pH	% Adsorption	pH	% Adsorption
4.11	0.50	4.34	2.22
4.55	4.04	4.53	3.56
4.77	8.98	4.72	8.52
5.61	52.58	5.65	51.10
5.79	62.46	5.91	65.04
6.22	82.76	6.12	75.04

A.3

Adsorption of copper onto goethite as a function of pH at 25.0 C

[Cu]	=	0.5 ppm
Goethite	=	0.6 g/l
Ionic strength	=	0.1 M $NaNO_3$

Batch A		Batch B-Day 1		Batch B-day 2	
pH	% Adsorption	pH	% Adsorption	pH	% Adsorption
4.31	0	3.97	0	4.04	0
4.75	12	3.98	0	4.11	0
4.85	18	4.60	6.4	4.79	12.4
5.09	28	4.64	5	4.82	12
5.27	33	5.35	51	5.40	48
5.58	69	5.33	47	5.46	54
5.85	86	6.09	91	6.04	89
6.46	95	6.19	94	6.09	90
		6.58	95	6.59	97

A.4

Adsorption of lead onto goethite as a function of pH at 25.0 C

Goethite = 0.6 g/l
Ionic strength = 0.1 M $NaNO_3$

Batch A-2 ppm		Batch B-2 ppm		Batch C-15 ppm		Batch D-15 ppm	
pH	% Adsorption	pH	% Adsorption	pH	% Adsorption	pH	% Adsorption
4.48	8.68	5.11	22.85	4.57	3.27	5.25	12.47
5.23	35.30	5.45	44.10	5.21	12.40	5.56	21.93
6.06	80.90	5.69	56.35	5.94	35.73	5.90	33.33
6.81	92.45	6.01	74.05	6.85	89.87	6.43	58.60
7.09	93.10	6.49	91.30	7.11	93.70	6.81	84.33

APPENDIX B

B.1

Adsorption of copper onto goethite as a function of pH at 25.0 C

Copper	=	0.5 ppm
Surface Area	=	30 m^2/l
Ionic strength	=	0.1 M $NaNO_3$

pH	% Adsorption
3.97	0
3.98	0
4.04	0
4.11	0
4.31	0
4.6	6.4
4.64	5
4.75	12
4.79	12.4
4.82	12
4.85	18
5.09	28
5.27	33
5.33	47
5.35	51
5.4	48
5.46	54
5.58	69
5.85	86
6.04	89

B.1 (cont.)

pH	% Adsorption
6.09	91
6.09	90
6.19	94
6.46	95

B.2

Adsorption of copper onto goethite as a function of pH at 25.0 C

Copper	=	1.0 ppm
Surface Area	=	280 m^2/l
Ionic strength	=	0.1 M $NaNO_3$

pH	% Adsorption
4.12	0
4.37	12
4.72	39.3
4.74	32.4
4.94	60.5
5.07	62.7
5.19	74.9
5.34	83.1
5.48	88.7
5.84	94.1
5.98	96.8

B.3

Adsorption of copper onto goethite as a function of pH at 25.0 C

Copper	=	5.0 ppm
Surface Area	=	30 m^2/l
Ionic strength	=	0.1 M $NaNO_3$

pH	% Adsorption
4.50	3.6
4.58	5.2
4.68	8.2
4.94	14.8
5.04	14.4
5.12	22
5.2	30
5.42	39.6
5.42	41.2
5.67	58.8
5.85	68.8
6.21	88

B.4

Adsorption of copper onto goethite as a function of pH at 25.0 C

Copper	=	5.0 ppm
Surface Area	=	60 m^2/l
Ionic strength	=	0.1 M $NaNO_3$

pH	% Adsorption
4.03	2.08
4.58	3.24
4.87	13.68
5.14	32.88
5.31	47.10
5.47	55.90
5.72	73.50
5.98	86.50
6.49	97.26

B.5

Adsorption of copper onto goethite as a function of pH at 25.0 C

Copper	=	5.0 ppm
Surface Area	=	145 m^2/l
Ionic strength	=	0.1 M $NaNO_3$

pH	% Adsorption
3.96	2.40
4.57	11.12
4.80	21.54
5.11	45.90
5.25	62.38
5.39	75.22
5.73	91.42
6.02	95.00
6.57	99.42

B.6

Adsorption of copper onto goethite as a function of pH at 25.0 C

Copper	=	5.0 ppm
Surface Area	=	280 m^2/l
Ionic strength	=	0.1 M $NaNO_3$

pH	% Adsorption
4.16	12.74
4.45	23.22
4.60	28.64
4.74	38.56
5.00	53.84
5.28	82.68
5.54	89.8
5.76	92.96
5.77	93.66
6.05	96.7
6.06	96.62

B.7

Adsorption of copper onto goethite as a function of pH at 25.0 C

Copper	=	10.0 ppm
Surface Area	=	30 m^2/l
Ionic strength	=	0.1 M $NaNO_3$

pH	% Adsorption
3.95	0
4.04	0
4.1	0
4.22	0
4.26	0.2
4.28	0.4
4.37	1.6
4.6	3.2
4.64	3.6
4.69	3.4
4.73	5.6
4.82	5.4
4.83	6
4.99	8
5.2	17.6
5.2	13.6
5.24	17.2
5.29	25.6
5.31	21.6

B.7 (cont.)

pH	% Adsorption
5.43	25.6
5.58	32
5.64	31.2
5.66	28
5.73	35.6

B.8

Adsorption of copper onto goethite as a function of pH at 25.0 C

Copper	=	10.0 ppm
Surface Area	=	280 m^2/l
Ionic strength	=	0.1 M $NaNO_3$

pH	% Adsorption
4.04	8.2
4.28	18.8
4.45	24.9
4.65	34.7
4.8	45.7
4.88	55.2
5.04	67.6
5.17	74.7
5.42	88.0
5.77	96.7
5.8	97.5
5.88	97.3

B.9

Adsorption of copper onto goethite as a function of pH at 25.0 C

Copper	=	5.0 ppm
Surface Area	=	30 m^2/l
Ionic strength	=	0.01 M $NaNO_3$

pH	% Adsorption
4.57	2.88
4.95	12.90
5.36	32.40
5.62	49.90
5.96	67.66
6.30	79.48
6.59	84.72

B.10

Adsorption of lead onto goethite as a function of pH at 25.0 C

Lead	=	2.0 ppm
Surface Area	=	12 m^2/l
Ionic strength	=	0.1 M $NaNO_3$

pH	% Adsorption
4.47	1.16
4.83	5.10
5.31	19.30
5.38	14.10
5.75	35.73
6.06	41.10
6.09	50.45
6.19	54.95
6.63	73.95
6.63	74.95

B.11

Adsorption of lead onto goethite as a function of pH at 25.0 C

Lead	=	2.0 ppm
Surface Area	=	30 m^2/l
Ionic strength	=	0.1 M $NaNO_3$

pH	% Adsorption
4.48	8.68
5.11	22.85
5.23	35.30
5.45	44.10
5.69	56.35
6.01	74.05
6.06	80.90
6.49	91.30
6.81	92.45
7.09	93.10

B.12

Adsorption of lead onto goethite as a function of pH at 25.0 C

Lead	=	5.0 ppm
Surface Area	=	30 m^2/l
Ionic strength	=	0.01 M $NaNO_3$

pH	% Adsorption
4.06	2.56
4.51	5.16
4.87	11.68
5.23	21.56
5.52	37.90
5.85	62.54
6.29	80.62
6.62	90.88
6.82	93.50
6.96	93.80

B.13

Adsorption of lead onto goethite as a function of pH at 25.0 C

Lead	=	5.0 ppm
Surface Area	=	30 m^2/l
Ionic strength	=	0.1 M $NaNO_3$

pH	% Adsorption
3.90	2.10
4.37	5.46
4.63	9.78
4.75	10.26
5.06	20.10
5.25	26.16
5.50	41.54
5.78	49.82
5.86	60.22
6.14	68.82
6.21	69.70
6.47	82.62
6.79	90.42
6.86	90.24
6.87	94.54

B.14

Adsorption of lead onto goethite as a function of pH at 25.0 C

Lead	=	5.0 ppm
Surface Area	=	30 m^2/l
Ionic strength	=	0.5 M $NaNO_3$

pH	% Adsorption
4.11	0.44
4.49	0.08
4.95	7.48
5.34	18.88
5.45	27.0
5.87	38.20
6.18	51.44
6.35	60.48

B.15

Adsorption of lead onto goethite as a function of pH at 25.0 C

Lead	=	5.0 ppm
Surface Area	=	60 m^2/l
Ionic strength	=	0.1 M $NaNO_3$

pH	% Adsorption
4.60	14.08
5.22	44.52
5.80	75.32
6.19	87.52
6.67	92.14

B.16

Adsorption of lead onto goethite as a function of pH at 25.0 C

Lead	=	5.0 ppm
Surface Area	=	120 m^2/l
Ionic strength	=	0.1 M $NaNO_3$

pH	% Adsorption
4.64	22.88
5.34	68.46
5.64	85.64
6.38	98.56
6.76	99.12

B.17

Adsorption of lead onto goethite as a function of pH at 25.0 C

Lead	=	10.0 ppm
Surface Area	=	30 m^2/l
Ionic strength	=	0.1 M $NaNO_3$

pH	% Adsorption
4.41	3.60
5.21	14.20
5.58	24.50
5.76	35.50
5.99	46.90
6.01	56.70
6.28	60.90
6.70	83.10
6.70	83.90
7.40	92.70

B.18

Adsorption of lead onto goethite as a function of pH at 25.0 C

Lead	=	15.0 ppm
Surface Area	=	30 m^2/l
Ionic strength	=	0.1 M $NaNO_3$

pH	% Adsorption
4.57	3.27
5.21	12.40
5.25	12.47
5.56	21.93
5.90	33.33
5.94	35.73
6.43	58.60
6.81	84.33
6.85	89.87
7.11	93.70

B.19

Adsorption of zinc onto goethite as a function of pH at 25.0 C

Zinc	=	5.0 ppm
Surface Area	=	30 m^2/l
Ionic strength	=	0.01 M $NaNO_3$

pH	% Adsorption
4.05	2.24
4.38	2.32
4.90	2.08
5.17	3.54
5.35	8.00
5.78	8.10
6.06	10.40
6.17	15.54
6.58	43.88
6.83	59.28

B.20

Adsorption of zinc onto goethite as a function of pH at 25.0 C

Zinc	=	5.0 ppm
Surface Area	=	30 m^2/l
Ionic strength	=	0.1 M $NaNO_3$

pH	% Adsorption
3.99	0
4.48	0
4.80	0
5.06	0
5.54	0.58
5.94	5.16
6.15	9.0
6.54	30.84
6.75	38.86
7.04	63.32

APPENDIX C

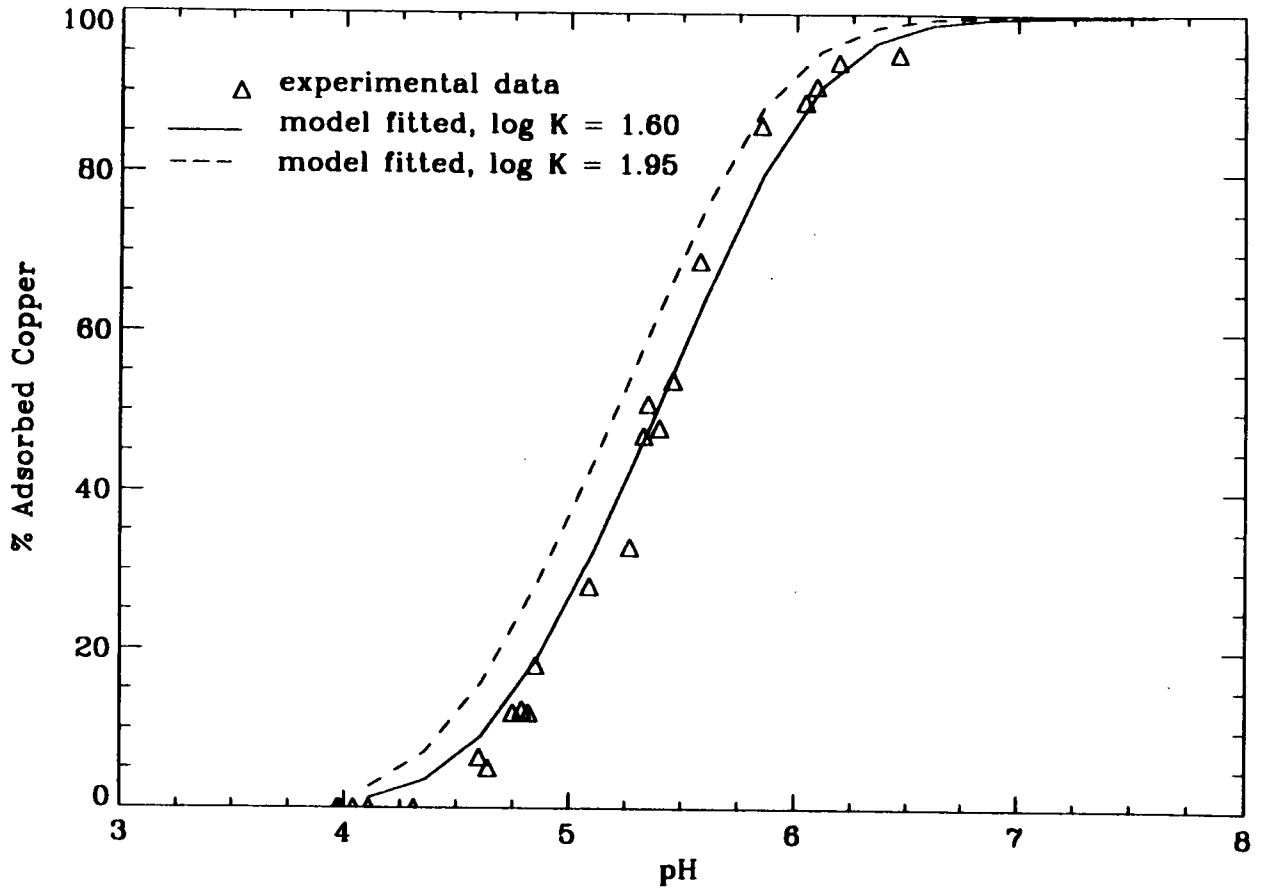


Figure C.1 Modeling the adsorption of copper onto goethite
ΣCu = 0.5 ppm (7.87×10^{-6} M); Surface area = 30 m^2/l; I = 0.1 M $NaNO_3$

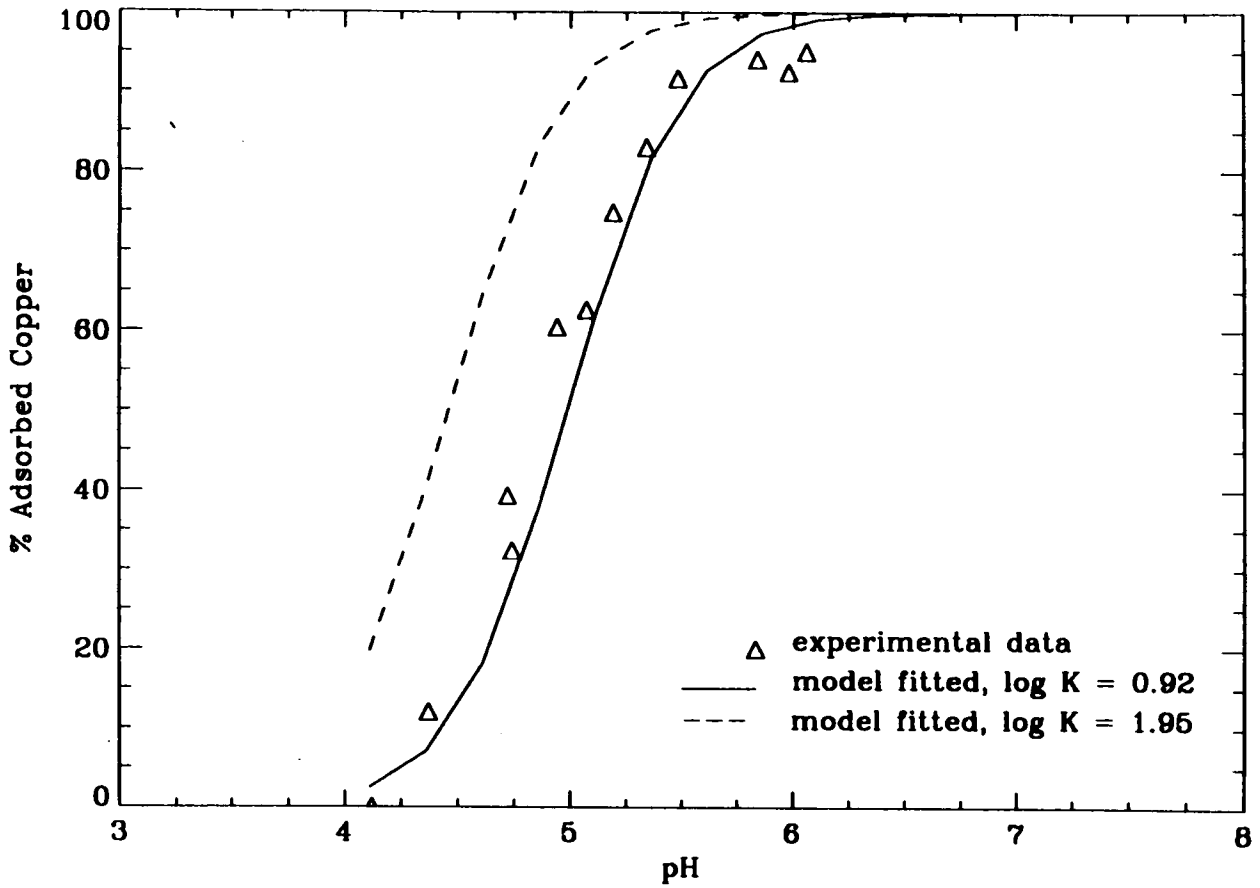


Figure C.2 Modeling the adsorption of copper onto goethite
ΣCu = 1.0 ppm (1.57×10^{-5} M); Surface area = 280 m^2/l; I = 0.1 M $NaNO_3$

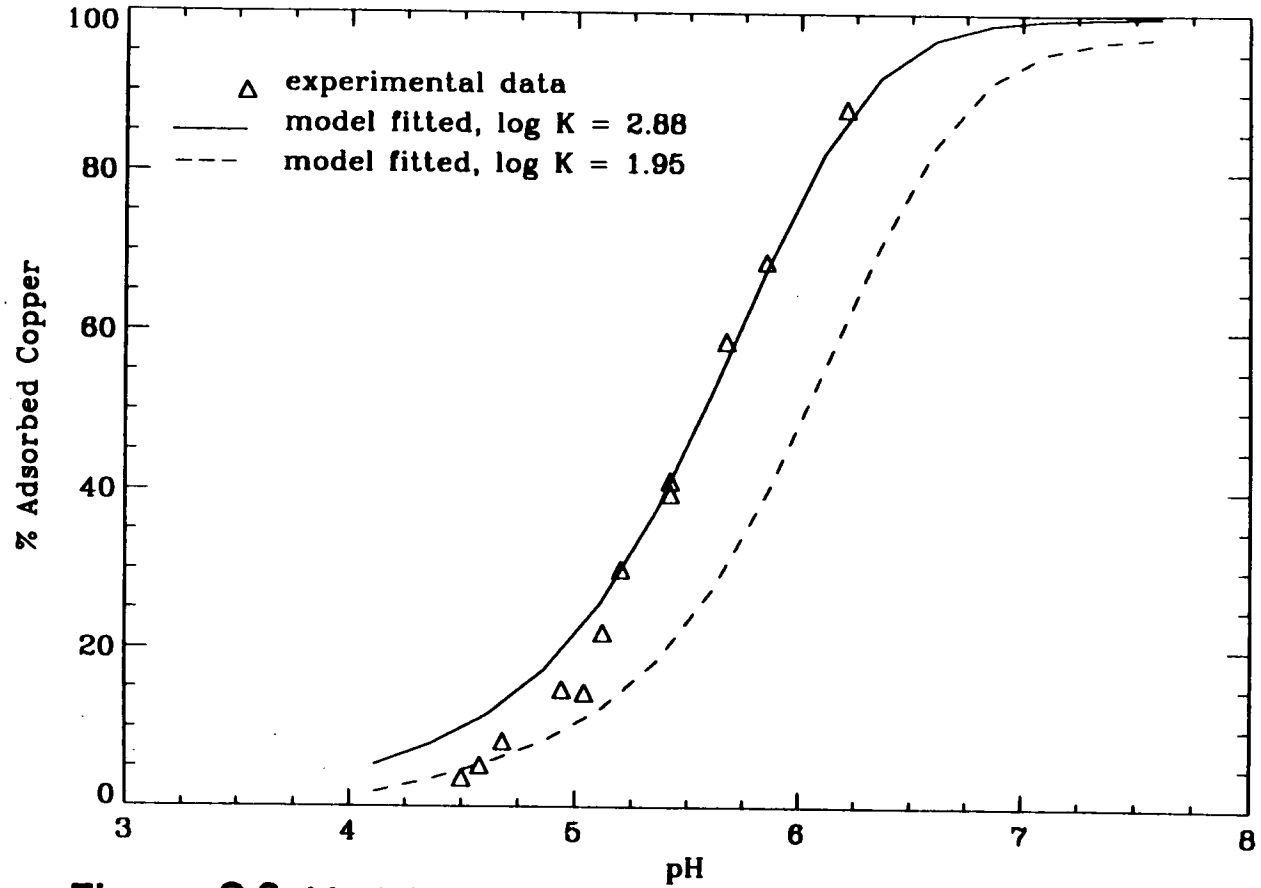


Figure C.3 Modeling the adsorption of copper onto goethite
ΣCu = 5.0 ppm (7.87×10^{-5} M); Surface area = 30 m^2/l; I = 0.1 M $NaNO_3$

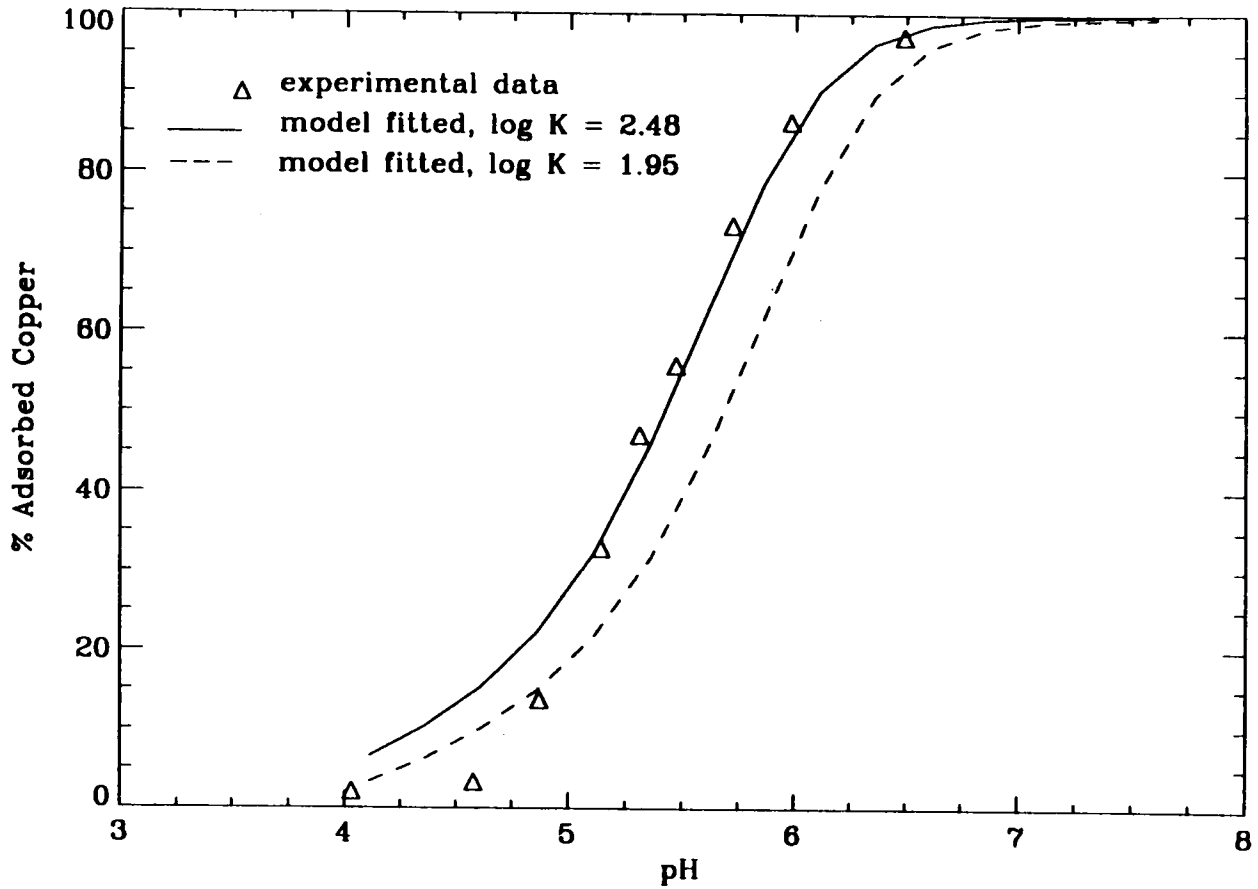


Figure C.4 Modeling the adsorption of copper onto goethite
ΣCu = 5.0 ppm (7.87×10^{-5} M); Surface area = 60 m^2/l; I = 0.1 M $NaNO_3$

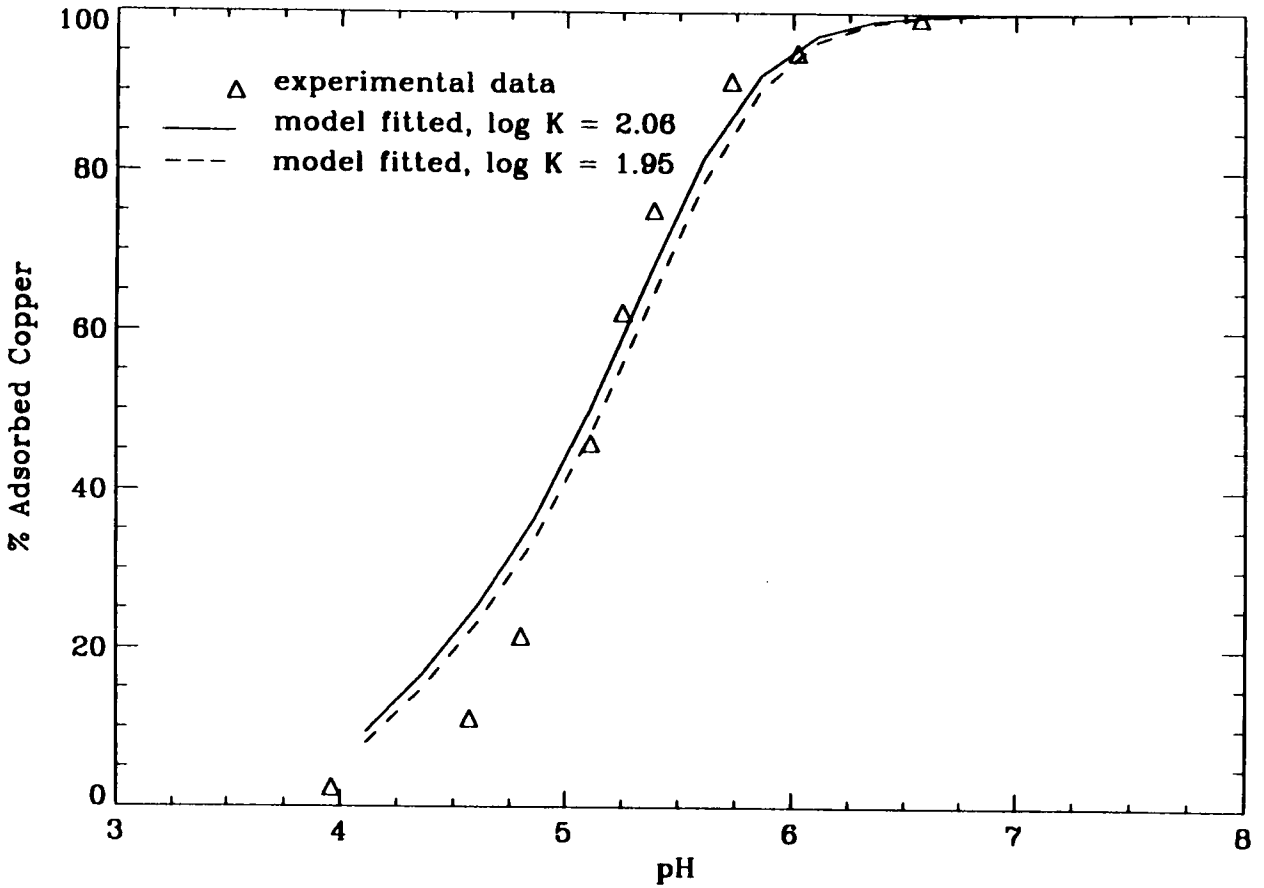


Figure C.5 Modeling the adsorption of copper onto goethite
ΣCu = 5.0 ppm (7.87×10^{-5} M); Surface area = 145 m^2/l; I = 0.1 M $NaNO_3$

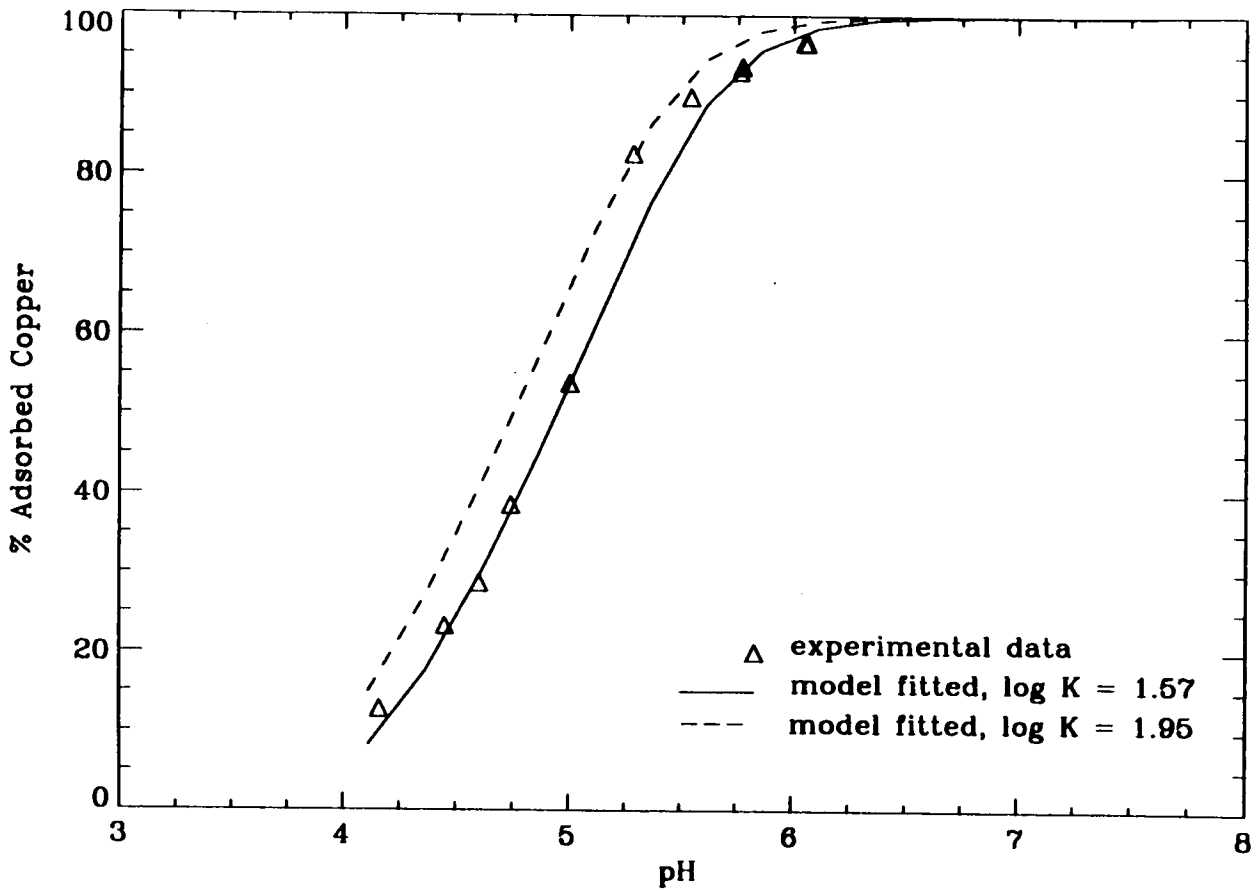


Figure C.6 Modeling the adsorption of copper onto goethite
ΣCu = 5.0 ppm (7.87×10^{-5} M); Surface area = 280 m^2/l; I = 0.1 M $NaNO_3$

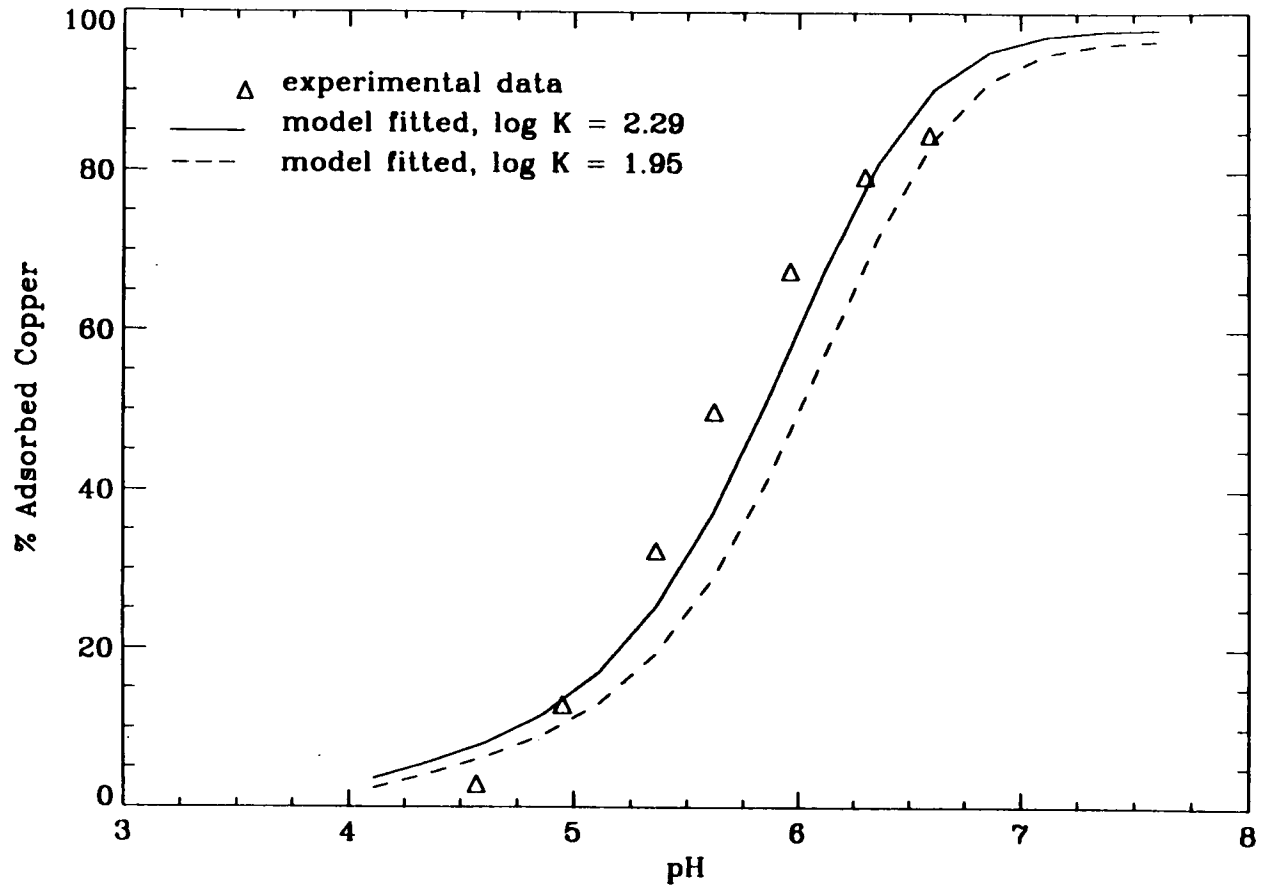


Figure C.7 Modeling the adsorption of copper onto goethite
ΣCu = 5.0 ppm (7.87×10^{-5} M); Surface area = 30 m^2/l; I = 0.01 M $NaNO_3$

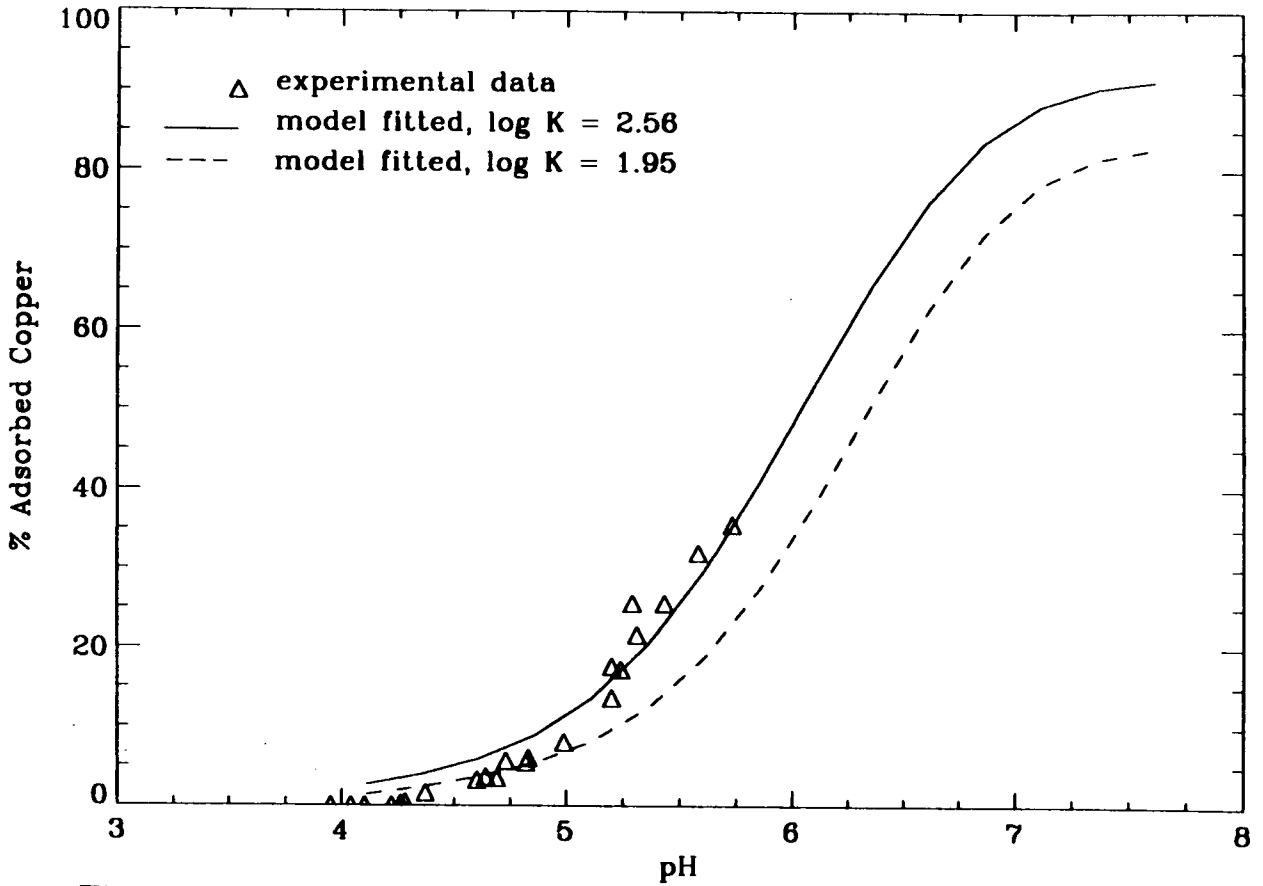


Figure C.8 Modeling the adsorption of copper onto goethite
ΣCu = 10.0 ppm (1.57×10^{-4} M); Surface area = 30 m^2/l; I = 0.1 M $NaNO_3$

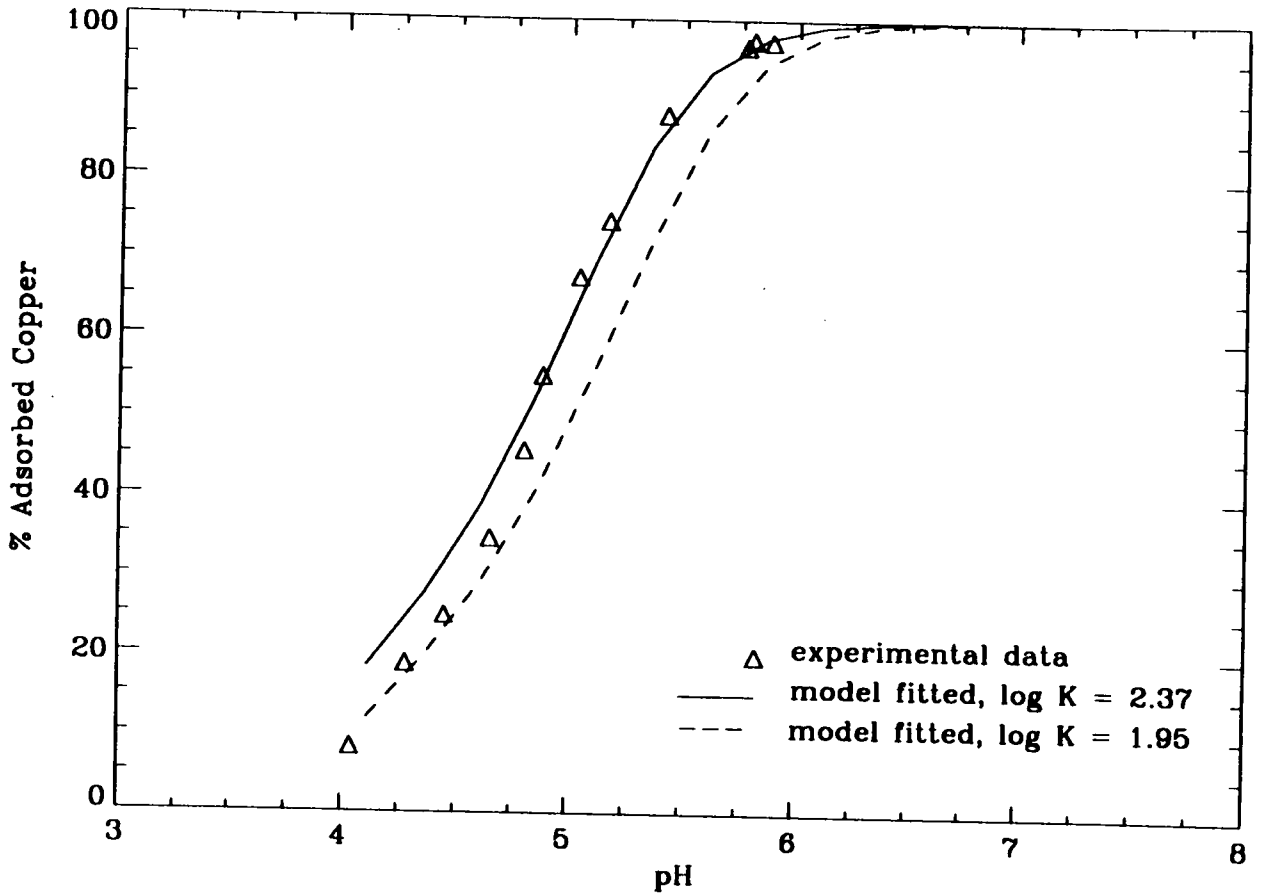


Figure C.9 Modeling the adsorption of copper onto goethite
ΣCu = 10.0 ppm (1.57×10^{-4} M); Surface area = 280 m^2/l; I = 0.1 M $NaNO_3$

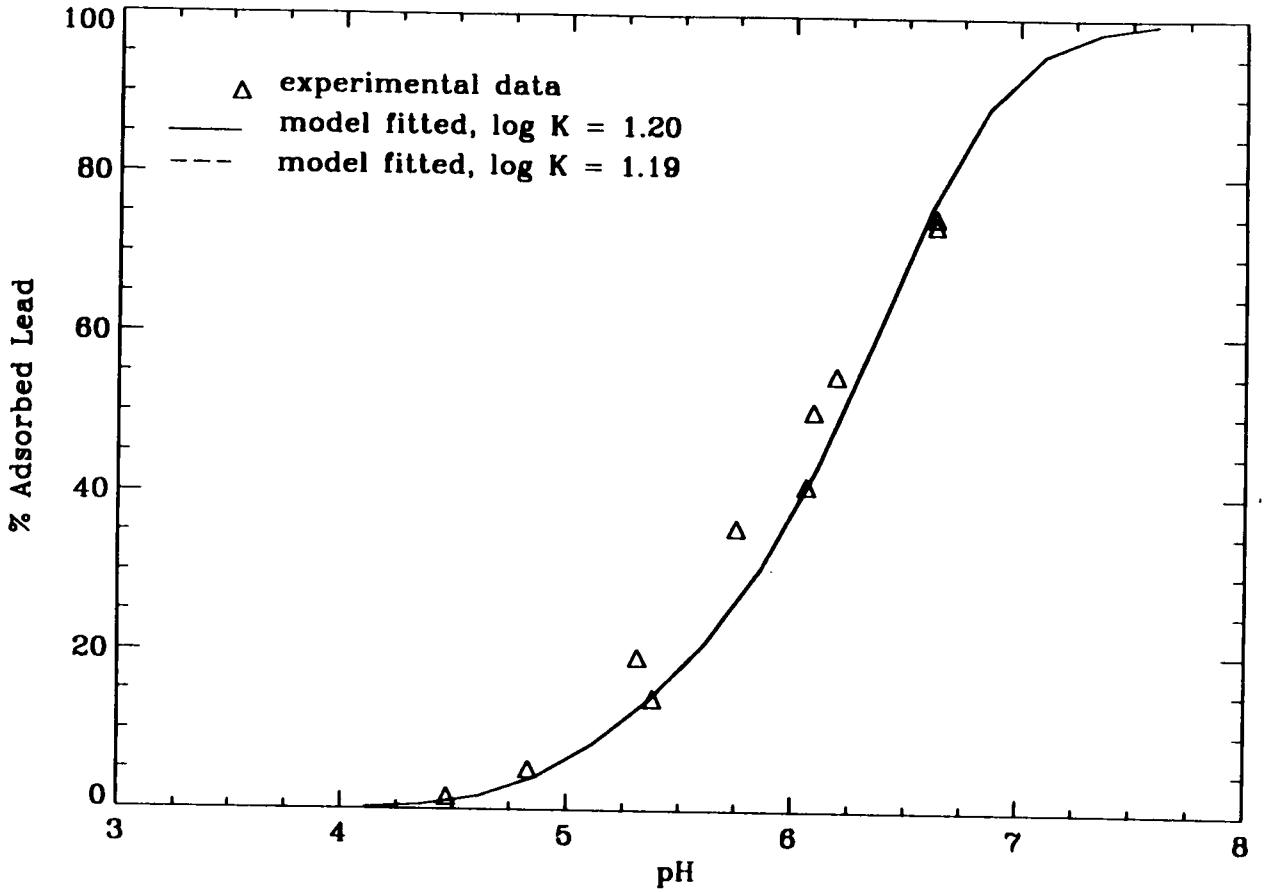


Figure C.10 Modeling the adsorption of lead onto goethite
ΣPb = 2.0 ppm (9.65×10^{-6} M); Surface area = 12 m^2/l; I = 0.1 M $NaNO_3$

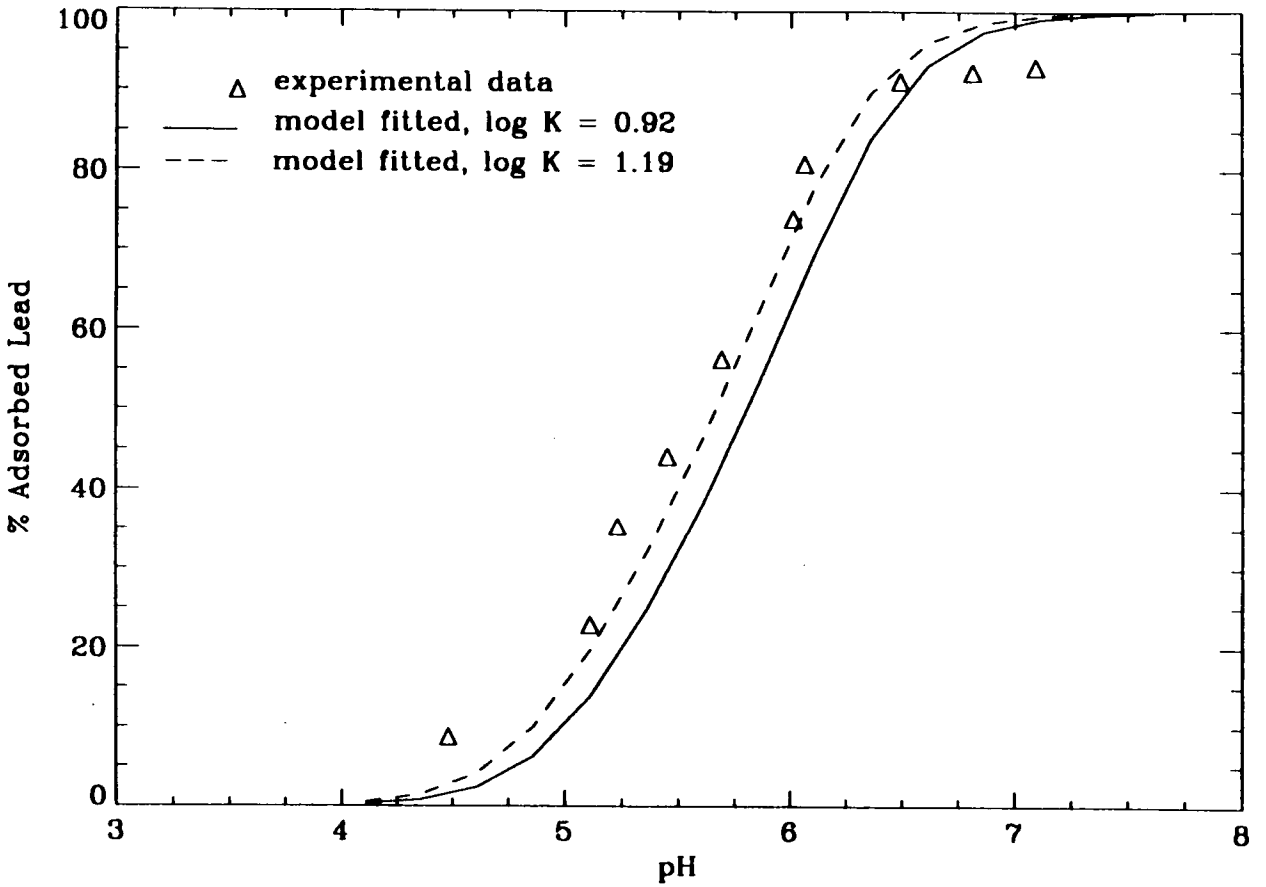


Figure C.11 Modeling the adsorption of lead onto goethite
ΣPb = 2.0 ppm (9.65×10^{-6} M); Surface area = 30 m^2/l; I = 0.1 M $NaNO_3$

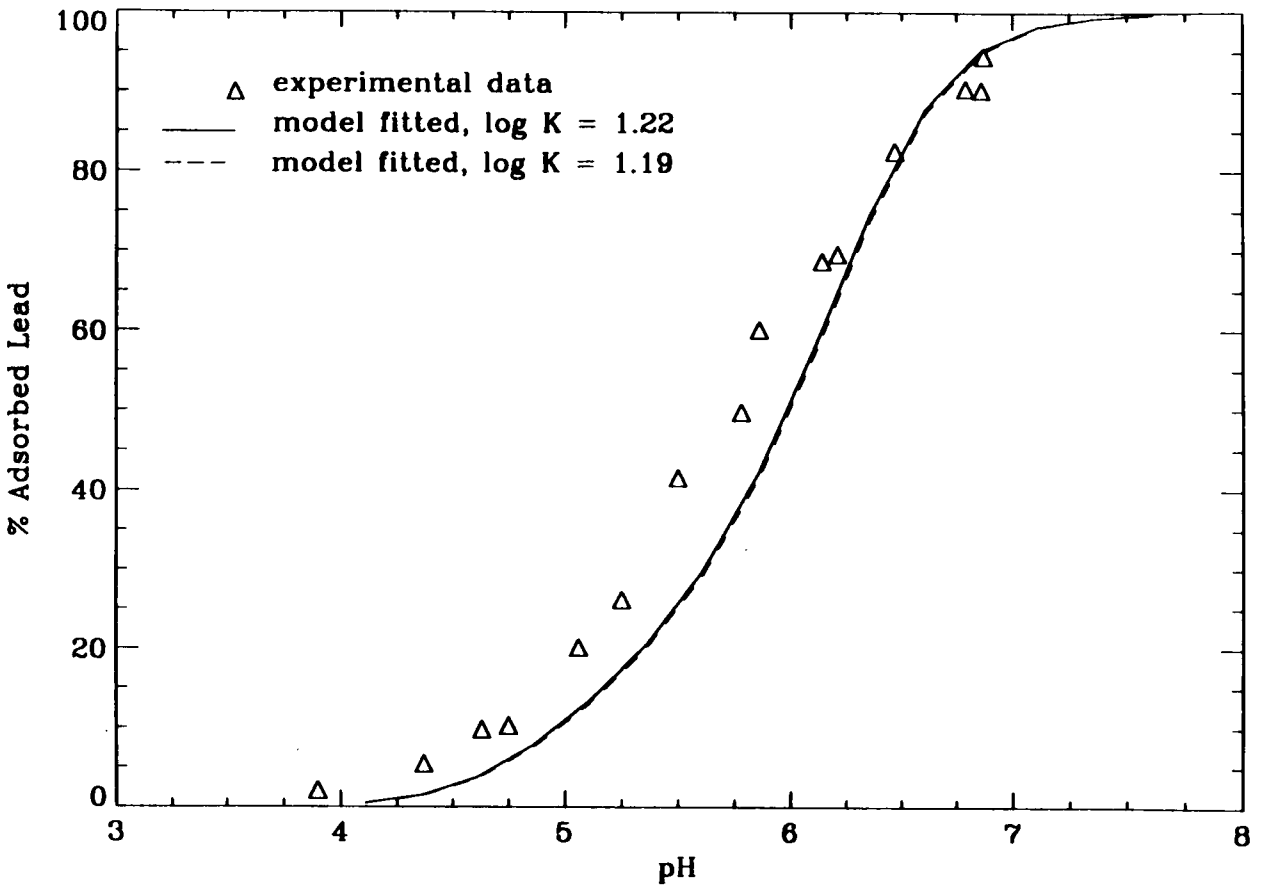


Figure C.12 Modeling the adsorption of lead onto goethite
ΣPb = 5.0 ppm (2.41×10^{-5} M); Surface area = 30 m^2/l; I = 0.1 M $NaNO_3$

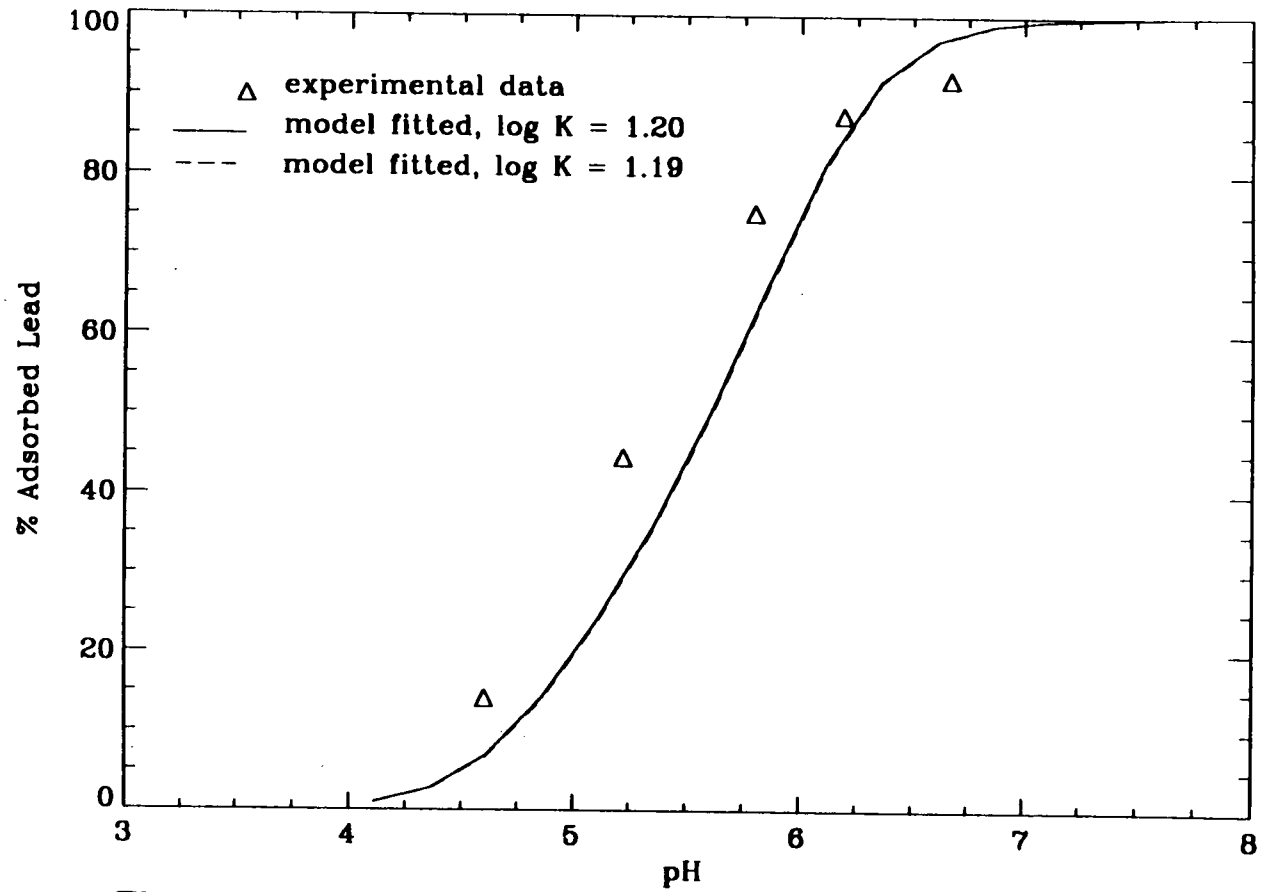


Figure C.13 Modeling the adsorption of lead onto goethite
ΣPb = 5.0 ppm (2.41×10^{-5} M); Surface area = 60 m^2/l; I = 0.1 M $NaNO_3$

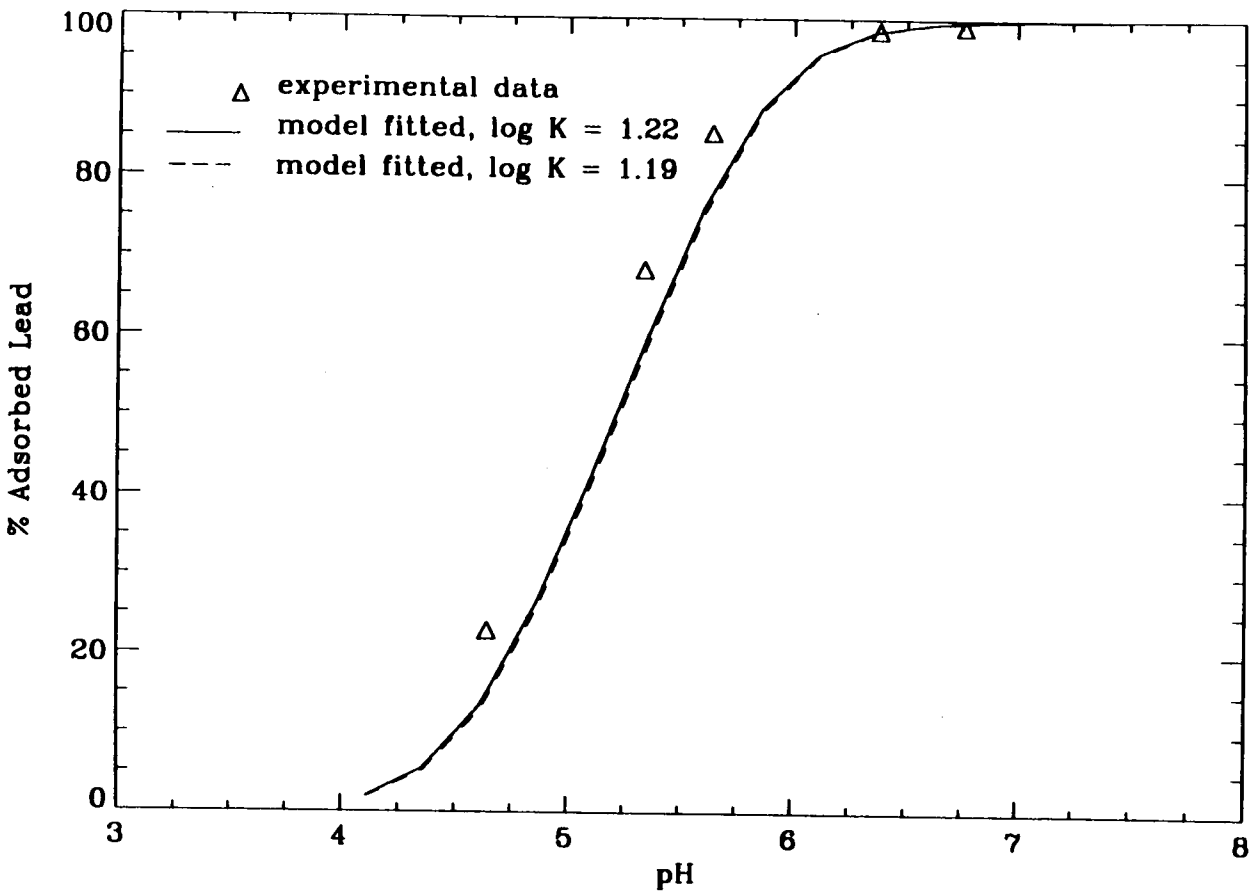


Figure C.14 Modeling the adsorption of lead onto goethite
ΣPb = 5.0 ppm (2.41×10^{-5} M); Surface area = 120 m^2/l; I = 0.1 M $NaNO_3$

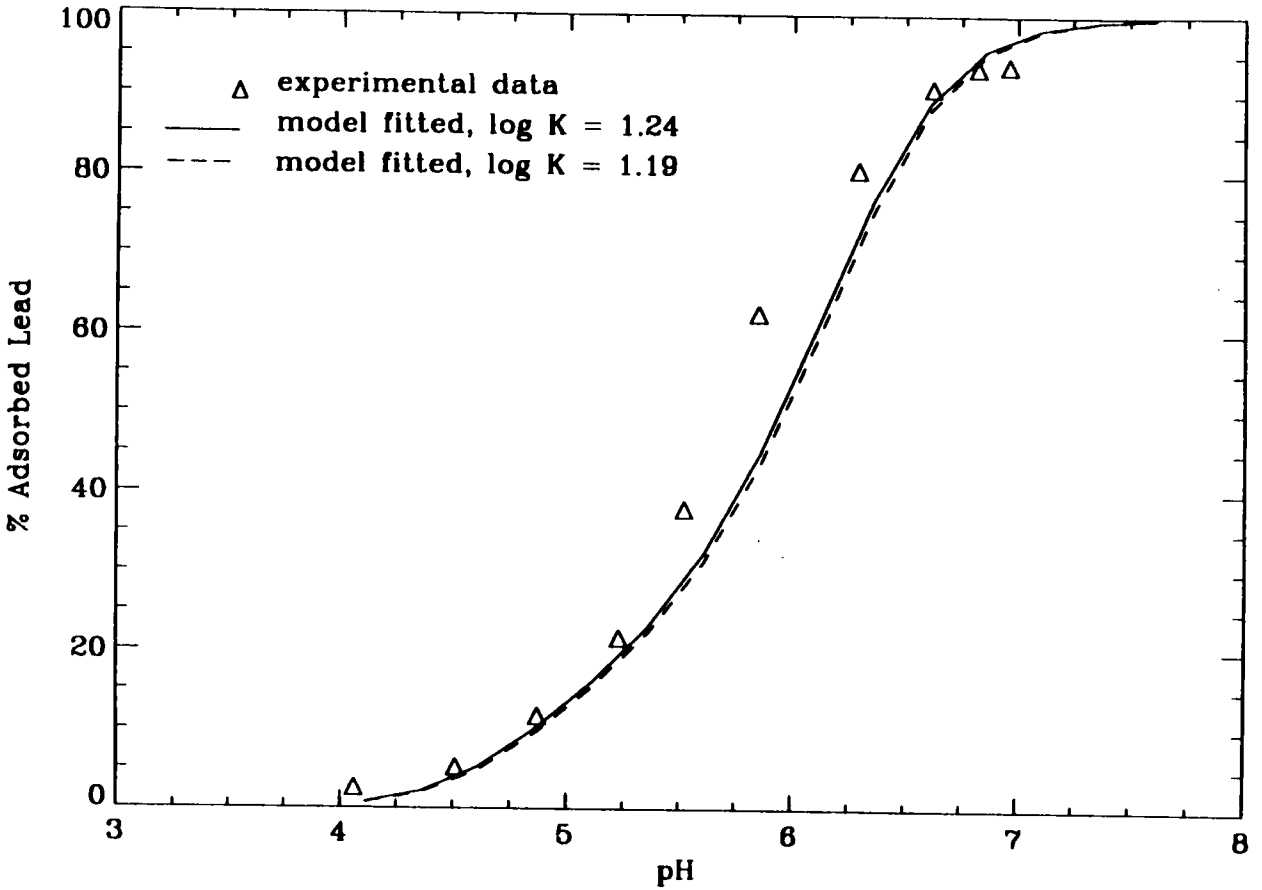


Figure C.15 Modeling the adsorption of lead onto goethite
ΣPb = 5.0 ppm (2.41×10^{-5} M); Surface area = 30 m^2/l; I = 0.01 M $NaNO_3$

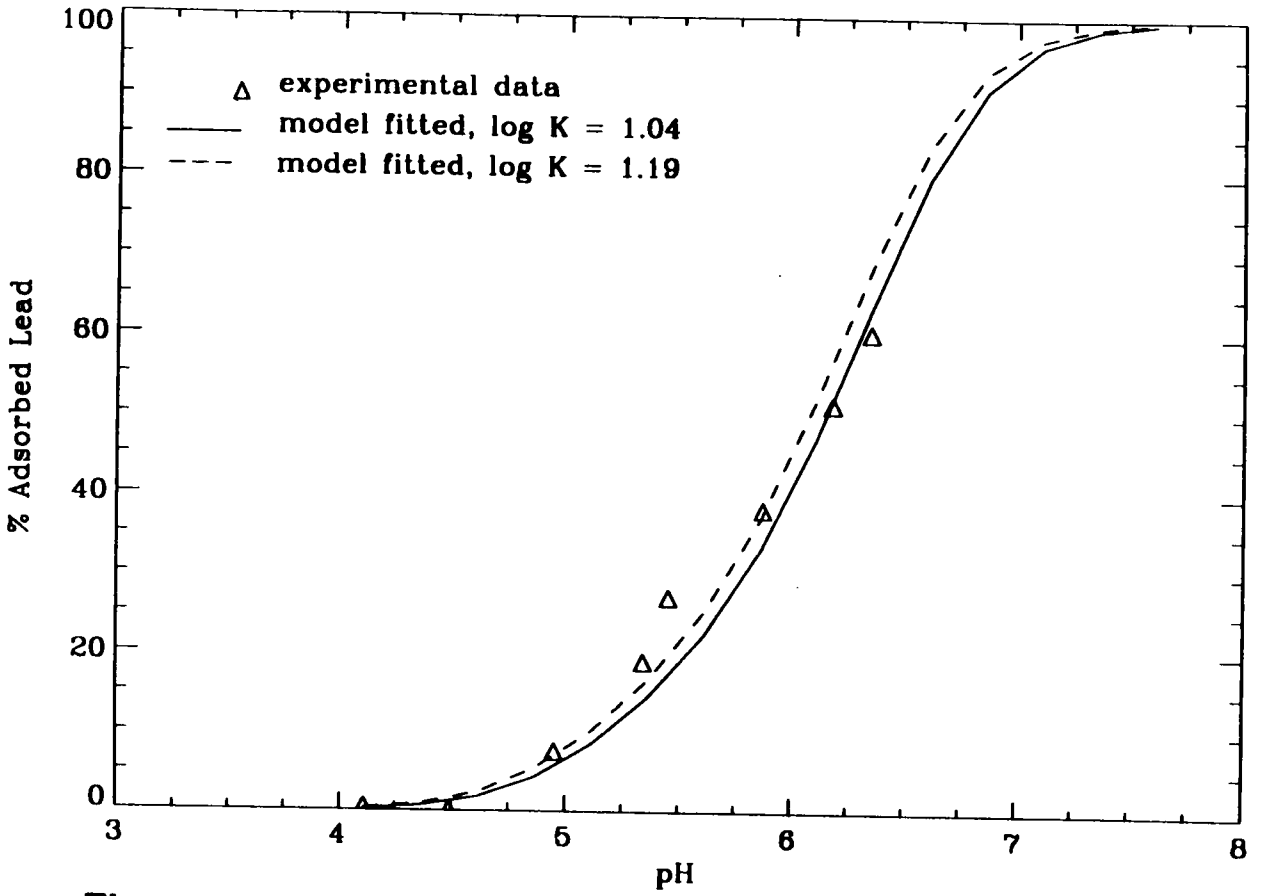


Figure C.16 Modeling the adsorption of lead onto goethite
ΣPb = 5.0 ppm (2.41×10^{-5} M); Surface area = 30 m^2/l; I = 0.50 M $NaNO_3$

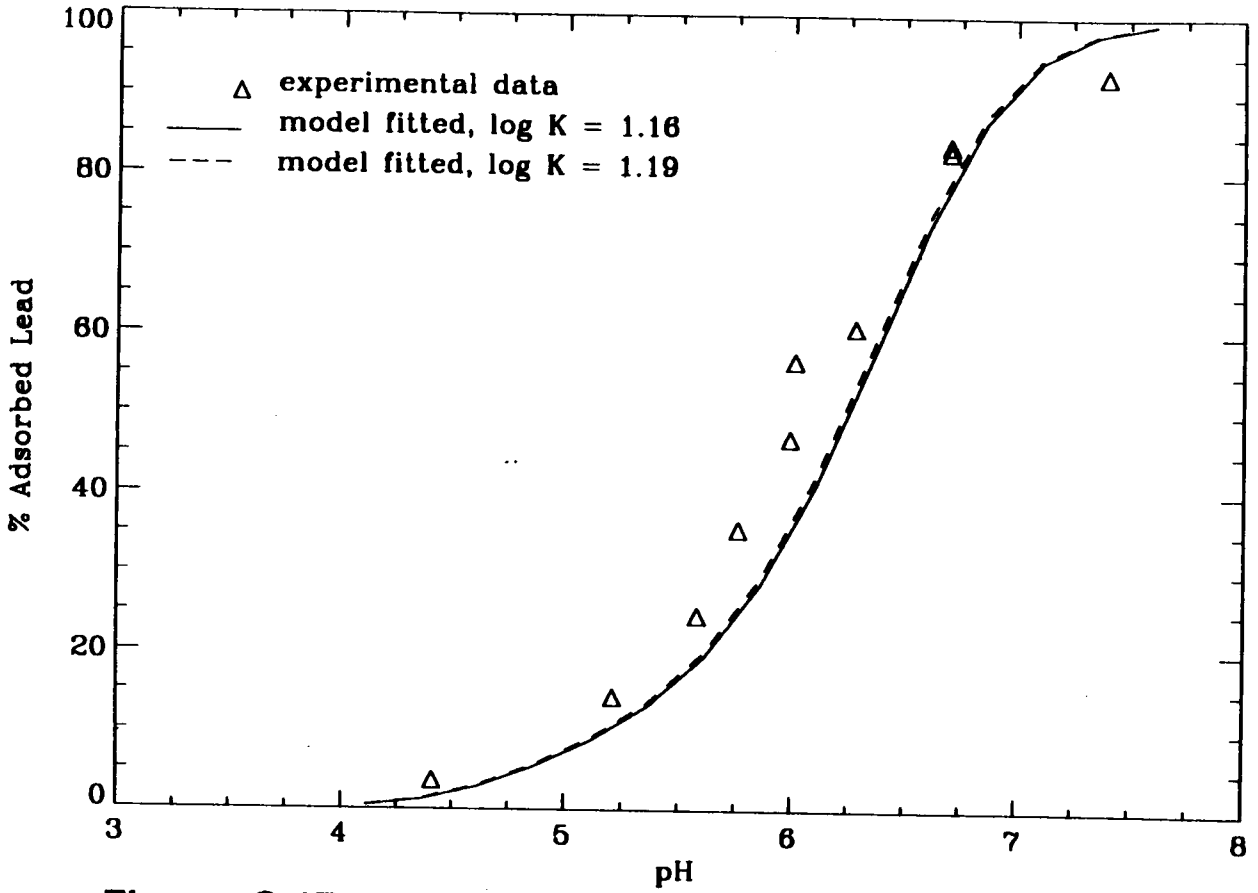


Figure C.17 Modeling the adsorption of lead onto goethite
ΣPb = 10.0 ppm (4.83×10^{-5} M); Surface area = 30 m^2/l; I = 0.1 M $NaNO_3$

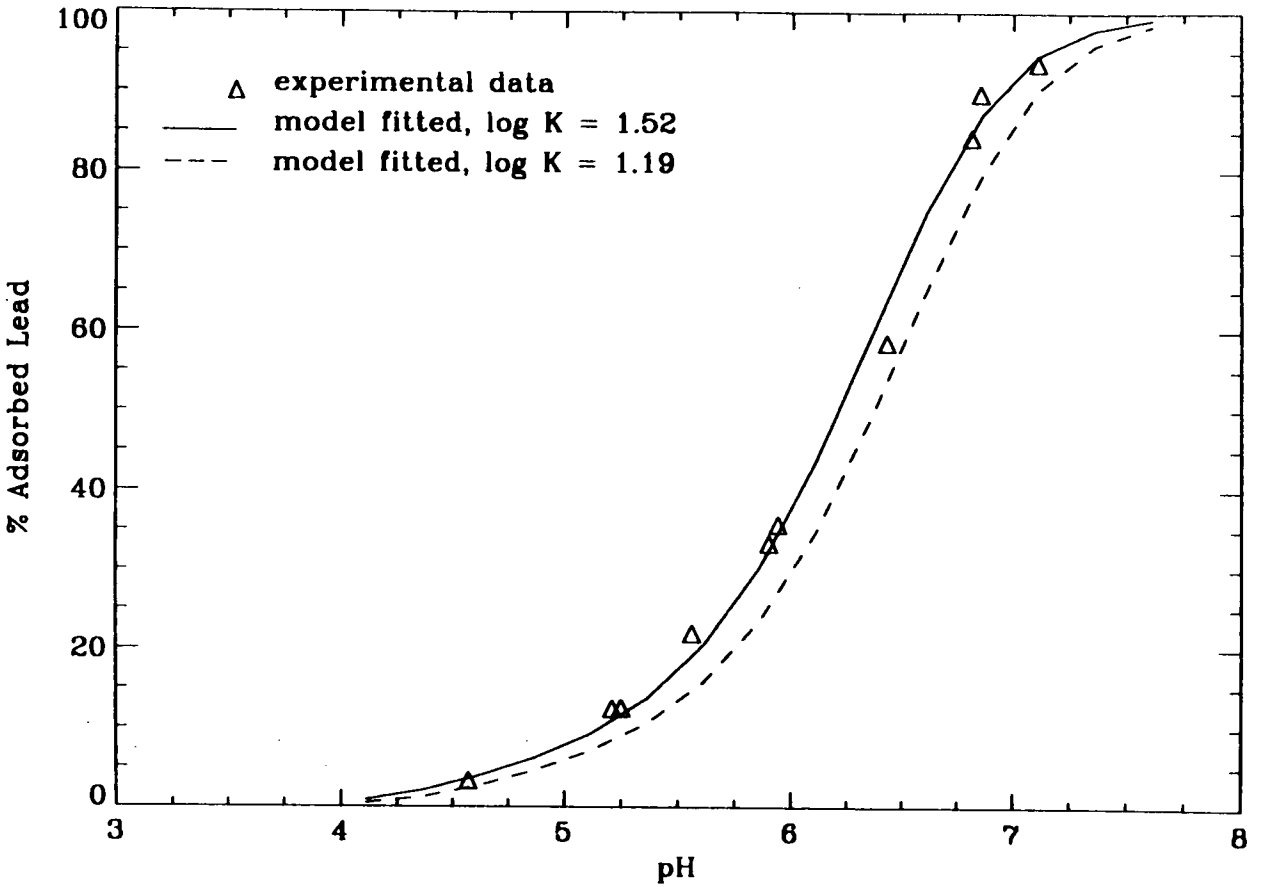


Figure C.18 Modeling the adsorption of lead onto goethite
ΣPb = 15.0 ppm (7.24×10^{-5} M); Surface area = 30 m^2/l; I = 0.1 M $NaNO_3$

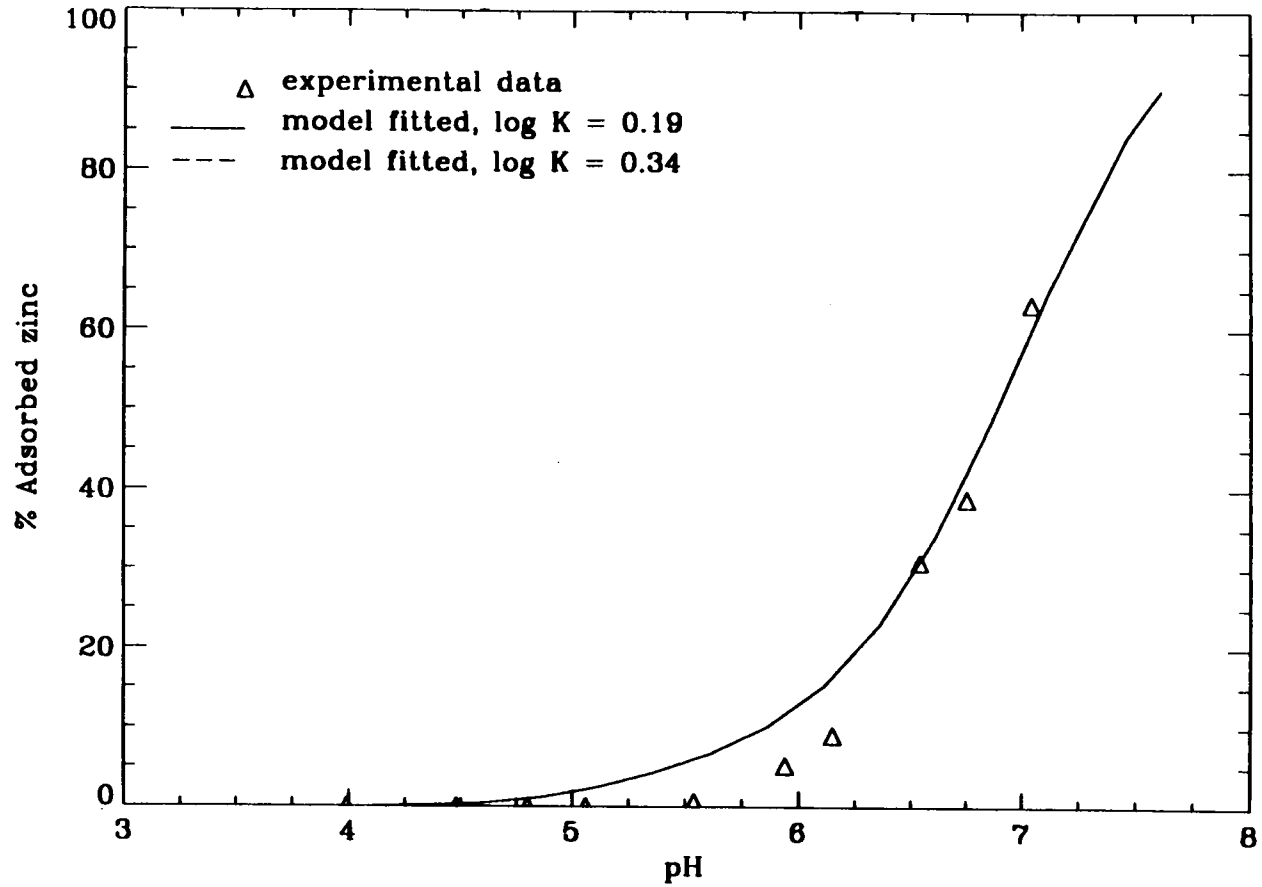


Figure C.19 Modeling the adsorption of zinc onto goethite
ΣZn = 5.0 ppm (7.65×10^{-5} M); Surface area = 30 m^2/l; I = 0.1 M $NaNO_3$

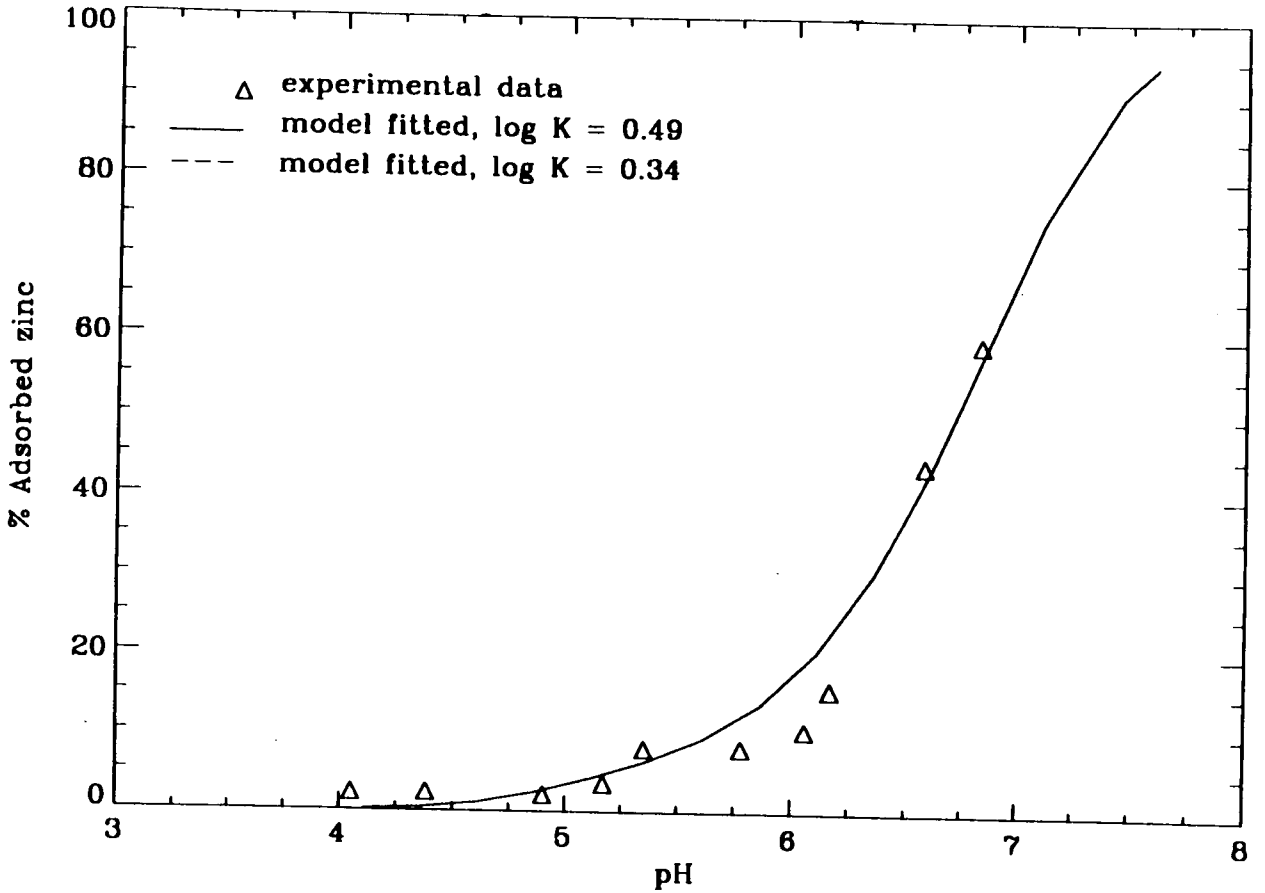


Figure C.20 Modeling the adsorption of zinc onto goethite
ΣZn = 5.0 ppm (7.65×10^{-5} M); Surface area = 30 m^2/l; I = 0.01 M $NaNO_3$

VITA

Zorawar Singh Kooner was born in India. He has a M.Sc. (Hons.) in chemistry from Panjab Agricultural University, Ludhiana, India, and a Ph.D. in physical chemistry from the University of Otago, Dunedin, New Zealand. He has published research papers in the area of physical and environmental chemistry. In the fall of 1990 he entered the University of Tennessee as a part time student while working at the Oak Ridge National laboratory in the Environmental Sciences Division and received a Master of Science in Environmental Engineering in Spring 1994.